Tectonic Structures and Glaciomarine Sedimentation in the South-Eastern Weddell Sea from Seismic Reflection Data

Tektonischer Aufbau und glaziomarine Sedimentation im südöstlichen Weddellmeer nach reflexionsseismischen Untersuchungen

---

László Oszkó

Ber. Polarforsch. 222 (1997)
ISSN 0176 - 5027

LÁSZLÓ OSZKÓ

Alfred-Wegener-Institut für Polar- und Meeresforschung
Postfach 120161
Columbusstraße
D-27515 Bremerhaven

Die vorliegende Arbeit ist die inhaltlich unveränderte Fassung einer Dissertation, die 1996 dem Fachbereich Geowissenschaften der Universität Bremen vorgelegt wurde.

Contents

Abstract

This thesis addresses the glaciomarine sedimentational and early tectonic history of the Southeastern Weddell Sea and proposes a model from the analysis of more than 25,000 km multichannel seismic data. The proposed seismic stratigraphic model includes the results of piston coring, drilling and bathymetric surveys. The tectonic interpretation was further supported by the compilation of published marine and satellite gravity surveys and magnetic anomaly maps.

The morphology of the investigated continental margin is characterised by a large trough-mouth fan, the Crary Fan, in front of the Filchner Shelf, and by numerous deeply incised canyons on the Queen Maud Land margin. The seismic data outline the principal tectonic structures of the survey area. They show a basement depression in front of the Filchner Shelf which is bounded by a basement ridge, the Andenes Escarpment, to the northwest and by the East Antarctic continental margin to the Southeast. Between 10°W and 20°W on the continental slope, the Explora Escarpment constitutes a step-like rise of more than 1 km. On the continental rise, a chain of three seamounts, the Polarstern Bank, has been found.

Glaciomarine sedimentation The uppermost sequence of the Crary Fan tapers downslope and consists of steeply dipping, prograding reflectors. On the continental slope, these reflectors downlap onto the underlying sequence of channel/levee complexes. On the lower slope, channel/levee complexes emerge from the cover of the prograding, steeply dipping reflectors that wrap the upper slope.

The correlation of the upper sequence with ODP Site 693 dates it to Middle Miocene to Recent. This upper sediment body is interpreted as a diamictit apron. It was deposited from a line source in front of the grounding line of an ice sheet when it extended to the shelf break. A tentative correlation of the channel/levee deposits with ODP Site 693 indicate an age of Early Oligocene to Middle Miocene for the formation of this seismic sequence. The channels are interpreted as conduits for turbidite flows and to a lesser extent thermohaline currents. Meltwater streams from wet-based glaciers fed the channels with sediments, levees formed from overbank deposits.

Near the slope base, some of the buried channels are partly eroded by and partly filled with transparent/chaotic acoustic sequences. These channel fills are interpreted as debris flows. The deeply incised canyons off Queen Maud Land drain turbidite flows.

They merge into a single, large channel running parallel to the slope base.

Hemipelagic, glaciomarine sedimentation occurred on the seamounts, with low sedimentation rates of 2.3 m/Ma. Levee deposits onlap on the older sediments on the seamount flanks.

The Cenozoic sedimentation of the Weddell Sea is controlled by glacial/interglacial climatic fluctuations. During glacial periods since the Middle Miocene, high sediment influx and growth of the diamictit apron have occurred. Interglacials are characterised by a sediment starving fan and by the generation of vigorous, strongly erosive thermohaline bottom currents flowing downslope. Before the Middle Miocene, meltwater streams from a temperate ice sheet fed the Crary Fan. Glacial and interglacial sedimentation rates differed during this period as well, but this difference was probably less pronounced than since the Middle Miocene.

Tectonic structures The compilation of the geophysical data confirms a failed rift arm underlies the Filchner Shelf. It probably formed in a broad back-arc extensional province during Middle-Late Jurassic times. With the initiation of seafloor spreading in the Somali and Mozambique basins, a major change occurred in the regional stress field at about 170 Ma. Strike-slip motion commenced between Africa and Antarctica forming the Explora Escarpment in a transform/transpressional regime. New data do not support the structural continuity of the Andenes and Explora Escarpments as representing the continent-ocean transition. The two structures have different morphology, their strikes are offset by about 70 km, and no basement high has been found to connect them. The Andenes Escarpment is probably an oceanic plateau that developed on a fracture zone during the strike-slip movement of Antarctica and Africa. The Polarstern Bank seamounts were formed by a delayed volcanic event on a pre-existing fracture or fault zone in the Late Jurassic/Early Cretaceous. The present structural continuity of the breakup-related tectonic structures indicates that no large-scale microplate movement has occurred in this area since the early opening of the Weddell Sea.

Zusammenfassung

Im Zentrum dieser Arbeit steht die glaziomarine Sedimentationsgeschichte und frühe tektonische Entwicklung des südöstlichen Weddell Meeres. Die dargestellte Interpretation basiert auf der Analyse eines Netzwerkes von mehr als 25 000 km mehrkanaliger seismischer Daten. Ergebnisse von Kolbenloten, Bohrungen und bathymetrischen Vermessungen wurden in das

seismostratigraphische Modell eingearbeitet. Die tektonische Interpretation wurde weiter durch veröffentlichte marine und Satelliten Schweremessungen und Karten von Anomalien des Erdmagnetfeldes unterstützt.

Die Morphologie des untersuchten Kontinentalrandes ist durch einen großen Trog-Mündungs-Fächer vor dem Filchner Schelf, dem Crary Fan, und einer Reihe tief eingeschnittener Canyons vor Queen Maud Land geprägt. Die tektonische Struktur des Untersuchungsgebiets zeigt ein unterschiedliches Bild. Vor dem Filchner Schelf zeigen die seismischen Daten eine Basement Depression. Diese wird durch eine Rückenstruktur, das Andenes Escarpment, im Nordwesten und den Ostantarktischen Kontinentalrand im Südosten begrenzt. Auf dem Kontinentalhang zwischen 10°W und 20°W bildet das Explora Escarpment einen stufenartigen Anstieg von mehr als 1 km. Eine Kette von drei Tiefseekuppen, die Polarstern Bank, wurde auf dem Kontinentalanstieg entdeckt.

Glaciomarine Sedimentation Die oberste Sequenz des Crary Fans keilt hangabwärts aus und besteht aus stark geneigten, progradierenden Reflektoren. Auf dem Kontinentalhang zeigen diese Reflektoren einen Downlap auf die liegende Sequenz des Channel/Levee Komplexes. Die Meeresboden–Morphologie des unteren Hang ist durch Channel/Levee Komplexe charakterisiert. Dort treten Channel/Levee Ablagerungen aus der Bedeckung der progradierenden stark geneigten Reflektoren hervor, welche den oberen Hang bedecken.

Die hängende Sequenz entstammt möglicherweise dem mittleren Miozän bis Rezent. Das Alter konnte über eine Korrelation der Sequenz mit ODP Site 693 entwickelt werden. Dieser obere Sedimentkörper wird als Diamiktit Schuttfächer interpretiert. Er wurde von einer Linienquelle vor der Aufsetzlinie einer Eisdecke abgelagert, als diese sich bis zur Schelfkante ausdehnte. Die liegende Sequenz der Channel/Levee Ablagerungen wurde über eine probeweise Korrelation mit ODP Seite 693 datiert, welche ein Alter von frühem Oligozän bis mittlerem Miozän für die Sequenz ergab. Die Kanäle werden als Rinnen für Turbiditströme und, zu einem geringeren Maß, als thermohaline Strömungen interpretiert. Schmelzwasserströme von Naß-Basis Gletschern transportierten Sedimente zu den Kanälen. Levees wurden durch Hochwasserablagerungen gebildet.

Einige der Kanäle nahe der Hangbasis wurden durch transparent/chaotische akustische Sequenzen zum Teil erodiert und verfüllt. Diese Sedimente werden als Schuttflüsse interpretiert. Die tief eingeschnittenen Canyons vor Queen Maud Land wurden durch

Turbiditflüsse entleert. Sie fließen in einer großem Kanal parallel zur Hangbasis zusammen.

Hemipelagische, glaziomarine Sedimente sind auf den Tiefseekuppen abgelagert mit niedrigen Sedimentationsraten von 2.3 m/Ma.

Die Känozoische Sedimentation des Weddell Meeres wird durch glazial/interglaziale Klimaschwankungen kontrolliert. Seit dem mittleren Miozän kam es während glazialer Perioden zu hohem Sedimenteintrag und Wachstum des Diamiktit Schuttfächers. Interglaziale sind durch niedrige Sedimentationsraten und die Bildung von kräftigen, stark erosiven hangabwärts fließenden thermohalinen Bodenströmungen charakterisiert. Schmelzwasserströme einer temperierten Eisdecke speisten den Crary Fan vor dem mittleren Miozän. Wärend jener Periode traten Unterschiede in Sedimentationsraten zwischen Glazialen und Interglazialen auf, die aber weniger ausgeprägt als die jüngeren waren.

Tektonische Strukturen Die Zusammenstellung der geophysikalischen Daten bestätigt das Vorhandensein eines "failed rift" Armes unter dem Filchner Schelf. Das "failed rift" Becken wurde wahrscheinlich während des mittleren-späten Jura in einer breiten "back-arc" Ausdehnungsprovinz gebildet. Mit dem Einsetzen der "seafloor-spreading" im Somali und Mozambique Becken kam es zu einer Änderung im regionalen Spannungsfeld um ca. 170 Ma. Strike-slip Bewegungen begannen zwischen Afrika und Antarktis, wobei das Explora Escarpment in einem Transform/Transpressions Regime gebildet wurde. Neue Daten unterstützen nicht die structurelle Einheit der Andenes und Explora Escarpments als Kontinent-Ozean-Übergang. Die beiden Strukturen haben unterschiedliche Morphologien, ihr Streichen ist um 70 km versetzt und es konnte kein verbindendes Basement Hoch gefunden werden. Bei den Andenes Escarpment handelt es sich wahrscheinlich um ein ozeanisches Plateau, welches auf einer Störungszone in der strike-slip Bewegung zwischen Antarctica und Afrika gebildet wurde. Die Polarstern Bank Tiefseekuppen entstanden durch ein verzögertes vulkanisches Ereignis an einem existierenden Bruch- oder Verwerfungszone größeren Ausmaßes im späten Jura oder in der frühen Kreide. Mikroplatten—Bewegungen seit der frühen Öffnungsphase des Weddell Meeres erscheinen unmöglich auf Grund der bestehenden strukturellen Kontinuität der tektonischen Aufbruchsstrukturen.

1. Introduction

Antarctica, the world's most southerly continent, also happens to be the last region on earth to have changed from theory to fact (Stefansson, 1947). As long ago as the 5th Century B.C., the Greek philosophers "knew" of its existence; but it took another 2200 years for the continent to be discovered.

The philosophers, the scientists of that day, believed the earth was spherical and that the sun was a great deal closer to the equator than we now know it to be. By induction and symmetry, they divided the earth into five great belts or zones: two polar caps extending to about 60° latitude, two mid-latitude zones and, finally, a great-circle belt girdling the equator. Of these, only the two mid-latitude Temperate Zones were inhabitable. The uninhabitable middle belt, the Torrid zone, was so near the sun and so directly beneath it that the rocks glowed red hot, and water boiled. By similar reasoning, the two zones at the poles, the Frozen Zones or Frigid Zones, were so far from the sun, and received rays so slanted and weak, that all was frozen and life there was impossible.

By happy circumstance, Greek civilisation lay within one of the two habitable zones. That flora and fauna also existed in the other Temperate Zone, south of the tropics, was accepted as anything from very probable to certain, as was the certainty of a great frozen land at the southern pole. Their existence, however, could never be fully known, for northern man could not venture south of the equator: first he had to pass through the unbearable Torrid Zone.

This Theory of the Five Zones held sway until the 15th Century, when sailors under the command of Prince Henry of Portugal proved the burning tropics could be crossed. Thereafter, the Great Southland was progressively reduced in size, through a series of reconnaissances that removed Africa, South America and Australia. These acts of geographical surgery culminated in James Cook's circumnavigation of the southern ice cap without sighting land in 1772-1775. When Antarctica, the continent, was finally discovered in 1820, by Edward Bransfield for England, Nathaniel Brown Palmer for America and F.G. von Bellinghausen for Russia, man had confirmed a more than 2200 year old Greek hypothesis - though the actual continent, and the world, for that matter, proved to be somewhat different than the Greeks had envisioned.

By the early 20th century, geographers felt sure about the main outlines of the continent; by the middle of the century, the solid land was beginning to break up into archipelagos, but there was still enough left to form a continent.

Personal and national ambition drove the first explorers to Antarctica. Ever since the mainland was first sighted in 1820, this

remote and mysterious land has fascinated the discoverer's imagination. But over the last few decades the motivation for Antarctic expeditions has fundamentally changed. Scientific co-operation during the International Geophysical Year in 1957/58 and the Antarctic Treaty in 1959 represent milestones of this still ongoing change. The Treaty dedicated the continent for peaceful use, established free exchange of scientific information and banned new territorial claims. It opened a new era for Antarctic research.

Already the first scientific findings showed that the exploration of Antarctica is not *l'art pour l'art* research. A natural or mankind induced change in the Antarctic environment would have drastic effect on the face of the Earth. On the other hand, the scientific results revealed that the continent is an unexplored treasury of natural resources.

If only 10% of the vast Antarctic Ice Sheet were to melt, sea-level would rise 7 m. The polar ice cap reflects as much as 90% of the solar radiation back to space. The loss of energy produces a temperature gradient which drives a global-scale atmospheric and oceanic circulation. A climatic warming could result in destruction of the polar ice sheet. Industrialisation may initiate such a change. Therefore, an understanding of the causes and preconditions of the Antarctic glaciation is of vital importance for being able to avert mankind induced global changes.

Before the development of the Antarctic ice sheet, a temperate to cool subtropical climate dominated on the continent. It provided favourable conditions for natural oil and gas formation in the large sedimentary basins, in the Weddell Sea, in the Ross Sea and in Prydz Bay. Antarctica was the core of the southern supercontinent, of Gondwana, which also encompassed South America, Africa, India and Australia. Hence, the geodynamic history of Antarctica may help to unravel the scenario of the breakup of Gondwana. An understanding of the tectonic history is also a prerequisite for predicting the location and amounts of natural resources.

This thesis applies geophysical investigations to deduce and constrain the glaciomarine sedimentational and early tectonic history of the Weddell Sea.

Marine glacial sediments contain a valuable record of Antarctica's glacial history. They are especially important where other data are non-existent or inaccessible. Onshore glacial sediments are disturbed, eroded and covered by thick ice. They can be accessed at only a few, sparse nunataks. Ice cores give a high resolution glacial history, but only for the last 150 kyears. Over longer time scales, the main source of information for reconstructing the glacial history is the glaciomarine sedimentary

record. Seismic reflection surveys can give a regional overview of the distribution of different sediment types. Seismic data can also provide indications of the depositional process.

The seafloor of the Weddell Sea was formed as Africa and South America drifted away from Antarctica. Possible movements of West Antarctica's microplates also imply generation and subduction of oceanic crust. Hence, the topography and physical properties of the seafloor contain remnants of the early opening history of the Weddell Sea. Geophysical investigations of the continental margin can reveal details of the tectonic development of this area.

In 1990 and 1992, the Alfred Wegener Institute collected about 8000 km of multichannel seismic data in the Weddell Sea Embayment to better understand the tectonic and glaciomarine sedimentational history of the Weddell Sea. Processing and interpretation of that data form the core of this thesis. The majority of the pre-existing seismic profiles collected by earlier expeditions and other institutions were also included in this study. Results of piston coring, drilling, bathymetric and potential field surveys were also considered to gain an integrated and consistent interpretation.

The first part of the thesis gives an overview of the data, and the physiography, glacial history and oceanography of the survey area. It then describes the glaciomarine sedimentational processes, introduces seismic stratigraphic models of the Antarctic continental margin and summarises previous geologic investigations in the study area including drilling results.

The second part of the thesis outlines the joint interpretation of the seismic surveys. It introduces a new synthesis of the glaciomarine depositional history of the Weddell Sea, and considers the implications for the glacial development of the investigated continental margin. It also discusses breakup and drifting history of the Weddell Sea. It investigates the major tectonic structures and earlier geodynamic models in light of the new geophysical data. Finally, it proposes a tentative breakup model for the Weddell Sea.

2. Multichannel Seismic Surveys, Bathymetric, Gravity and Magnetic Maps of the Weddell Sea

2.1 Processing and Compilation of the Seismic Data

A harsh climate and unpredictable ice conditions make geophysical surveys in the Weddell Sea technically difficult and put heavy demands on equipment. The first multichannel seismic measurements were carried out by the Norwegian Antarctic Research Expeditions in 1976/1977. Since this reconnaissance, the seismic network has been expanding quickly. During the relatively mild summer months, icebreakers and ice-strengthened research vessels with towed seismic equipment can penetrate the coastal areas of the southeastern Weddell Sea and collect geophysical data. This study analyses the multichannel seismic profiles obtained by three principal investigators: the Federal Institute of Geosciences and Natural Resources (BGR), the Norwegian Antarctic Research Expeditions (NARE) and the Alfred Wegener Institute for Polar and Marine Research (AWI).

Over 25,000 km multichannel seismic lines have been compiled into a joint dataset during this study. This work included the final processing of about 8,000 km data collected by the Alfred Wegener Institute in 1989/90 and 1991/92. The seismic profiles acquired by the Norwegian Antarctic Research Expeditions and by the Federal Institute of Geosciences and Natural Resources of Germany were available as stacked or migrated sections in SEG-Y format. Processed seismic data collected by the Alfred Wegener Institute during the season 1986/87 were stored in DISCO internal format (discussed later). Separate files contained the shotpoint coordinates. The principle acquisition parameters of these profiles are listed in Table 1; more detailed descriptions are given by Hinz & Krause (1982), Haugland et al. (1985), Hinz & Kristoffersen (1987), Miller et al. (1988), Kuvaas & Kristoffersen (1991) and Kaul (1991).

This chapter first details acquisition and processing of the seismic data collected by the Alfred Wegener Institute in 1989/90 and 1991/92, then describes the compilation of the combined dataset. The fundamentals of the standard seismic data processing are not addressed here. A systematic approach to this topic is given by Sheriff & Geldart (1983) and Yilmaz (1987). Technical details of the data acquisition and special problems encountered in ice covered regions are discussed in Jokat et al. (1994).

Year	Institution	Vessel	Seismic Source		Receiver		Coverage	Sampling Rate (ms)	Total Suvey (km)
			Volume (l)	No. of Guns	Streamer (m)	No. of Channels			
1977	**NARE**	**POLARSIRKEL**	**3**	**1**	**800**	**16**	**8**	**4**	**1000**
1978	**BGR**	**S.V. EXPLORA**	**24**	**24**	**2400**	**48**	**24**	**4**	**5854**
1979	**NARE**	**POLARSIRKEL**	**5**	**1**	**900**	**18**	**9**	**4**	**1012**
1981	SAE								750
1982	SAE								820
1983	SAE								700
1983	JNOC	HAKUREI MARU	7	1	600	24	6		1500
1985	**NARE**	**ANDENES**	**13**	**2**	**1200**	**24/28**	**12**	**4**	**2600**
1985	SAE								800
1986	**BGR**	**POLARSTERN**	**25**	**10**	**1500**	**30**	**15**	**4**	**6263**
1987	**AWI**	**POLARSTERN**	**5**	**2**	**600**	**24**	**6**	**2**	**2800**
1989	SAE								1340
1990	**AWI**	**POLARSTERN**	**6**	**3**	**600**	**24**	**6**	**2**	**4100**
1990	BGR	POLARSTERN	25	10	2400	48	24	4	3000
1992	**AWI**	**POLARSTERN**	**24**	**8**	**600/2400**	**96**	**24**	**2**	**3900**
1995	AWI	POLARSTERN	24	8	600/2400	96	24	2	2063
									IN TOTAL 27529 of 38502 used

Data listed in bold were used in this study

NARE: Norwegian Antarctic Research Expedition
BGR: Federal Institute for Geosciences and Natural Resourches
AWI: Alfred Wegener Institute for Polar and Marine Research
SAE: Soviet Antarctic Expedition
JNOC: Japanese National Oil Corporation

Table. 1 Overview of existing multichannel seismic surveys in the Weddell Sea. Datasets used in this study are listed in bold.

Data acquisition

In 1989/90, an airgun array of 3 (2.5, 2.0 and 1.2 l) Prakla Seismos "VLF" airguns was used as seismic source. In 1991/92, the source was an array of 8 (8 x 3 l) Prakla Seismos airguns. The arrays were shot with a pressure of 140 MPa and a time triggering of 10 - 20 sec depending on the profiles.

Two different streamers were used to record the seismic signal. In 1989/90, a Prakla Seismos streamer with an active length of 600 m comprising 96 hydrophone groups (8 hydrophones/group) was used such that the 96 hydrophone groups were clustered into 24 channels. In 1992 each hydrophone group of this streamer was recorded on a separate channel (96 channels). Adding the lead-in section and passive stretch-sections, the total streamer length was 800 m. In 1992, part of the data were acquired with a SYNTRON streamer of 2400 m active length and 96 hydrophone groups (16 hydrophones/group) in a 96 channel configuration. With lead-in and passive stretch sections, the total streamer length was 2480 m. An EG&G GEOMETRICS ES2420 seismograph recorded the seismic data on 6250 bpi 9-track tapes in SEG-D format. The recording time varied between 7-12 sec for different profiles with a sampling rate of 2 msec.

Data processing

For data processing and interpretation DISCO®, FOCUS® (CogniSeis Development), LANDMARK® and ZYCOR® (Landmark Graphics Co.) software packages were used on a CONVEX C3420 vector computer and on SUN Sparc 4 and 20 Workstations.

The main steps of the digital data processing are displayed in Fig. 2.1 and detailed below:

DEMULTIPLEXING (DEMUX) The signals, stored on tape in the order of registration as successive samples of different channels, were reorganised into separate channels. The demultiplexed data were saved on IBM 3480 Tape Cartridges.

GEOMETRY DEFINITION (GEOM. DEF.) The shotpoints were assigned to a one-dimensional line by using the shotpoint coordinates. Equidistant, 25 m, "theoretical" common mid-point (CMP) locations were also defined on the same line. From the shotpoint locations and receiver array configuration, the "real", non-equidistant CMP coordinates were computed, and the corresponding channels were ordered to the nearest, pre-defined CMP.

SORTING (SORT) On input, traces of the same shot follow each-other until the first trace of the next shot arrives. The output traces were

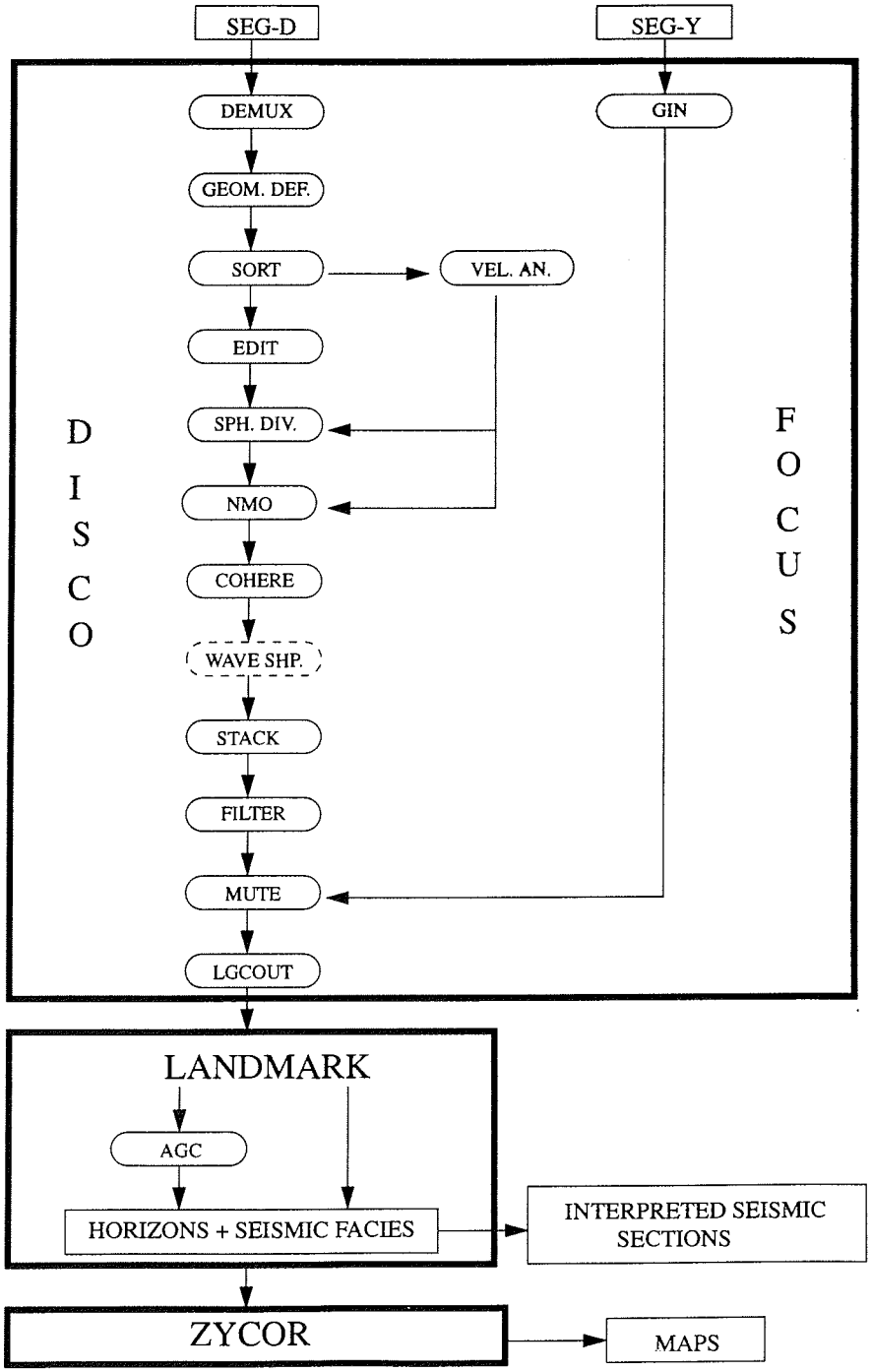

Fig. 2.1 Data processing scheme

sorted into groups of CMP gathers, based on the information stored by the "geometry definition".

EDIT Noisy or dead traces were eliminated.

VELOCITY ANALYSES (VEL. AN) At different source-receiver offsets the travel-time of the reflected signal depends on the velocity-depth function. The velocity analyses used this relation to determine the velocity-depth function. Constant-velocity stack panels, constant-velocity moveout corrections on CMP gathers, semblance contour plots and interactive velocity analyses were applied. Sonobuoy data and published depth-velocity functions (Hinz & Krause, 1982; Haugland et al., 1985; Kaul, 1991; Hübscher, 1994) were also included, since the majority of the lines have been observed with the 800 m streamer in a water depth of 4000 m, which does not give sufficient resolution. Velocities from sonobuoy recordings were computed by conventional velocity analyses similar to those used for CMP gathers (Fig. 2.2). Most of the recordings were very noisy, however, and even the four best sections (9209, 9215, 9220, 9230) gave velocities only for the upper 1-2 sec of sediments (glacial deposits). Interpretable arrivals as first breaks were largely undetected (Fig. 2.2).

SPHERICAL DIVERGENCE (SPH. DIV.) A correction was applied for the decrease of the signal amplitude with time. It eliminates the effect of the signal energy loss caused by spherical propagation of the wavefield.

NORMAL MOVEOUT CORRECTION (NMO) The offset dependence of the reflection travel-times was removed. The corrected reflections were moved to the travel-time of the corresponding zero-offset trace reflection.

COHERENCY FILTER (COHERE) An f-k filter was used to remove non-horizontal coherent noise from the CMP gathers.

WAVE SHAPING (WAVE SHP.) On a few selected sections wave shaping was used to compress the effective source wavelet and increase the temporal resolution by deconvolution (Fig. 2.3). On sections with stable source wavelet, good results were obtained, but the presence of ice often resulted in major waveform variations and thus prevented the successful application of the deconvolution filter.

STACK The corresponding samples of the different traces of a CMP gather were summed to improve the signal to noise ratio.

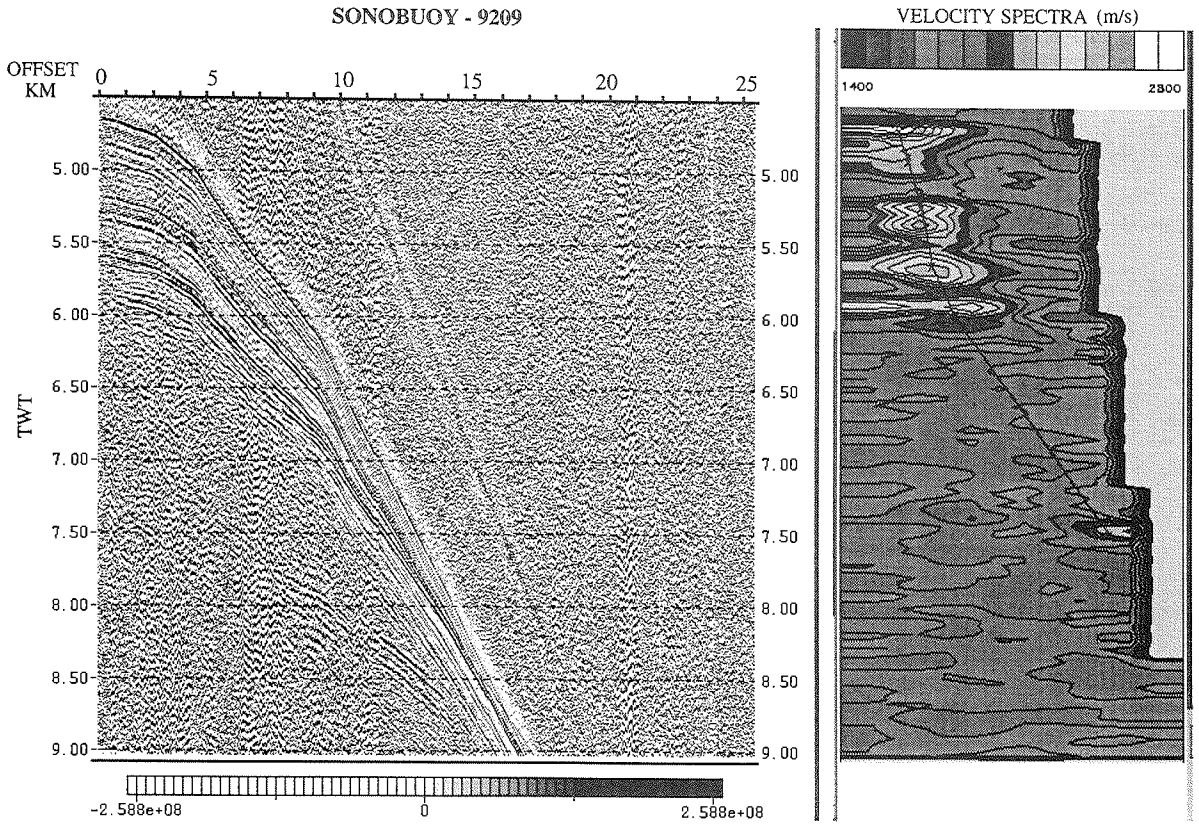

Fig. 2.2 Sonobuoy recording (SB-9209) and its velocity spectra. The sonobuoy was deployed on the seismic reflection profile AWI-92020

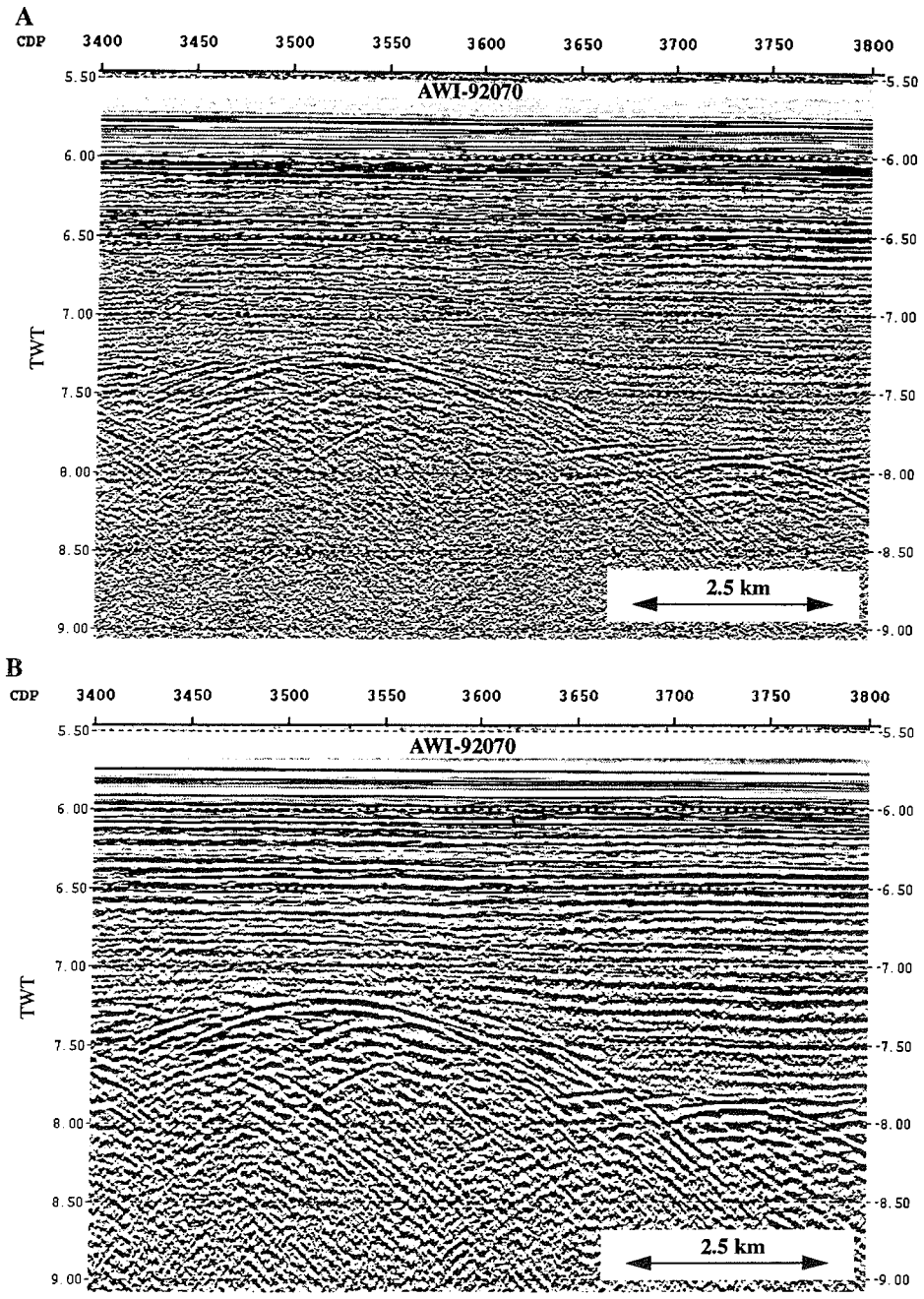

Fig. 2.3 Stacked section A) with no deconvolution, B) with wave shaping

FREQUENCY FILTER (FILTER) A time-variant bandpass filter was used to eliminate or suppress frequencies with a low signal to noise ratio. Filter parameters were derived from frequency analyses and filter panels. A 10-120 Hz bandpass filter was applied to most of the data with a decreasing high-cut frequency with increasing travel-time.

MUTE The signal was "wiped" down to the sea-bottom reflection to improve the aesthetic.

GIN Processed seismic lines of the BGR and NARE were transformed from SEG-Y to DISCO internal format.

LGCOUT The seismic and line-location data were then transformed from DISCO internal format to LANDMARK format. During loading, each 32-bit floating point trace was normalised to the same average amplitude level, and stored as 16-bit integer to save disk space. Each section was saved in two different formats, with and without auto gain control (AGC). The version with AGC is optimal for correlating seismic horizons, the one without for determining amplitude relations and seismic facies (Fig. 2.4).

Despite the different source signals, acquisition parameters, processing and navigation systems, the seismic horizons generally show a good correlation at crosspoints (Fig. 2.5). In some cases, however, the effective seismic signal strongly varies from one section to the other and only the most prominent horizons can be traced with confidence (Fig. 2.6a and 2.7). Already, uniform bandpass filtering makes the different sections similar (Fig. 2.6b), though some mistie still can be observed, partly due to the different wavelets, and partly due to positioning errors. The most prominent differences in data quality are well demonstrated in Fig. 2.6a: the BGR profiles have good penetration at greater depths, but with a rather bad resolution; the AWI lines have high resolution and are excellent for stratigraphic analyses, but the acoustic basement is often hardly detectable. The NARE profiles lie midway between the AWI and BGR profiles both in penetration and resolution. Some, prominent mistie occurs in places, most obviously detectable at the sea bottom reflection. These misties are probably due to major navigation errors. Such sections must be omitted from the interpretation. Other, minor discrepancies were caused by the occasionally missing relation between the shotpoint and CMP numbers: the line locations were defined at shotpoints; the sections were stored as subsequent CMP traces. The shot-CMP relation was generally derived from the information stored in the seismic database by the geometry definition. For foreign lines, this information was not available. In this case, shot-CMP pairs were

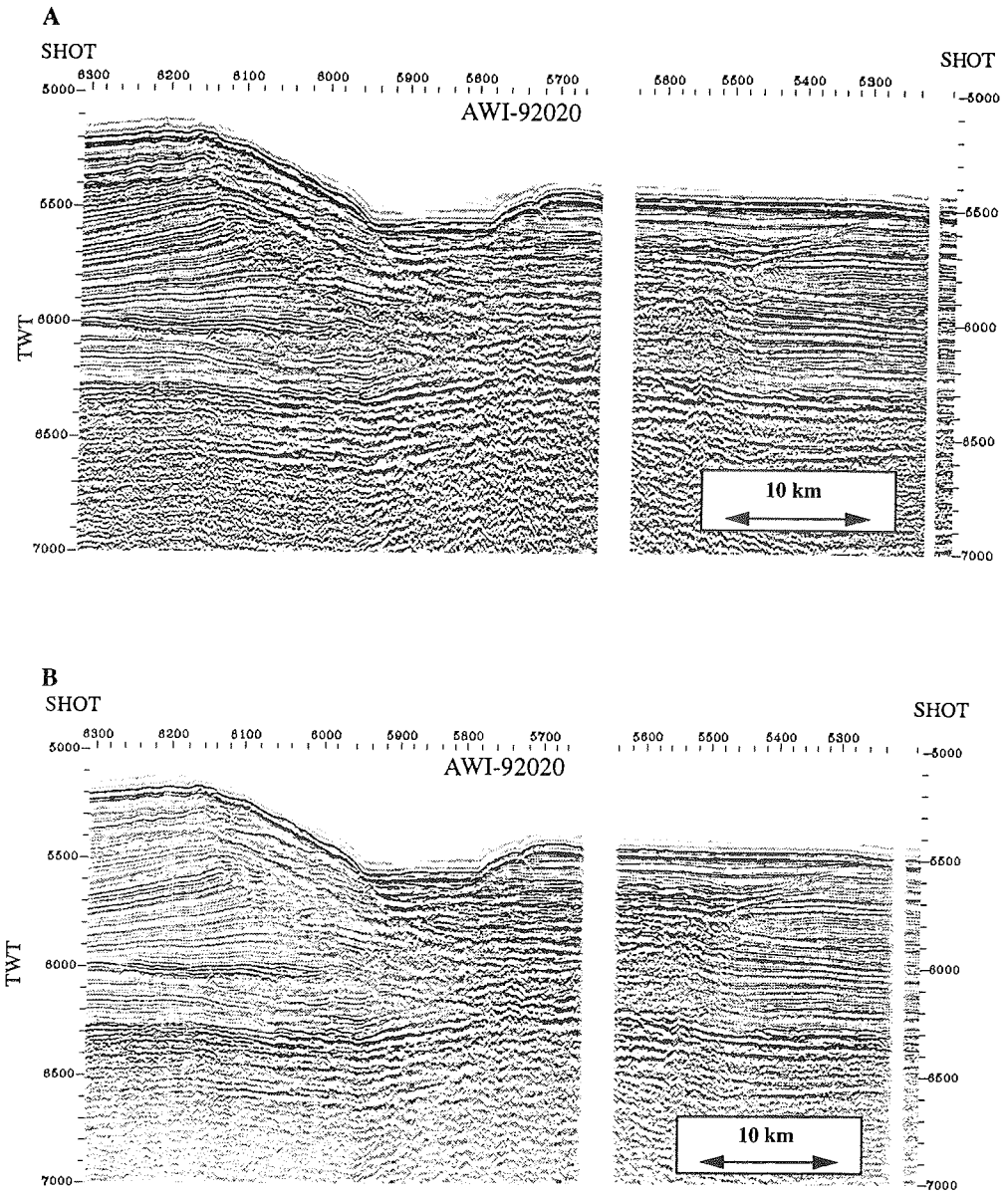

Fig 2.4 Stacked section A) with AGC, B) with correction for the spherical propagation of the acoustic wave

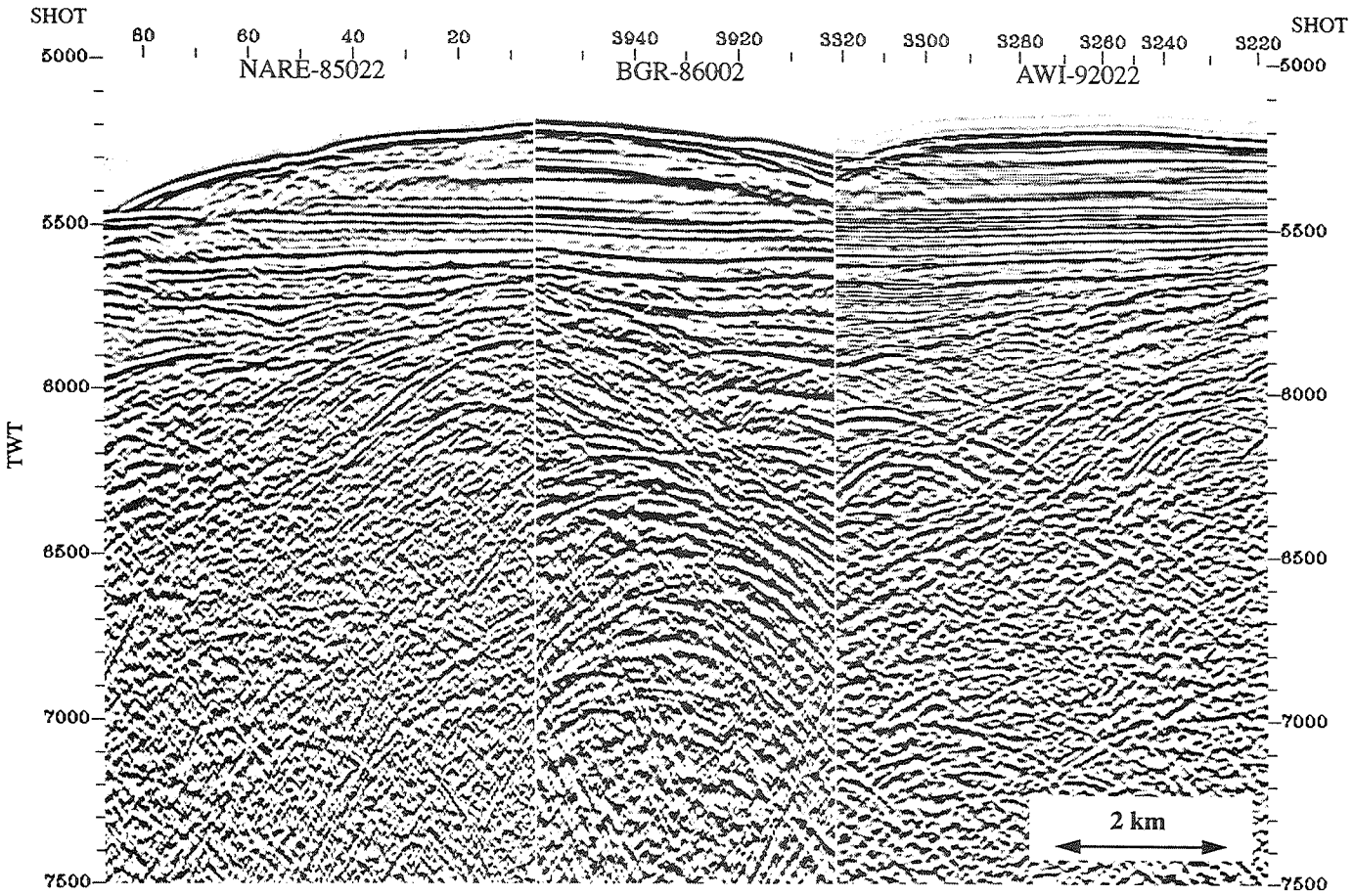

Fig 2.5 Intersecting seismic sections of different projects

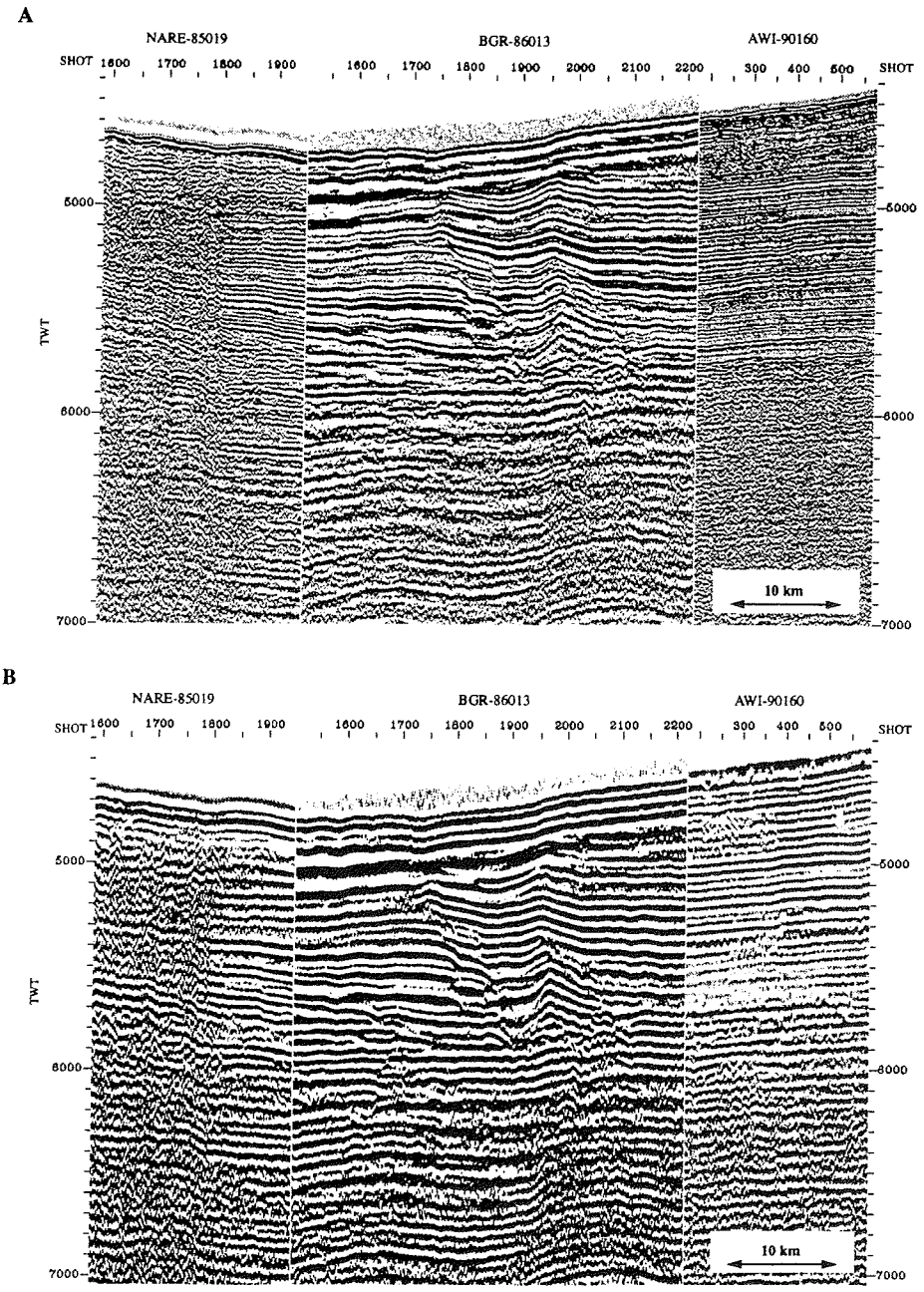

Fig. 2.6 Intersecting seismic sections. A) The different acquisition parameters and processing resulted in a prominent variance of the seismic signal. The amplitude spectra of the displayed sections are shown in Fig. 2.7 B) The same sections after the application of a uniform bandpass filter resulting in a rather similar seismic signal

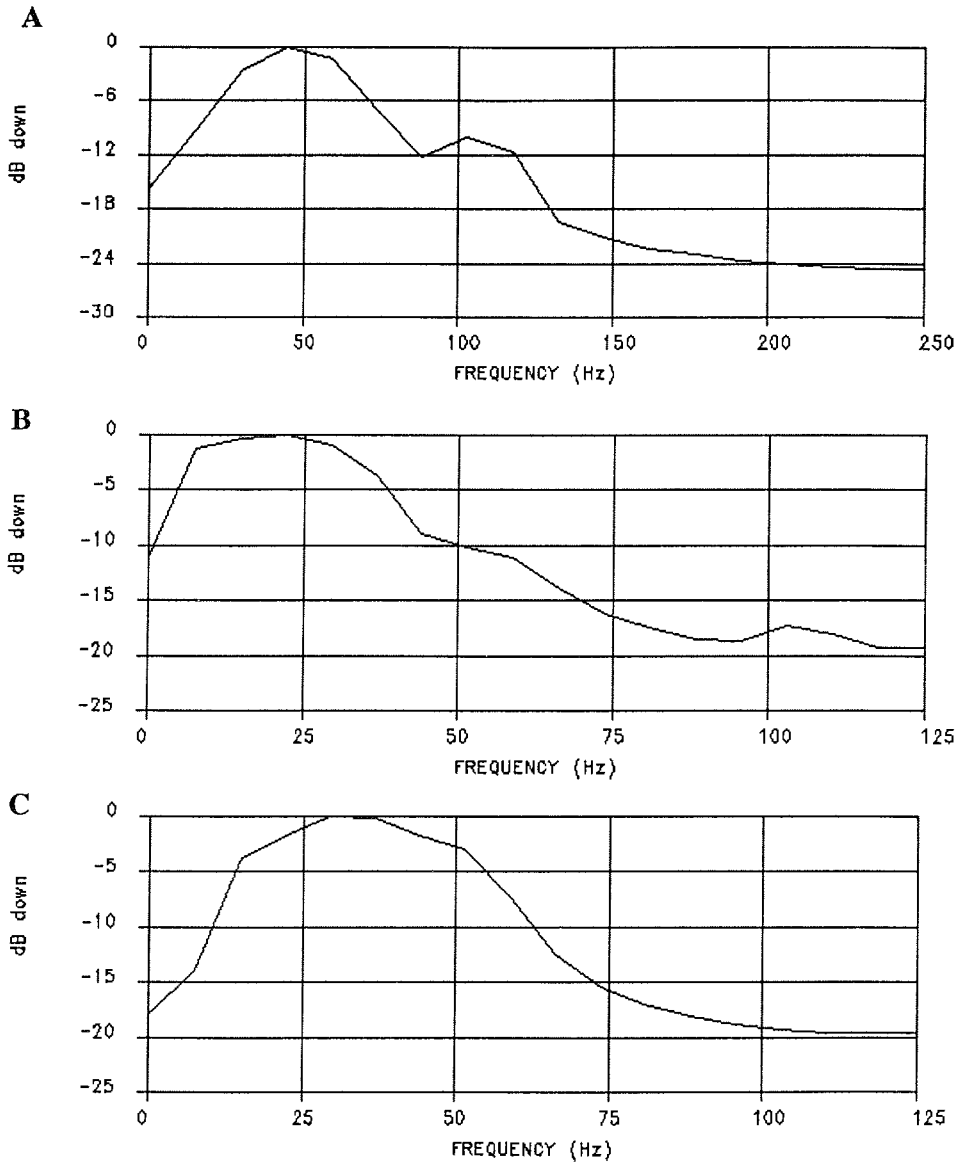

Fig. 2.7 Ampitude spectra of the seismic signals shown in Fig. 2.5A; A) AWI-90160, B) BGR-86013, C) NARE-85019. Note that horizontal scales are different corresponding to the Nyquist frequencies of the data

read from the trace headers, which for our purposes was still a good approximation. Where these header entries did not exist, a linear interpolation was used for the shot-CMP relation: the first CMP was defined at the first shot, the last CMP at the last shot. This interpolation led to minor, but detectable misties at crosspoints, especially at data gaps or along sections with varying shot distances.

LANDMARK An interactive program package was used to interpret the seismic profiles. Seismic horizons were traced party automatically, partly interactively; ties were proved at every possible crosspoints. The interpreted horizons were than digitally exported to the mapping software. The lateral extension of the seismic facies was manually picked. As a whole, the applied interpretation flow is quite similar to paper-and-pencil mapping, but the effectiveness and reliability of the work are multiplied through the system´s quick display, correlation, horizon tracing, zoom options, real amplitude display, control maps etc. Another major advantage of the system is that new lines can be easily added to the existing network. The interpretation, since it is stored digitally, can be quickly revised with new lines, and updated maps can be rapidly prepared.

ZYCOR Interactive mapping software was used for cartographic display of the interpreted horizons and seismic facies. A uniform projection was used for the most important maps to make the displayed geological structures directly comparable. Interpreted seismic horizons were imported from LANDMARK. The sources of other geophysical and cartographic data are discussed in § 2.2.

Predictive deconvolution was tested, but finally omitted from the processing flow. Firstly, because wave shaping can only increase the temporal resolution of the seismic section at the expense of worsening of signal to noise ratio. This was undesirable in this study, where a rather good temporal resolution was occasionally accompanied by a poor signal to noise ratio, especially at greater depths. Secondly, predictive deconvolution was omitted because it can easily cause unpredictable results when applied for signal compression. The method´s mathematical assumptions are mostly, but never perfectly fulfilled. This changes the output wavelet from trace to trace, since a new filter (or new filters, if time variant) are computed for each trace. The artifacts of predictive deconvolution may then later be interpreted in terms of geological changes. In addition, due to the difficult acquisition circumstances, the effective wavelet of the seismic sections discussed here often strongly changes. To distinguish the geological structures from the changes

in signal shape, a limited processing is more appropriate, even if the processed sections are less pleasing in appearance.

Migration was also not included in the applied processing flow. Though proper migration is valuable for interpretation, the lack of sufficient velocity profiles and the vast amount of data made the completion of an acceptable migration for all of the lines a hopeless task. To build a homogeneous database, seismic lines were loaded into the LANDMARK system as stacked sections (with the exception of some NARE lines).

Stacking was tested with different options such as median, coherency weighted and mixed mean-median stack. No improvement of the signal-noise ratio could be observed compared to the conventional mean stack. The results were of rather poorer quality, suggesting a gaussian-like noise distribution for the tested profiles. However, horizontal "mixing" of the adjacent traces was applied to the deep sea sections. The neighbouring two traces of each trace were added to the trace itself, with a weight of 0.5, to improve the signal to noise ratio. The neighbouring traces are quite similar, since the horizontal resolution in the deep sea is about a factor ten lower (210 m at 4 s, TWT) than the defined CMP distance (25 m). More complicated post-stack coherency filters were also tested, but did not significantly improve the data quality compared to the simple trace-mixing.

2.2 Maps and Potential Field Measurements

Gravity, magnetic and bathymetric maps served as auxiliary information for the seismic interpretation. A new bathymetric chart of the Weddell Sea was prepared by Schenke & Hinze (in prep.) and a marine gravity map compiled by Meyer (in press). An aeromagnetic map based on Russian data was available in digital form (Johnson & Smith, 1992). Marine Gravity field derived from Geosat measurements (Sandwell & McAdoo, 1988) provided a northward extension of the shipboard gravity data. An unpublished satellite gravity map was made available by Schöne (personal communication). Microplate boundaries of West Antarctica were provided by Lawver (personal communication). Coastlines and bathymetric contours (2000 m, 3000 m) used in Gondwana reconstructions were taken from the GEBCO CD-ROM (Canadian Hydrographyc Service, 1982).

3. Physiography

The southeastern Weddell Sea is bordered on the east by the East Antarctic margin and on the south by the broad Filchner-Ronne Ice Shelf (Fig. 3.1). The continental shelf of this area has an average depth of 400-500 m and dips landward. The inner shelf is covered by the East Antarctic Ice Sheet and by the Filchner-Ronne Ice Shelf.

The upper continental slope is generally steep and smooth. It is only in some places incised by v-shaped *canyons* (Fig. 3.2). The lower continental slope is more gently dipping, but has a varied topography. It is dominated by u-shaped *channels* bounded by asymmetric ridges, called *levees*. The channels and the associated levees form *channel/levee systems*. Individual channel/levee systems are stacked onto each other building *channel/levee complexes*. Downslope, the channel/levee complexes turn gradually eastward (Fig. 3.3). Levees can rise more than 1 km above the

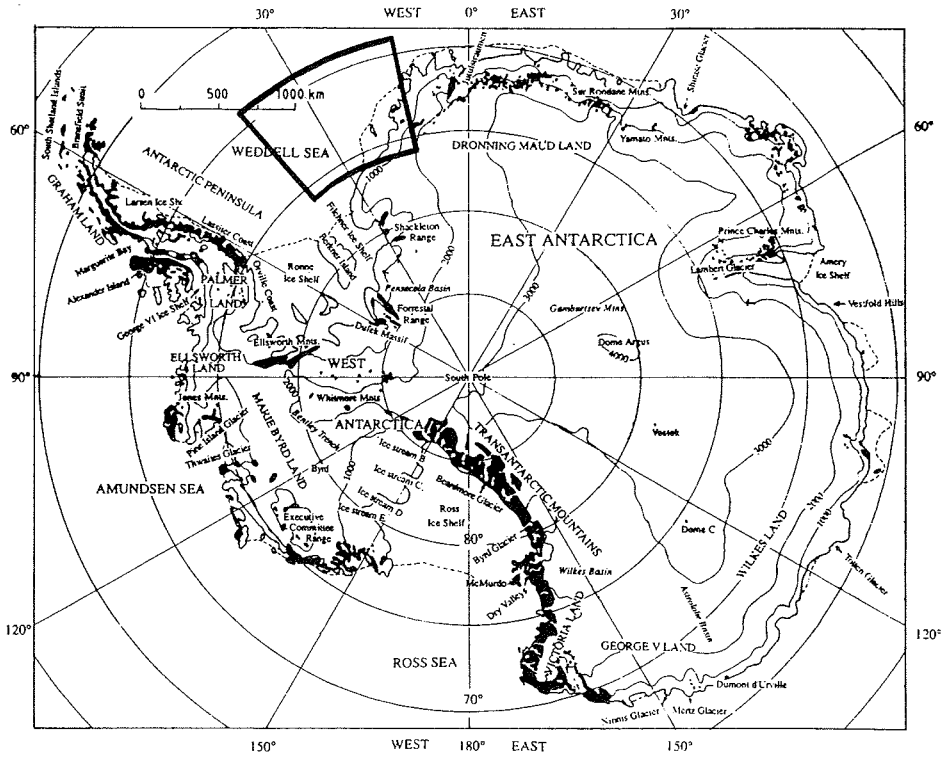

Fig. 3.1 Index map of Antarctica (from Huybrechts, 1992) showing the study area and the main geographic features. Black regions denote rock outcrops. Dashed lines show ice shelf edges.

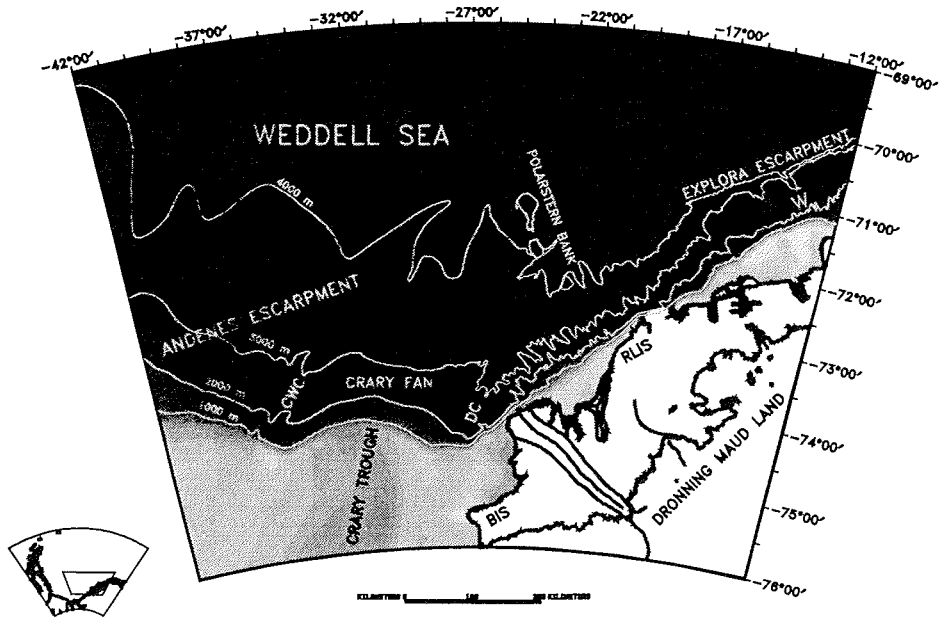

Fig. 3.2 Bathymetric map of the survey area (Schenke et al., in prep.) sowing the key morphologic features. Cold Water Channel, CWC; Deutschland Channel, DC; Wegener Canyon, W; Brunt Ice Shelf, BIS; Riiser-Larsen Ice Shelf (RLIS). Map location is indicated in Fig. 3.1.

seafloor and are up to 100 km wide. Many of the channels on the lower slope terminate against a smooth upper slope without any continuation or sign of large scale mass movement above the channel. The continental rise descends to approximately 4000 m onto the Weddell Sea abyssal plain.

The topography of the Filchner Shelf is dominated by the Crary (or Filchner) Trough (Fig. 3.2), a landward dipping, bathymetric depression with a maximum observed axial depth of 1140 m near the ice shelf (Haugland et al., 1985) and a sill depth of 630 m at the shelf edge (Fig. 3.3). The trough extends southward beneath the ice shelf for more than 600 km (Vaughan et al., 1994). The continental margin in front of the Crary Trough is characterised by oceanward-convex bathymetric contours and by an upper continental slope that is more gently dipping than in adjacent areas. The average dip at 1-2 km depth in front of the Crary Trough is about 1.5°. The upper continental slope in front of the trough has but two major bounding canyons/channels (Fig. 3.2): the Deutschland Canyon/Channel (DC) to the east and the Cold Water Channel (CWC)

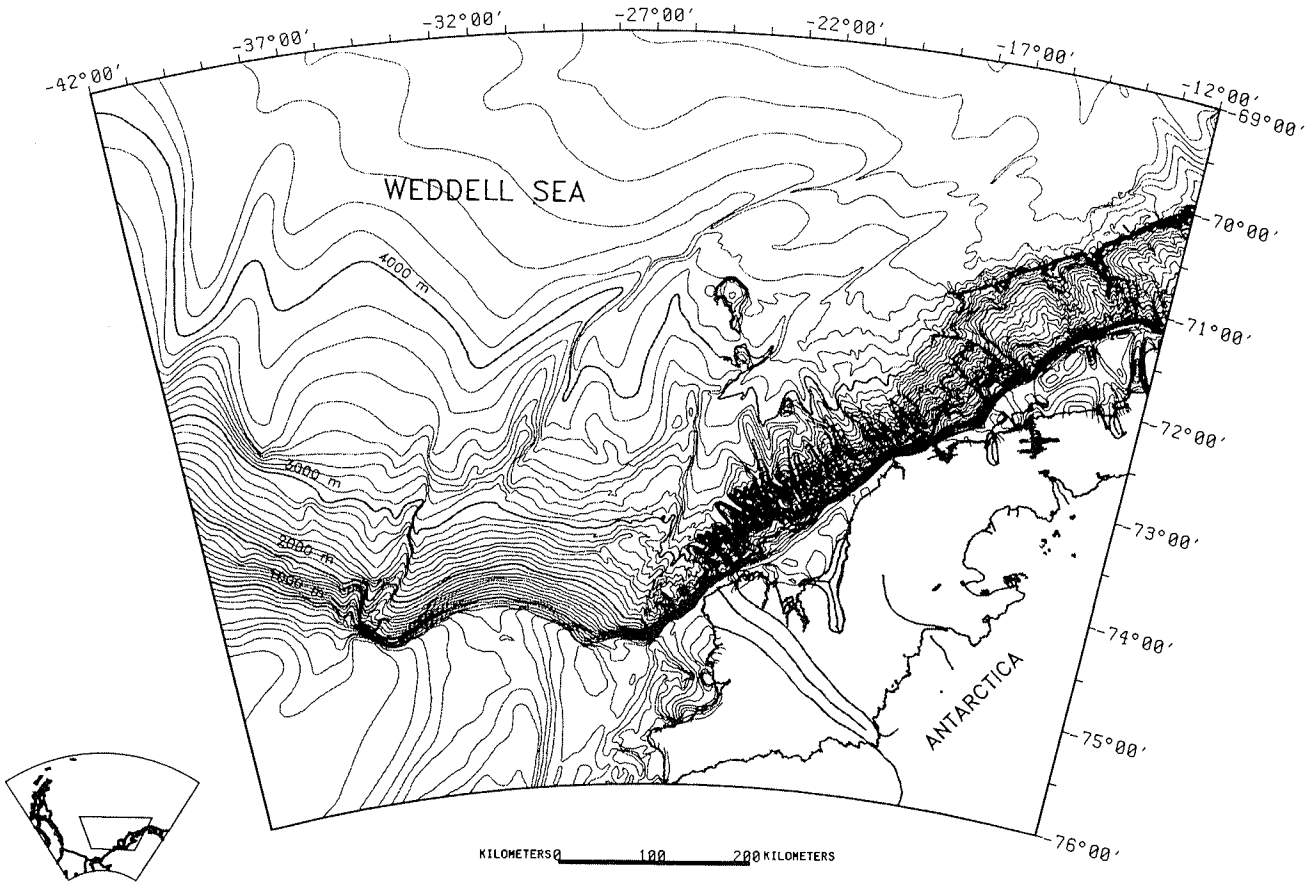

Fig. 3.3 The survey area bathymetry (Schenke et al., in prep.)

to the west. Numerous large channels rise, however, in 3000 m water depth in this area. The channels can be followed downslope over several hundred kilometres before they disappear. Between 26°W and 36°W, these changes in the sea-floor topography, i.e. the bathymetric bulge, the channel/levee systems and the gently dipping upper slope outline the Crary Trough Mouth Fan (CF).

To the east of the Crary Fan, the upper slope is very steep, about 15°, but shows a smooth topography. The lower slope has a normal dip of 1.5° and a large number of canyons and channels. The gentle dip and the channels are below 1500-2000 m, in relatively shallow depth compared to those in front of the Crary Trough below 3000 m water depth.

East of 20°W, the Weddell Sea margin has a two-step morphology, an overdeepened continental shelf, a very steep and narrow upper continental slope, and a gently dipping (1.5°) mid-slope bench (Fig 3.3). The bench is about 80 km wide and stretches from 1700 m to 3100 m depth. It descends to the continental rise in a steep escarpment having a maximum inclination of 30°. This *Explora Escarpment* (Fig. 3.2; Hinz & Krause, 1982) forms a cliff-like wall which descends more than 1300 m to the abyssal plain (Fütterer et al., 1990). The wall of the escarpment has a linear SW-NE trend. Towards the west, the escarpment becomes more subdued; and west of 20°W, it disappears as a topographic feature.

The escarpment is cut by several submarine canyons, the biggest of which is the *Wegener Canyon* (W). The Wegener Canyon system (Fig. 3.2) deeply incises the mid-slope bench and shows a rather linear trend towards the southeast approximately perpendicular to the strike of the Explora Escarpment. At the seaward edge of the mid-slope bench, the canyon walls are at least 1000 m high and incline at an angle of 10°-15° (Fütterer et al., 1990). Upslope of the center of the mid-slope bench, the Wegener Canyon branches into several morphologically less prominent tributaries and loses its deeply incised, steep-walled character.

On the continental rise, a chain of three seamounts, the *Polarstern Bank* (Fig. 3.2), constitute a NNE-SSW trending structure. The seamounts appear as isolated, 500 m highs on the bathymetric map. The northernmost has a slightly elongated shape and is about 30 km wide and 50 km long; the other two are smaller, more circular and have diameters of 10 km.

A 15-30 km wide basement ridge, the *Andenes Escarpment* continues along the strike of the Explora Escarpment towards the southwest (Kristoffersen & Haugland, 1986). The escarpment has a basement relief of 600 m, but does not show up in the sea bottom topography as it is buried by sediments (Fig. 3.2).

4. Glacial Sedimentation In the Weddell Sea, Overview

4.1 The Antarctic Ice Sheet and Its Glacial History

Ice covers 98% of the Antarctic continent to an average thickness of 2200 m (Huybrechts, 1992). Its total volume of 30 million km^3 (Drewry, 1983) represents more than 70% of the Earth's fresh water, and if melted, it would raise sea level by about 66 m (Huybrechts, 1992). Clearly, the Antarctic Ice Sheet is the salient feature of the continent and has a major effect on the climate of the Earth.

Most of the Antarctic ice is discharged into the sea as ice shelves, floating glacier tongues or tidewater glaciers. At the *grounding line*, the ice sheet separates from the bed and becomes a *floating ice shelf*. Within the grounded ice sheet, quickly flowing *ice streams* surrounded by relatively stagnant ice, *ice walls*, transport much of the inland ice to the *ice shelves* and rock-lined *outlet (or valley) glaciers*. Floating ice slabs can exist only in sheltered bays that protect the floating ice from currents, tides, waves and wind (Powell, 1984). They are always of cold ice, because ice at the pressure melting point has a lower tensile strength which allows easier fracture propagation (Powell, 1984). The formation of ice shelves requires high grounded-ice discharge rates. Rapid calving prevents the existence of floating ice shelves: such ice sheets terminate in the sea in cliff-like walls, called *tidewater front*, where the grounding line coincides with the calving zone (Powell, 1984).

Typical flow velocities for ice streams and glaciers are 500-1000 m/years. Typical ice shelves are over 1000 m thick at their inland margin and taper off to 250 m at the ice shelf front.

During the austral winter, the sea almost completely freezes around Antarctica and forms an ice pack which extends to approximately 60°N with the exception of a few polynias of open water. Sea ice covers 0-50% of the study area during the austral summer and well over 80% during the winter. (Sea Ice Climatic Atlas, 1985).

The coastline of the study area can be divided into three sections from a glaciological point of view. In the South, lies the outlet of the Filchner Ice Shelf. Further to the NE, offshore of Coats Land, several glaciers enter the sea. Along most of the coast landward of the seismic network, stand the Brunt and Riiser-Larsen ice shelves.

The huge drainage area and the relatively narrow outlet of the Filchner Ice Shelf (Fig. 4.1.1), compared to the smaller drainage area of the rest of the Eastern Weddell Sea coast is one of the main factors causing morphologic differences of the continental margin. In glacial times the Filchner Ice Stream carved out the deep trough beneath it, the Crary Trough, and fed the continental slope with sediments.

A major morphological difference exists between the East and West Antarctic Ice Sheets. The West Antarctic Ice Sheet (WAIS) is marine based: it largely rests on bedrock lying below sea level (Drewry, 1983). If the ice sheet was removed, West Antarctica would isostaticly rebound and become a few islands separated by deep (>1000 m) trenches. The East Antarctic Ice Sheet (EAIS) is a continental ice sheet: were the ice removed, East Antarctica, practically all its bedrock, would rise above sea level (Huybrechts, 1992).

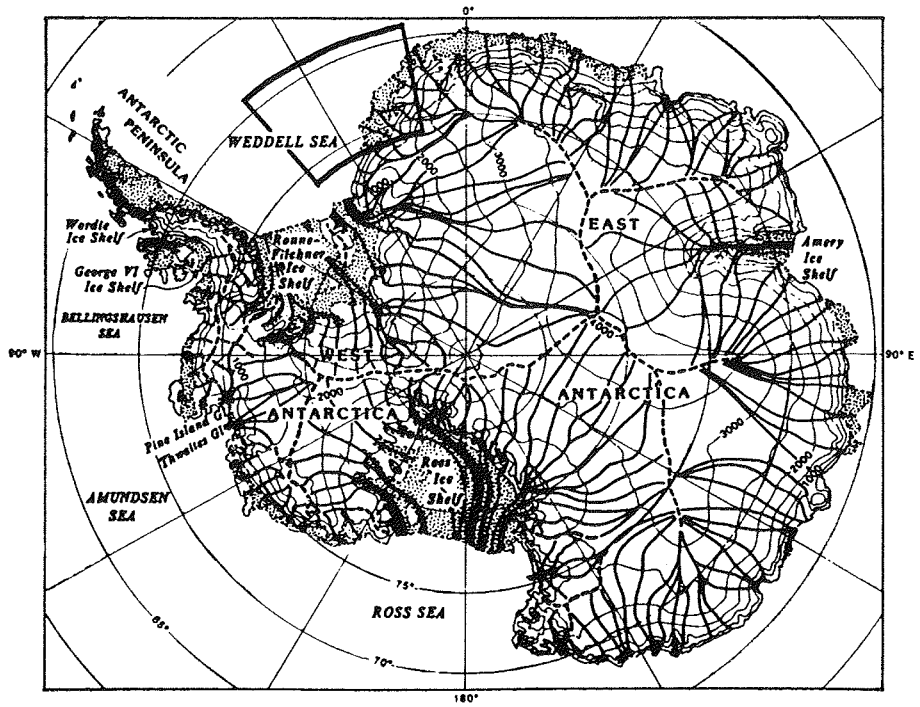

Fig. 4.1.1 Major ice flowlines and surface topography of Antarctica (from Drewry, 1983). Ice divides are shown by dashed lines. Ice shelves are stippled. Survey area is also indicated.

The EAIS is a vast, relatively flat dome with a maximum elevation of just over 4000 m. The surface configuration of the WAIS is more complicated consisting of several domes resting on islands and a number of seabed-based ice shelves filling the trenches. The WAIS has a maximum altitude of 2400 m. The marine nature of the WAIS makes it rather sensitive to sea level changes and climatic variations. The continental nature of the EAIS makes it relatively stabile (Huybrechts, 1992).

To understand the glacial development of Antarctica it is important to know how the ice sheet responds to different environmental changes. The glaciological modelling results of Huybrechts (1992) elucidate the fundamental components and effects of an environmental change:

At present, the mean annual surface temperature is about -15°C along the Antarctic coast and gradually falls to below -60°C over the East Antarctic Plateau. Due to these low temperatures, almost everywhere over the continent, surface melting and run off is virtually absent and the surface mass balance is positive. Presently ice ablates from Antarctica through iceberg calving and through basal melting below ice shelves. An increase of the mean annual temperature has two effects on the mass balance. It increases the precipitation rate, and thus the ice accumulation. But at the same time, it also increases the ablation rate, thus the ice discharge, through higher surface melting. The net effect of 5°C or less temperature rise is a moderate growth of Antarctica's ice volume (Fig. 4.1.2). A 10°C and 15°C temperature increase would result in a 10% or 50% shrinkage of the ice volume, respectively. A temperature rise of 20°C would remove practically the whole Antarctic Ice Sheet with the exception of a few mountain glaciers. Region by region, a 5°C temperature rise would result in an overall ice growth, but a 9-10°C temperature change would mainly affect the WAIS. A 9°C increase would separate the Peninsula Ice Cap from the rest of the WAIS creating an open seaway between Palmer Land and Ellsworth Land. (Fig 4.1.2). A 10°C temperature increase, the first threshold predicted by the model, would yield a total destruction of the marine portion of the WAIS. A 19-20°C temperature rise would cross the next threshold, now associated with the EAIS. This change would disintegrate the previously continuous EAIS into several ice domes situated on top of mountains.

Besides temperature, another crucial environmental factor in determining the glacial extent is the sea level change. For a sea level fall of 130 m, even assuming constant climatic conditions, the model predicts a vast ice sheet that would advance to the shelf edge of the Antarctic continent. Since the growth and the decay of

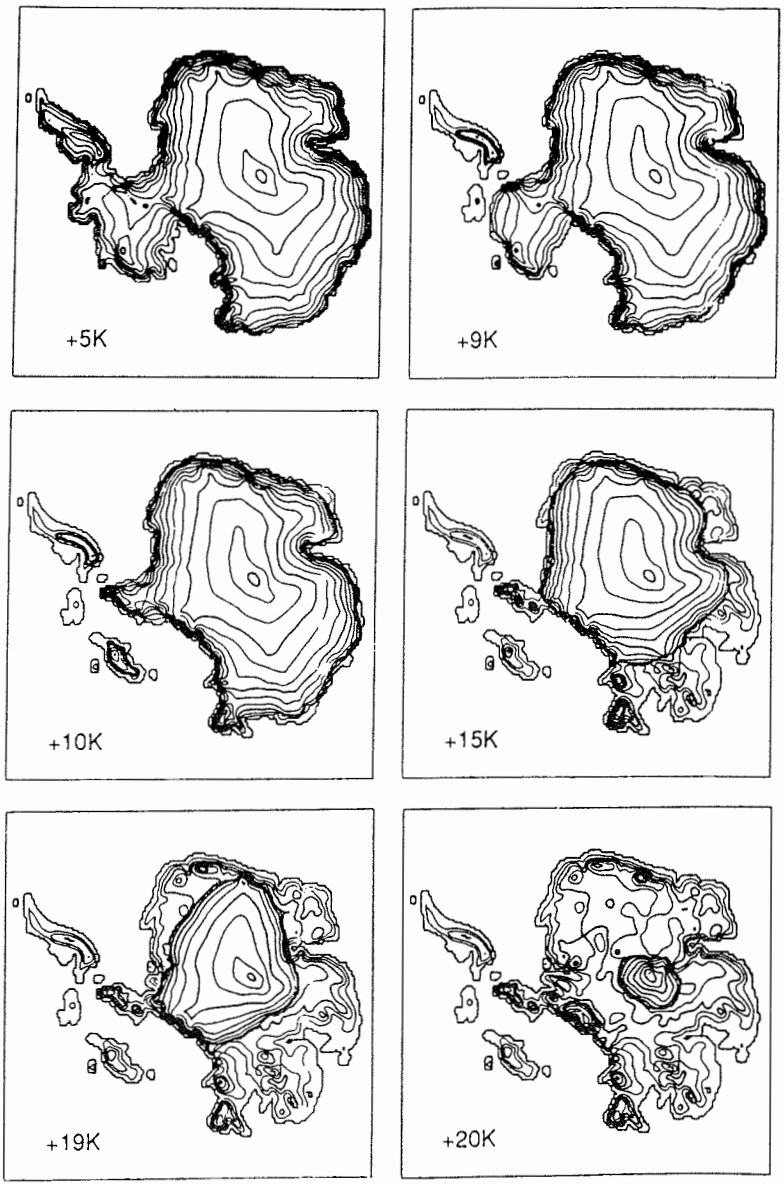

Fig 4.1.2 Steady state ice sheet geometries for temperature perturbations above present level as indicated. Isolines are for surface elevation. Contour interval is 333 m. From Huybrecths (1993).

Northern ice sheets can affect sea level, sea level change may be responsible for the observed coupling of the Northern and Southern cryospheres (Ehrmann, 1993).

The erosion potential for wet-based glaciers, whose bases are at the pressure melting point, is significantly higher than that of the cold based glaciers. Climatic amelioration is often considered to cause large scale basal melting of the Antarctic glaciers and thus high erosion rates. The implication of modelling studies for EAIS, however, show that this instability mechanism evoking widespread change in basal melting is unlikely to have played a major role in the ice sheet's history (Huybrechts, 1992).

Typical time scales for ice sheet build-up are on the order of a few tens of thousands of years (20-40 kyear), and for ice sheet decay 5000-10000 years, that is significantly shorter. Compared to this, the isostatic rebound with a time constant of 3000 years is a relatively quick process (Huybrechts, 1992). The rigidity of lithosphere would result in deviations from the local isostatic equilibrium on the order of 50 m (or 155 m after Cooper et al., 1991) in steady state ice sheet model.

The cryospheric, paleoceonographic and paleoclimatic development of Antarctica are basic components of an understanding of the continent´s geologic and tectonic history. Despite increased interest and strenuous effort, however, our present knowledge of Antarctica´s glacial history suffers severe inconsistencies. On land, the thick ice cover allows us to examine the geologic record of Antarctica at only a few sparsely spaced outcrops and nunataks. Ice cores taken from the ice sheet give a high resolution record of the last glacial/interglacial cycles covering some 150 kyears. Over longer time scales, the marine geological record provide a wide range of parameters that reveal details of the cryospheric development: stable oxygen isotopes of benthic and planctonic foraminifera, lithofacies, clay mineralogy, ice-rafted debris, microfossil assemblages and seismic stratigraphy.

The main stages of the Antarctica´s glacial history, from the synthesis of Ciesielski (1983), Kennett & Barker (1990), Grobe & Mackensen (1992) and Ehrmann (1993), can be summarised as follows.

Most of the sedimentological and isotopic data argue against glacial conditions at sea level during Cretaceous times. Valley glaciers could have existed, however, descending to 1000 m above sea level. At about 60 Ma, a distinct warming began and continued through the rest of the Paleocene and Early Eocene. Surface water temperatures on the Maud Rise and Kerguelen Plateau rose up to 17-18°C. About 52 Ma, close to the Early/Middle Eocene boundary, a long term cooling trend began. At 45.5 Ma, we find the first

indications of glacier ice reaching the coast, even though the climate was still temperate and humid and most of Antarctica certainly remained ice free. At 35.9 Ma, in Earliest Oligocene, numerous sediment parameters and stable oxygen isotope values reflect an intense growth in ice volume: the development of a continental East Antarctic Ice Sheet. On West Antarctica, only the highest regions are assumed to have been covered by ice. The ice sheet was subject to major fluctuations: between 30 and 25 Ma, the grounding line advanced five or six times across the Ross Sea Shelf, and between advances it retreated to the inner shelf. The ice did not have the polar character it has today, but was temperate and wet-based. The long term Cenozoic cooling trend and build-up of Antarctic ice continued throughout the Miocene. Cooling and significant growth of Antarctic ice volume occurred during the Middle Miocene, between 15 Ma and 12 Ma. During the Late Miocene, a further cooling step caused the development of ice shelves on East Antarctica and for the first time, on West Antarctica. The Late Miocene was the time of the maximum ice volume on Antarctica since the onset of the Cenozoic glaciation. A climatic optimum occurred between 4.8 and 4.1 Ma and resulted in the disintegration of the WAIS. From about 2.5 Ma to Recent, a complex interaction of sea-level variations, paleoceanographic and paleoglaciological changes caused intense glacial/interglacial cycles typically lasting about 100 ka.

4.2 Oceanography

The general circulation and structure of the Antarctic waters (Gordon & Goldberg, 1970; Foldvik & Gammelsrod, 1988; Orsi et al., 1993) is dominated by the deep reaching, clockwise Circumpolar Current (CC) which encircles Antarctica. Because of its small amount of attenuation with depth, this current transports a large quantity of water and constitutes the mightiest current in the world's oceans. The Circumpolar Current, or West Wind Drift, is caused by westerly winds driven by the earth's rotation. It could first be formed after continental migration opened the seaways around Antarctica. Opposed to the easterly flow of the Circumpolar Current, in the vicinity of the Antarctic coast, a westward flow is found called the East Wind Drift or Antarctic Coastal Current (ACC). At the western side of the Weddell Sea, the Antarctic Coastal Current is deflected northward. Hence, the overall circulation of the Weddell Sea takes the form of a clockwise gyre, the Weddell Gyre (Fig. 4.2.1). In the Southern Hemisphere, wind induced Ekman transports are directed to the left of the wind stress. The southerly Ekman transports in the Antarctic Coastal current and the northerly Ekman transports in the Circumpolar Current give rise to a divergence of the surface water, the Antarctic Divergence (AD), which facilitates upwelling of deeper waters (Foldvik & Gammelsrod, 1988; Fig. 4.2.2).

A general meridional circulation is superimposed on the ACC and CC. The warm, highly saline, low-oxygenated deep water, the Circumpolar Deep Water (CDW), has a component of flow towards the south and upwells at the Antarctic Divergence (Fig. 4.2.2). Approaching the surface, it is altered into two different water masses by sea-air exchange of heat and water. These two new water masses are cold with high dissolved oxygen content. One of these water masses remains at the surface and is known as Antarctic Surface Water. The other sinks to the seafloor and forms the Antarctic Bottom Water. The Antarctic Surface Water ends relatively abruptly at a latitude between 50°S and 60°S. Here it encounters less dense Subantarctic Surface Water, sinks below this water mass and contributes to the formation of Antarctic Intermediate Water which flows northward (Fig. 4.2.2). The contact between the two surface water masses is known as the Antarctic Convergence or Polar Front. The southward flow of Circumpolar Deep Water is compensated by the northward flow of Antarctic Bottom Water and Antarctic Surface Water. The downward flow of Antarctic Surface Water and Antarctic Bottom Water is compensated by the upwelling of Circumpolar Deep Water at the Antarctic Divergence.

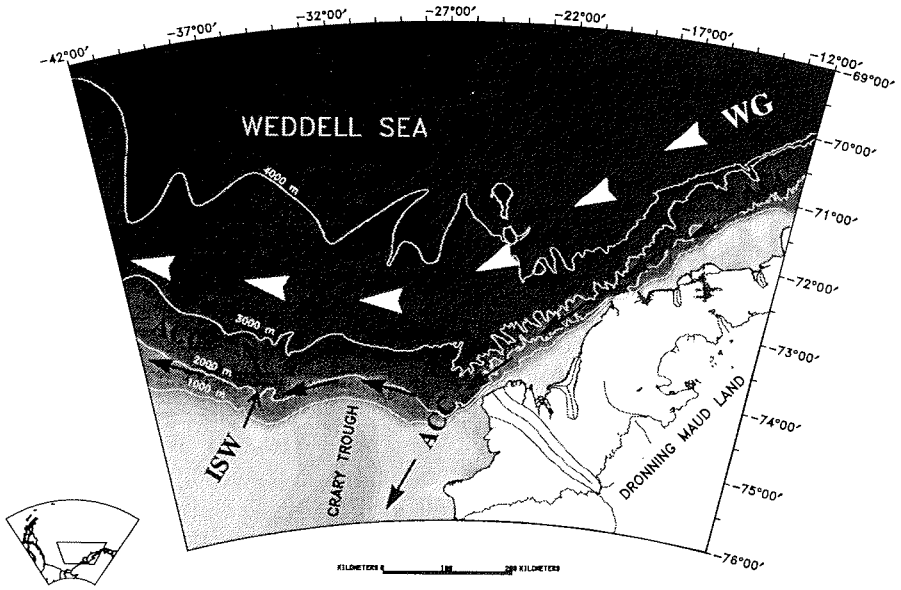

Fig 4.2.1 The principal of water currents in the survey area: the Ice Shelf Water (ISW), the Antarctic Coastal Current (ACC) and the Weddell Gyre (WG).

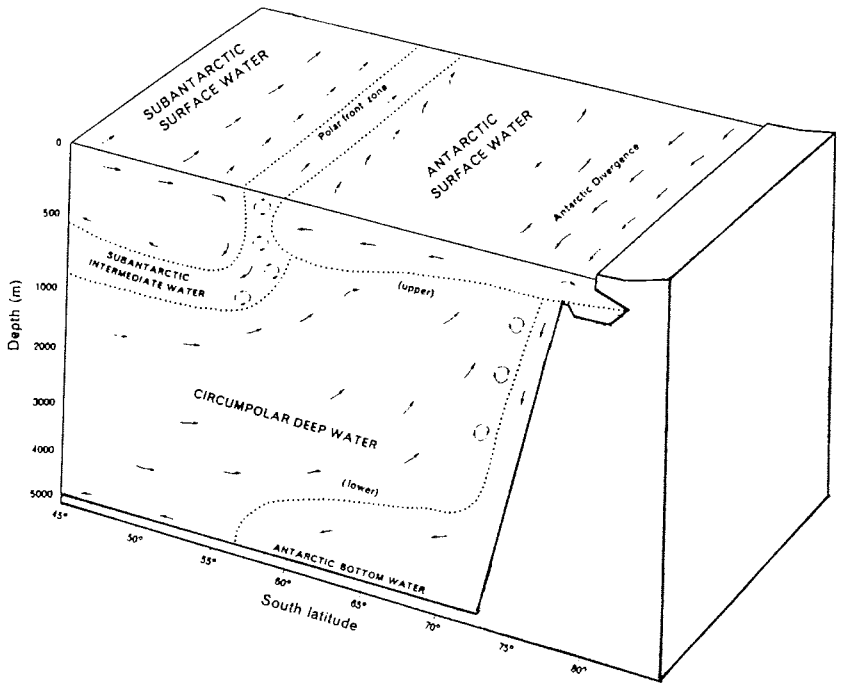

Fig 4.2.2 Schematic representation of water masses in the Antarctic. From Gordon&Goldberg (1970).

The Circumpolar Current has a major effect on the global climate: it isolates Antarctica from the northern warming influences resulting in the development of the polar ice cap. The upwelling at the Antarctic Divergence supplies heat and a vast quantity of nutrients to the surface water producing a rich plankton growth. South of the Circumpolar Current core, the carbonate compensation depth (CCD) is generally shallow, so that calcareous sediments are rarely found on the deep sea floor. The Weddell Sea provides about 80% of bottom water in the Southern Ocean (Foldvik & Gammelsrod, 1988).

The circulation pattern of the study area is dominated by the Antarctic Coastal Current near the coast, by the Weddell Gyre in the abyss and by a strongly erosive thermohaline water mass, the Ice Shelf Water, that flows down the continental slope in front of the Crary Trough (Fig. 4.2.1).

The Antarctic Coastal Current follows the bathymetric contours westward along the shelf break until about 27°W, where it splits. One branch continues along the shelf break while the other flows southwards on the eastern side of the Crary Trough (Foldvik et al., 1985a; Fahrbach et al., 1992.) The near-surface average speed (Fahrbach et al., 1992; Fahrbach et al., 1994) east of 27°W reaches a maximum of 16 cm/s and then quickly drops approaching the interior of the basin, decreasing to less than 1 cm/s about 400 km from the shelf edge (Fig. 4.2.3). Average current velocities also quickly drop with depth and are below 1 cm/s and of varying direction beneath 4000 m depth (Fig 4.2.3). At shallow depths, west of 27°W, in front of the Filchner Shelf, typical mean speeds are 6-7 cm/s (Foldvik et al., 1985a)

While the annual mean velocities within the ACC are small, from 2 to 15 cm/s, the maximum velocity, still measured as an hourly average was 68.8 cm/s (Fahrbach et al., 1992). As a rule of thumb, maximum velocities can be an order of a magnitude larger than the annual means. Comparing these values to Hjulström´s curve (Fig. 4.2.4) shows the significant erosive power of the Antarctic Coastal Current being able to transport clay, silt and sand at times of maximum current velocities. As kathabatic winds and thermohaline flows are the driving forces of the Antarctic Coastal Current and since both result from Antarctica´s cold climate, the existence of a strong ACC depends on the existence of the Antarctic Ice Cap and on the presence of open water in front of the ice shelves. A temperate Antarctic climate or a complete ice pack around Antarctica would dramatically reduce the erosive power of the ACC.

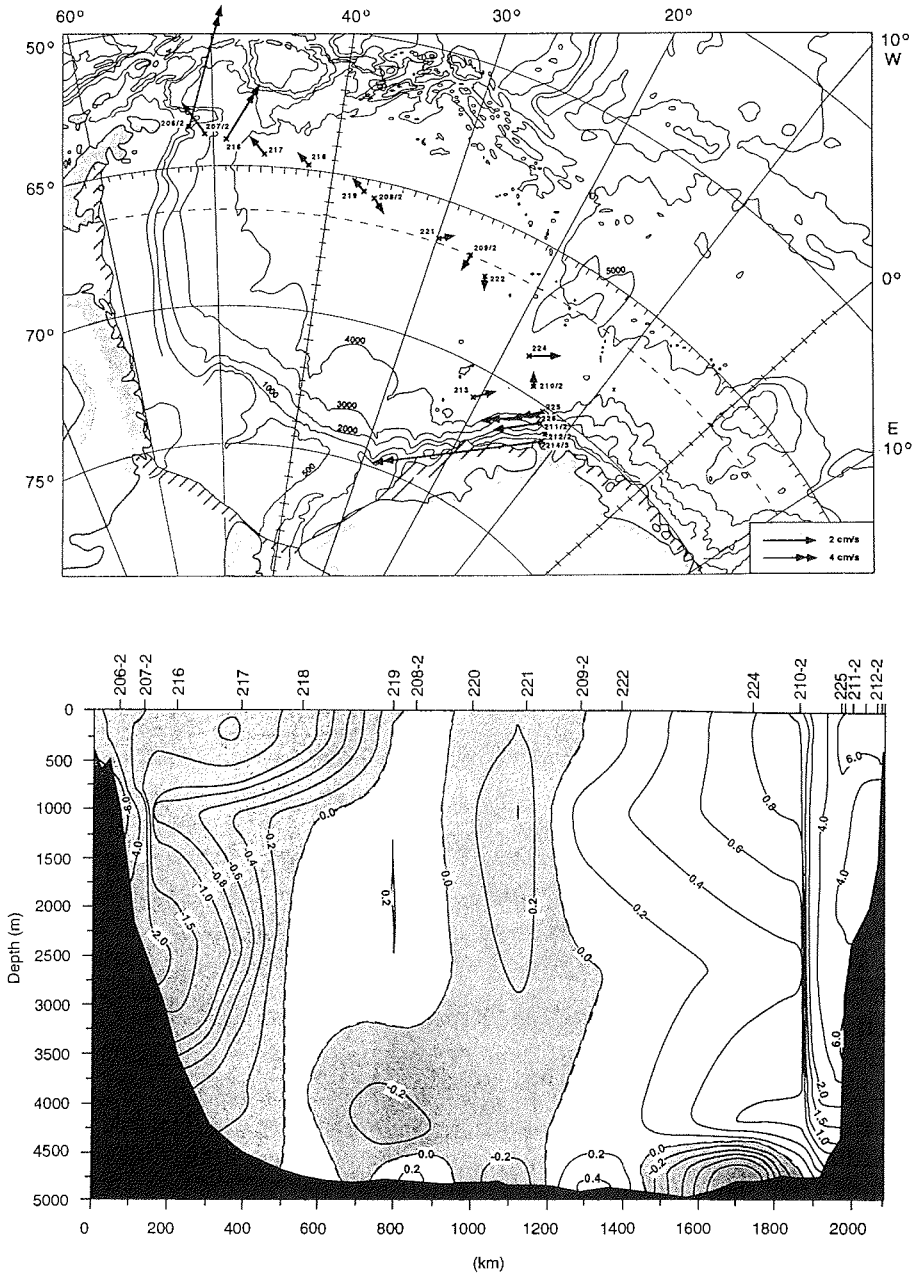

Fig 4.2.3 Mean current vectors about 50 m above sea-bottom (above) and the corresponding cross section showing mean current velocities of the Weddell Gyre (below). From Fahbach et al. (1994).

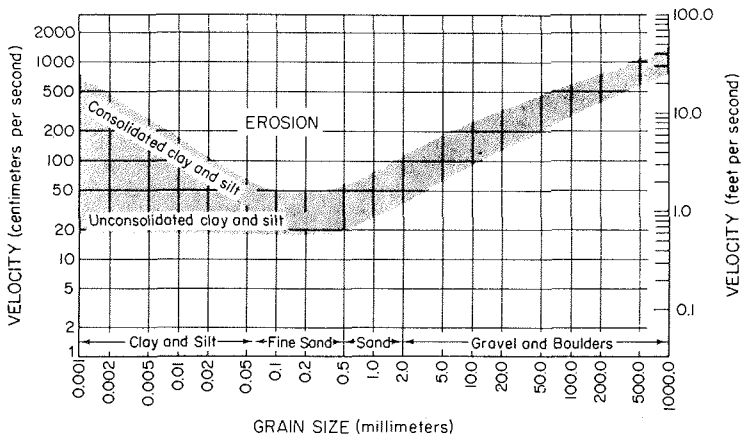

Fig. 4.2.4 Hjulström's diagram, showing critical velocity for movement of quarz grains on a plain bed at a water depth of one meter, as modified by Sundborg (1956). The shaded area indicates the scatter of experimental data.

The circulation of the deep Weddell Sea (Fig. 4.2.1) is dominated by the cyclonic Weddell Gyre. It extends from the Antarctic Peninsula to 20°-30°E and from 55°-60°S to Antarctica (Orsi et al., 1993). The current reaches the bottom, but the mean speed in the abyss is rather weak, about 1 cm/s, below 4000 m (Fig. 4.2.3). Even if its peak velocities are an order of magnitude higher than average values, the Weddell Gyre has little erosive power in deep waters. Nevertheless, the Gyre may influence the sediment transport directions by drifting icebergs at times when sedimentation of Ice Rafted Debris (IRD) dominates.

Two unusual arrows at moorings 213 and 224 indicate bottom currents that flows contrary to the Weddell Gyre (Fig. 4.2.3). The two measurements are from long-term recordings and are mutually consistent, thus they can not be simply explained as measurement error. Their mean velocities are 1.5 cm/s (Fahrbach et al., 1994) and are parallel to the channels found on the sea bottom. Their peak velocity measured as an hourly average was 9 cm/s (Fahrbach, personal communication). Kuhn & Weber (1993) suggested that this or similar thermohaline flows create the channels during glacial times. The origin of this bottom current is unclear. The current may rise in the Filchner Shelf as Ice Shelf Water (ISW) and gradually change its properties as it flows down following the sea bottom morphology (Fahrbach, personal communication). Or it may be a branch of the ACC turned back by topographic obstacles at approximately 27°E (Hoppema, personal communication). Whatever its origin, this current is not strong

enough to erode or transport sediment or to produce current-controlled sedimentation (cf. Fig. 4.2.4). But it can not be excluded that in glacial times strong, erosive thermohaline currents were formed by a different process.

At 36°W, a strong, bottom-trapped current, the Ice Shelf Water crosses the sill of the Filchner Shelf and flows downslope (Foldvik et al. 1985b; Fig. 4.2.1). It can also be observed at 2000 m to 3500 m depth on the slope near 40°W. At the sill of the Filchner Depression the flow is approximately 100 km wide, about 100 m thick and its maximum velocities exceed 100 cm/s without any appreciable seasonal variation (Foldvik & Gammelsrod, 1988). Foldvik et al. (1985b) proposed that the Ice Shelf Water forms as follows. During the winter, very dense water is formed near the barrier of the Filchner-Ronne Ice Shelf due to freezing and cooling of sea water and connective mixing. This process is intensified by offshore winds which carry the ice away. This very dense water flows downwards underneath the ice shelf where it is deflected eastward by the Coriolis force. The flow then is steered by the bathymetric contours around the Berkner Island until it appears, as observed, on the eastern side of the Filchner Depression. Cooling at the underside of the ice shelf is associated with net melting of glacier ice. ISW is therefore colder, less dense and less saline than the shelf water it originated from. Bottom water formation in the Weddell Sea can thus be explained as the result of mixing the downward flowing ISW with the overlying water mass on the continental slope.

The high observed velocity of the ISW shows that this water mass can erode and transport large quantities of sediments and thus plays an important role in the sedimentation of the study area. Kuvaas & Kristoffersen (1991) have attributed the formation of the Cold Water Channel to the erosion caused by the ISW. The formation of the ISW requires the existence of a floating ice shelf. Hence, this process is restricted to interglacial times. It can not be ruled out, however, that during glacial times, high density thermohaline bottom currents were formed by a process similar to formation of the high density shelf water (Fahrbach, personal communication).

In the geologic past the circulation of the Weddell Sea was significantly different. The main factors determining the prevailing oceanic circulation are the position and distribution of land masses and the global climate. Both factors have changed considerably during the Cenozoic with development of paleo-seaways around Antarctica as the result of the Gondwana break-up.

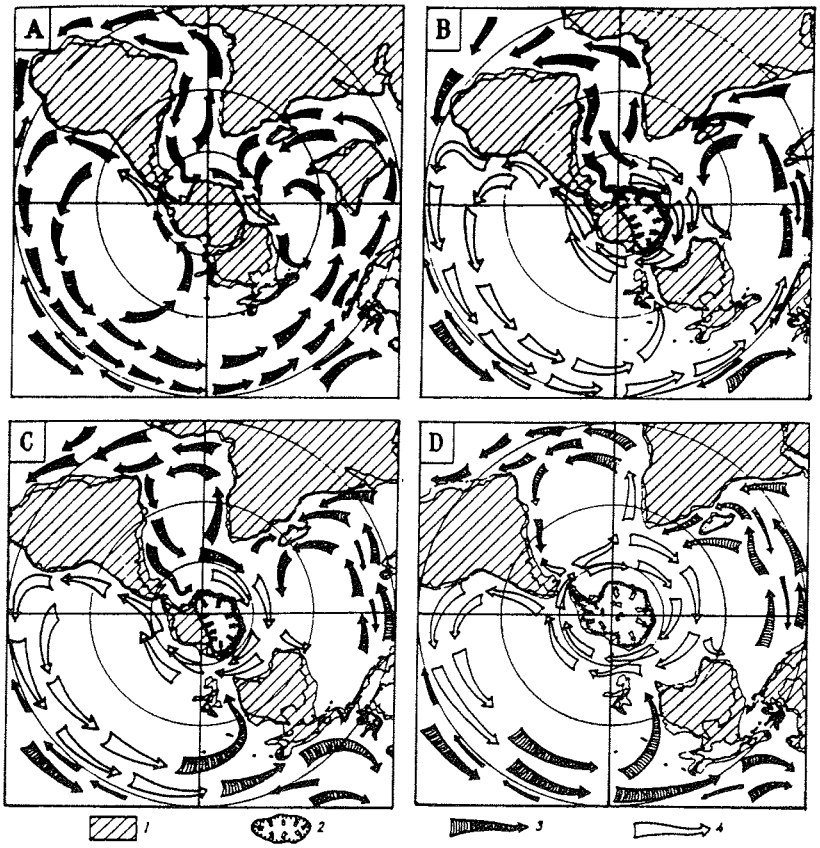

Fig. 4.2.5 Currents in the oceans of the Southern Hemisphere. (A) Paleocene (60 Ma ago); (B) beginning of Oligocene (35 Ma ago); (C) beginning of Miocene (20 Ma ago); (D) currents at present. (1) Continents with epicontinental seas, (2) ice sheets; (3) warm currents; (4) cold currents. From Kvasov&Verbitsky (1979)

In the Paleocene and Eocene, a powerful longitudinal circulation existed (Kvasov & Verbitsky, 1981; Fig. 4.2.5) balancing the surface temperature of the ocean to about 28°C in the tropics and 12°C near the Antarctic shore (Salvin et al., 1975) and causing a temperate Antarctic climate. ODP Leg 113 indicates that at times during the Eocene a deep water was present in the Weddell Sea that was warmer and more saline than surface waters (Kennett & Barker, 1990). This suggests that Antarctica may not have been the primary source of deep waters. In the Paleogene, warm deep waters are inferred to have been produced at middle or low latitudes. At the boundary between the Eocene and Oligocene, a deep strait developed between Antarctica and Australia (Lawrence et al., 1992; Fig. 4.2.5). This strongly affected the oceanic circulation in the Southern Hemisphere. A not closed circum Antarctic current, the South Ring Stream, formed (Kvasov & Verbitsky, 1981) which

encircled almost the whole Antarctic. It was interrupted only by the barrier between the Antarctic Peninsula and South America. With this change, warm low latitude waters had enough time to cool considerably, which is reflected in a general temperature fall of 7°C in Antarctic waters (Salvin et al., 1975). The cooling of the circum-Antarctic water masses resulted in a climatic deterioration that led to the development of the East Antarctic Ice Sheet (Lawver et al., 1992; Kvasov & Verbitsky, 1981). Due to higher annual temperatures than at present, however, the main ice discharge was accomplished not through iceberg calving, but through melting (Ehrmann, 1993). This process may explain the low amount of the Ice Rafted Detritus (IRD) in Oligocene sediments and the formation of extensive submarine fans from meltwater streams. The presence of shallow, partly ice free East Antarctic continental shelf is indicated by the occurrence of benthic diatoms of Oligocene to Early Miocene age at ODP Site 693. At the same time, traces of IRD found in Oligocene sediments suggest cryospheric activity on the continental margin (Kennett & Barker, 1990). The absence of the Circumpolar Current and the Polar Front is indicated by the biogeographic similarity between Maud Rise and Falkland Plateau areas during the Oligocene. But the presence of a temperature gradient between Maud Rise and colder areas south and west of it implies a clockwise circulation in the Weddell Sea (Kennett & Barker, 1990). The Eocene/Oligocene boundary is also associated with formation of a widespread hiatus in the Weddell Sea and in other deep sea basins. This probably reflects the development of the modern upwelling regime in Antarctica that was also typical for the late Neogene, and the formation of more vigorous deep water currents resulting from basal thermohaline circulation (Kennett & Barker, 1990).

Until the Middle/Late Miocene, the Weddell Sea was penetrated by a warm current flowing along the eastern shore of South America (Kvasov & Verbitsky, 1981). Nothofagus forests could grow on the South Shetland Islands. The separation of South America from Antarctic Peninsula began 29 Ma ago, but the passage opened not earlier than 23.5 +/-2.5 Ma ago (Barker & Burell, 1982). At first, however, the passage was narrow and not very deep. According to Kvasov & Verbitsky (1981), it was not until 11-14 Ma ago (or Early Miocene after Barker & Burell, 1982) that the South Ring Stream could overcome this last obstacle, encircled the entire Antarctic continent, formed the Circumpolar Current and the Polar Front (Fig 4.2.5). With that, the water exchange between middle and low latitudes has considerably decreased resulting in a cooling of the circum Antarctic waters and a warming of the low latitude oceans. This climatic cooling initiated ice sheet formation on West Antarctica and a renewed growth of the East Antarctic Ice Sheet

(Kvasov & Verbitsky, 1981). It is reflected in the increase of Ice Rafted Detritus contents of Miocene sediments (Kennett & Barker, 1990).

During the last 12 Ma, the oceanic circulation and climate have constantly been favourable for glaciation in Antarctica. The main factor has probably been the fluctuation of sea-level associated with glaciation in the northern hemisphere which controlled the waxing and waning of the Antarctic Ice Sheet (Kvasov & Verbitsky, 1981).

4.3 Processes of Glaciomarine Sedimentation

Glaciomarine regimes Glaciomarine sedimentation is a complex and diverse process, but its basic characteristics can be described by three main variables. (Powell, 1984). These variables determine the type of the glacial debris and how and where debris is introduced to the ocean. The three main variables are: (1) the type of the glacial ice source (ice sheet or valley glacier); (2) the condition of a grounded glacier (melting/freezing or frozen base and cold or warm internal ice); and (3) the type of glacier front (ice shelf or tidewater). Combinations of these variables define different glaciomarine regimes.

(1) The type of the terrestrial glacier source determines the volume of the supraglacial and high level englacial debris. Valley glaciers receive debris at their surface from rockfall and generally contain significant volumes of englacial debris from side wall and nunatak erosion. Ice sheets contain little or no supraglacial derived debris (other then perhaps aerosol particles) because they override most topography.

(2) The condition of the grounded glacier determines the volume of basal debris transported by ice. Frozen based glaciers cause nearly no erosion and therefore are practically clean based. Alternate areas of basal melting and freezing provide the largest volume of basal debris and are capable of introducing large volumes of sediments into the sea. If the melting area is too large, the basal debris content can be also very low because it is released from ice and transported away by subglacial streams. By and large, temperate mountain glaciers produce large volumes of glaciomarine sediments whereas polar and ice sheet conditions produce smaller volumes (Powell, 1984).

The type of ice-distal sedimentation also depends on the basal conditions: cold-based ice margins are not capable of producing large deep-sea channels, whereas warm-based ice margins generate deep-sea channel-levee systems with coarse-grained channel floors bordered by muddy levees (Kuvaas & Kristoffersen, 1991).

(3) The type of glacier front is the major factor influencing the composition of ice-proximal sediments. Ice shelves deposit sediment at the grounding line. These deposits have a basal debris source, high level englacial debris is deposited at a more distal position. In the corresponding position of a tidewater glacier, debris comprises mixed basal and high level englacial debris (Powell, 1984).

Sediment transport by ice. Glacial sediments destined for deposition in the ocean are incorporated into grounded ice masses at their surface, in their interior, but mainly by entrainment at their beds.

Debris rich basal layers extend from a few centimetres to several tens of meters. Typical values for margins of polar ice sheet appear to place the thickness of the debris layer at 1% of the ice depth. The average concentration of the debris is extremely variable from 0.01% to 70%, but for a polar ice sheet, the value is probably 1%. (Drewry & Cooper, 1981).

Fast flowing ice streams also transport basal debris by dredging of subglacial till. Alley et al. (1987) have suggested that this process alone could advance the grounding line by several kilometres per thousand years. The sediments transported by this process also contribute considerably to the build-up of the diamict apron (discussed later).

Debris can also be transported to the sea after falling or being blown onto the glacier surface, or as englacial debris eroded from side walls or nunataks. This debris is quantitatively not important, however, sediment from this source can be deposited as far as icebergs can reach, because it is carried on the top or within the ice. Such debris can be readily recognised by its well-sorted fine-grained nature (aeolian sand) or angular shape (rock talus).

Sedimentation by ice

- Subglacial zone: Subglacial deposition from a grounded glacier occurs during periods of glacial advance and produces lodgement and melt-out tills (Powell, 1984). These sediments derived from the base of a grounded ice sheet are flat-lying and overcompacted (Cooper et al., 1991) and have high seismic velocities (1.9-2.6 km/s).
- Ice proximal zone: Where the ice sheet flows into the sea, most of the basal debris melts out close to (within a few kilometres of) the grounding line through basal melting (Drewry & Cooper, 1981). If the grounding line is more or less stationary for thousands of years, sediments deposited at the grounding line build-up a *diamict apron* (= till delta; Dimictit is a non-sorted terrigenous sediment containing a wide range of particle sizes, regardless of genesis).

At the grounding line, freezing-on of sea water can prevent sedimentation from the basal debris layer and the build-up of a diamictit apron. Sediments protected from melt-out by this process can reach the edge of the ice-shelf and produce debris laden ice bergs. Freezing-on of sea water seawards of the grounding line is observed beneath the Filchner-Ronne, Ross and Amery Ice Shelves (Ehrmann, 1993). At present, however, in Antarctic seas, icebergs calved from ice shelves are free of basal debris. These icebergs do not play an important role in the deposition in the open ocean,

because basal freezing takes place only after the bulk of the debris has melted out (Drewry & Cooper, 1981).

Sediment in suspension can enter the marine environment directly from supraglacial and subglacial meltwater channels resulting in an extremely high sedimentation rate near the grounding line. Plumes emanating from the ice front deposit hemipelagic mud which is intermixed with graded sandy-to-gravely beds deposited from debris flows and turbidity currents (Syvitski, 1994). Fluvial/plume deposits are more common from melting base glaciers compared to frozen base ones, from warm ice glaciers compared to cold ice ones and from tidewater fronts compared to ice shelves (Powell, 1984). Presently, the temperate tidewater glaciers of SE Alaska produce large amount of meltwater, whereas little meltwater emanates from the floating and polar ice-margins of Antarctica.

- Ice shelf zone: In polar climates under cold based ice regimes the grounding line can deform into an ice shelf or floating glacier tongue. In such conditions, basically no sediment is actively deposited beneath the floating ice shelf (Powell, 1984).
- Ice distal zone: Icebergs can transport sediments to distal areas. These deposits are often preserved during both glacial advances and retreats. Ice shelves and floating glacier tongues bar the movement of ice offshore. The slow seaward progression of ice leads to the early release of basal debris through melting close to the grounding line. Thus, ice shelves do not play an important role in deposition in the open ocean. In contrast, valley glaciers have high sediment content, calve rapidly and produce debris rich icebergs (Ehrmann, 1993). However, debris laden icebergs calved from polar ice shelves can transport sediment over large distances. Icebergs of temperate tidewater regimes melt quickly and deposit the glacial debris near their source (Powell, 1984).

Glacial versus interglacial The position of the grounding line plays an important role in determining the sedimentation in different ice-margin environments (Fig 4.3.1). In glacial periods, when the grounding line is at the continental shelf edge, large volumes of debris may be dumped down the continental slope to create a submarine wedge (rather than fan) at the continental rise out onto the abyssal plain (Powell, 1984). The wedge consists of sediment gravity flow sequences and glaciomarine diamictons. From a melting base glacier, large discharge of glacial rock flour produces high concentrations of suspended sediment later deposited on the continental slope, rise and the abyssal plain. During rapid glacial retreat, a high portion of the englacial and basal debris that under quasi-stable conditions melts out at the grounding line, is instead rafted away, and later deposited by icebergs. A gradual ice retreat,

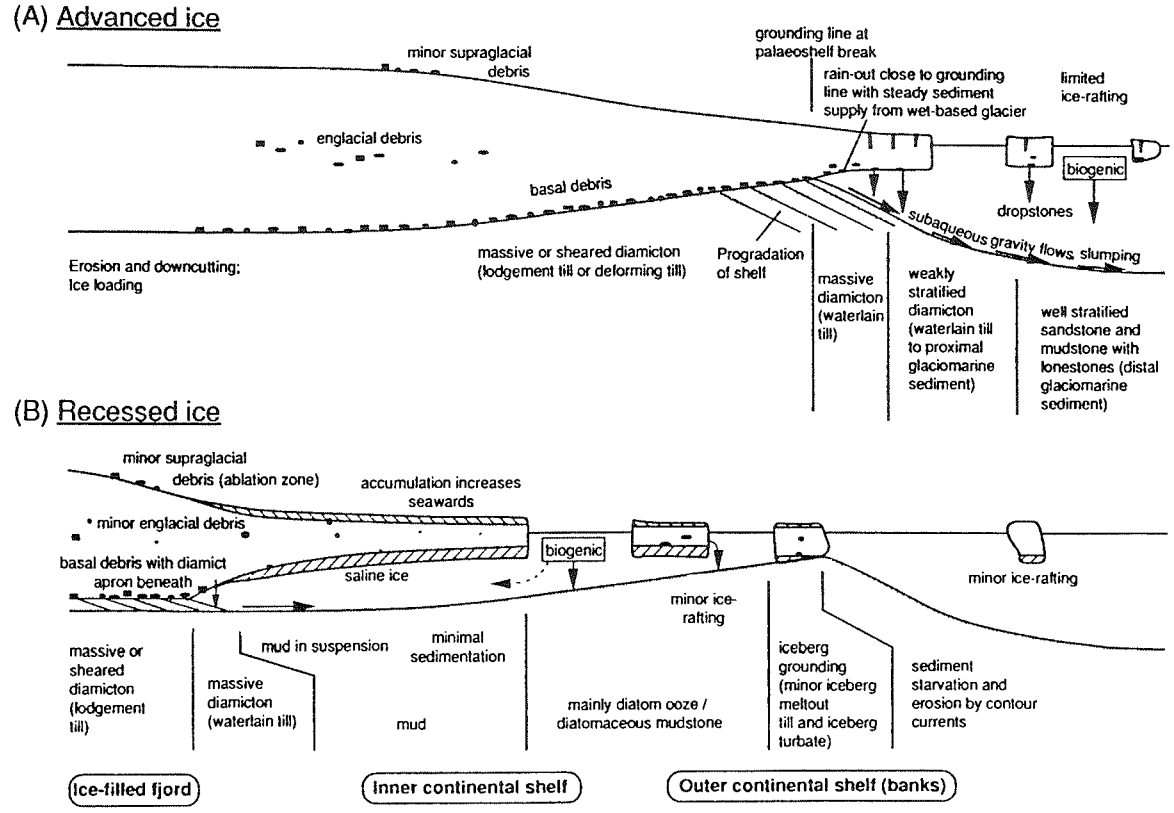

Fig 4.3.1 Sedimentary models illustrating (A) ice advanced to the continental shelf break, and (B) recessed ice with melt-out of most basal debris close to the grounding line, followed by freeze-on of oceanic ice beneath the ice shelf, as occurs today. From Hambrey et al. (1992).

produces eskers or erosional channels (Powell, 1984). As the grounding line retreats from the shelf edge to the continental shelf, sedimentation occurs mainly on the shelf; deposition on the slope, rise and plain noticeably decreases. Wet-based glaciers, however, produce sediment rich plumes that contribute to the deep-sea sedimentation even during interglacials (Powell, 1984). During glacial re-advance most of the sediments deposited during interglacials on the continental shelf are eroded, reworked and re-deposited at the new, more advanced grounding line.

Sediments deposited from glaciers are subject to reworking by gravity flow processes (turbidity currents, debris flows, sliding and slumping), by iceberg scouring (down to a depth of 250 m) (Elverhoi, 1984) and by bioturbation.

4.4 Seismic Stratigraphy of the Antarctic Continental Margin: Models and Examples

Cooper et al. (1991) have proposed a general model for the Cenozoic sedimentary sequences of the Antarctic continental margin. They suggested that these sequences could be divided into two types denominated IA and IIA:

(1) Type IA sequences are most commonly characterised by strongly prograding strata, that have relatively thin topset beds and steeply dipping (4-15°) foreset beds. The topset beds are flat lying, often eroded, show high seismic velocities (2-2.6 km/s) and overcompaction (Fig. 4.4.1).

(2) Type IIA sequences lying beneath IA sequences are of relatively gently dipping and continuous reflections, that principally aggrade the buried paleo-shelf edges (Fig. 4.4.1). The abrupt angular unconformities and terminated topset reflectors typical for IA sequences are absent. The sequence shows the characteristics of the seismic sequences of low- and mid-latitude continental margins described by Vail et al. (1977a).

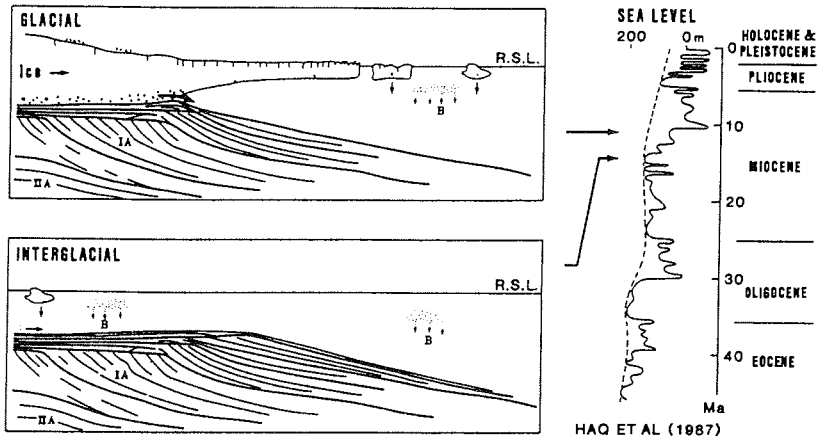

Fig. 4.4.1 The grounded ice-sheet model of Cooper et al. (1991) proposed to explain the origin of IA and IIA sequencies beneath the Antarctic margin. Such ice-sheet fluctuations are probably closely linked to sea-level changes. The type IIA sequences may be deposited during non-glacial and early glacial periods on a normal depth shelf, whereas type IA sequences may be deposited during glacial maxima periods on an overdeepened shelf at the front of grounded ice sheets that extend to the paleo-shelf edge. Little sediment is deposited during interglacial periods. B = biogenic debris; RSL = Relative Sea Level. From Cooper et al. (1991)

According to their interpretation, the IA sequences are caused by sediment deposition from a grounded ice sheet that episodically advanced to the shelf edge. Most deposition occurred directly from the base of the ice sheet onto the upper continental slope. Multiple erosion and overcompaction of the topset reflectors were caused by repeated ice advances. Thin topset reflectors may record cycles of grounded ice sheet advance, lift off by floating, and retreat. According to this model, the sequence of IA reflectors was deposited on an overdeepened continental shelf. The transition between IA and IIA sequences signals the onset of major advances of grounded ice to the continental shelf edge and the formation of the present overdeepened shelf geometry. The type IIA sequences were deposited by non-glacial and open-marine glacial processes on normal depth shelves; such sequences do occur on low-latitude margins.

The overdeepened shelf geometry was preserved (a) during glacial times, by grounded ice sheets episodically crossing the shelf, eroding sediments from onshore and inner shelf areas and depositing them at the front of the ice sheet as outer shelf topset banks and on the continental slope as foreset aprons. (b) During interglacial times, the overdeepened shelf geometry was preserved by the little or no clastic sedimentation on the continental shelf. Deposition occurred only beneath the retreated ice shelves that lay far from the continental shelf edge.

Ice streams carve broad depressions across the shelf and carry abundant basal sediments directly to the continental shelf edge, creating trough-mouth fans and sheet-like prograding sequences. On the shelf, progradation of the paleo-shelf edge increases whereas the thickness of the topset beds decreases towards the axis of the trough.

The model of Cooper et al. (1991) is based on reflection seismic data from the Ross Sea and Prydz Bay regions, the only places in Antarctica where the continental shelf has been drilled.

In Prydz Bay, five sites were drilled during Leg 119 of the Ocean Drilling Program along a 180 km long transect extending across the continental shelf to the slope. The area was chosen because it lies at the mouth of the Lambert Graben (Fig. 3.1) through which about one fifth of the East Antarctic Ice Sheet currently drains. It was expected to show the earliest indication of ice reaching the coast of Antarctica. The drilling encountered glacial deposits at all sites, mostly diamicts ranging in age from Middle Eocene to present. At the two inner sites, beneath this glacial sequence, preglacial deposits were sampled and interpreted as fluviatiles. Reflection seismic profiles along the ODP transect show at least seven

sequences that are considered type IA (Fig. 4.4.2). Below this, a unit of gently dipping, aggrading reflectors build a transitional IIA sequence. Sediments recovered from the seaward-dipping parts of the type IA and transitional IIA sequences are diamicts. These diamicts were interpreted as water-lain tills and proximal glaciomarine sediments deposited near or at the front of a grounded ice sheet. Contorted glacial sediments of glaciomarine/lacustrine and possibly fluvial origin were sampled from the transitional IIA sequence about 100 m above the inferred base of the glacial section and also from the top of the IIA sequence (Cooper et al. 1991). The ODP lithologies and acoustic stratigraphy are consistent with (1) an ice-sheet advancing onto, and probably deepening, the continental shelf with deposition of transitional IIA sequences starting in the Middle to Late Eocene, and (2) a grounded ice sheet having reached the shelf edge, and deposited a type IA sequences by Earliest Oligocene time. In Prydz Bay, the transitional IIA sequences lie directly on the inferred unconformity between pre-glacial and glacial rocks.

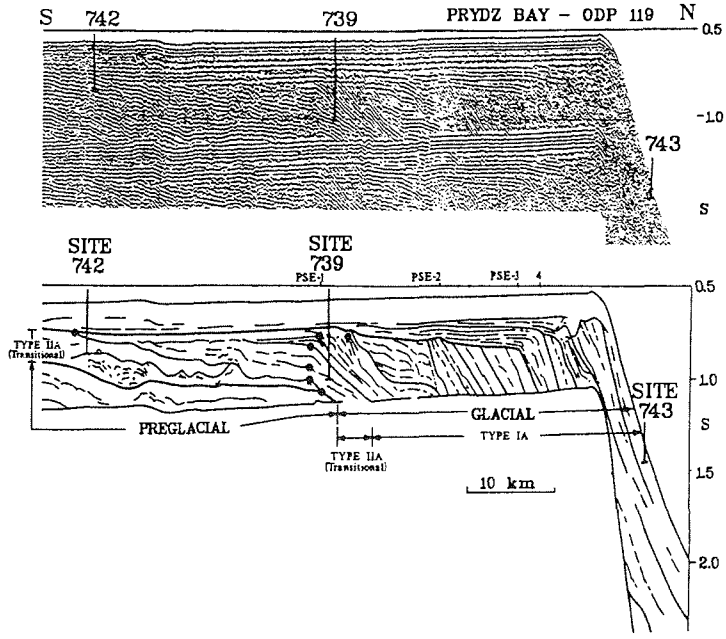

Fig. 4.4.2 Seismic section and line drawing across the type IA and transitional IIA glacial sedimentary sequences underlying the outermost shelf beneath Prydz Bay. The upsection change from type IIA to IA geometries generally corresponds to a transition from early glacial conditions to full glacial conditions. From Cooper et al. (1991).

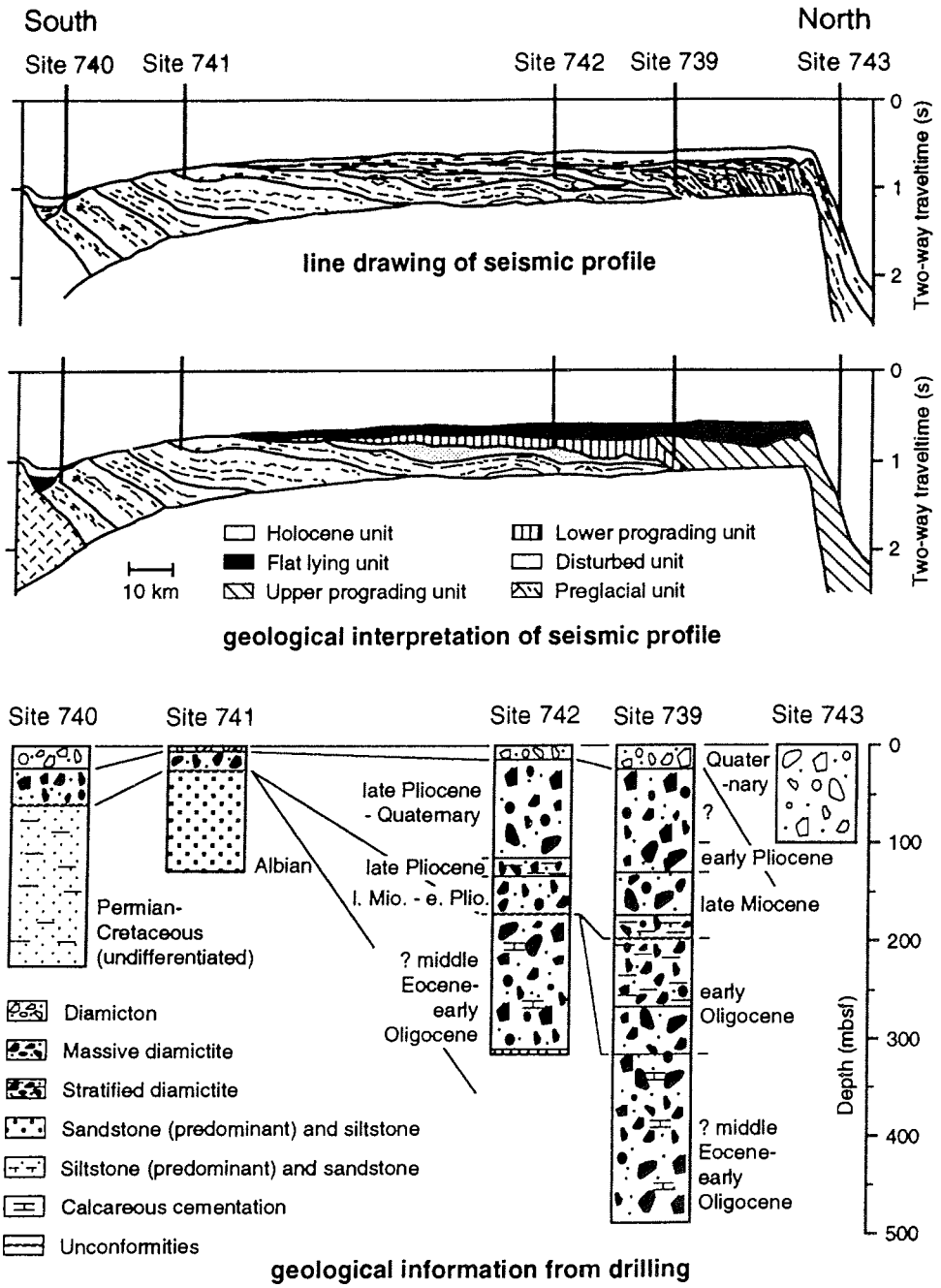

Fig. 4.4.2 (continued) Transect across Prydz Bay showing an interpreted seismic profile and the stratigraphic information from ODP Leg 119 drill sites. From Ehrmann (1993).

In the Ross Sea (Fig. 3.1), well data (DSDP Leg 28, CIROS 1 and 2, MSSTS) document glaciomarine sedimentation back to at least Middle Eocene times. From DSDP data on the continental shelf, Savage & Ciesielski (1983) suggested that the formation of small ice shelves began in the Middle Miocene. The near-shore CIROS 1, 2 and MSSTS wells in McMurdo Sound sampled sediments from the Middle Eocene to Recent times, and documented a series of glacial advances. The sequence from the Eocene to Late Oligocene exhibits relatively deep water environment and testifies a significantly lower amount of glaciation during this period (Hambrey et al., 1992; Brancolni & Darey, 1994). CIROS 1 recovered fossil leaf and pollen from the Late Oligocene. The climate during the Oligocene was probably more temperate than today. Sediment structures indicate higher meltwater production; the presence of well-developed flora suggests temperatures above freezing for much of the year and the presence of a temperate ice sheet (Hambrey et al., 1992). Cooper et al. (1991) identified nine type IA sequences on seismic reflection profiles which overlie the transitional IIA and the IIA sequences, respectively (Fig. 4.4.3). From correlation of drill hole and seismic data, Cooper et al. (1991) suggest the change in acoustic geometry of the paleo-shelf edge reflections from IA to IIA signals the onset of major glacial advances of grounded ice to the continental shelf in Early Miocene time. Grounded ice sheets may have existed previously, however, on an overdeepened inner shelf. The initial advance of grounded ice sheets towards the shelf edge may explain the "transitional" geometries between type IA and IIA units.

Similar prograding sequences have also been identified on the Antarctic Peninsula (Larter & Cunningham, 1993; Cunnigham et al., 1994) and on the Wilkes Land margin (Tanahasi et al., 1994).

The continental slope and rise of Antarctica is a less favoured target of stratigraphic and drilling studies compared to the Antarctic shelf. Even the deposits from there, however, show several common features, that distinguish them from low-latitude margins. Since they are not affected by ice erosion and can be better dated than ice-proximal deposits, the continental slope and rise sequences contain a valuable record of the glacial history of the continent.

The present upper continental slope is generally smooth and steep and uncut by major canyons. (Antarctic Peninsula: Larter & Cunningham, 1992; Weddell Sea: Fütterer & Melles, 1990). The downslope sediment transport is dominated by slumps, debris flows and turbidity currents (Antarctic Peninsula: Larter & Cunningham, 1993; Weddell Sea: Melles & Kuhn, 1993). The prograding continental margins of Antarctica show more elongated depocenters reflecting the deposition from a "line source" quite unlike the river deltas of low-latitude margins deposited from a "point source"

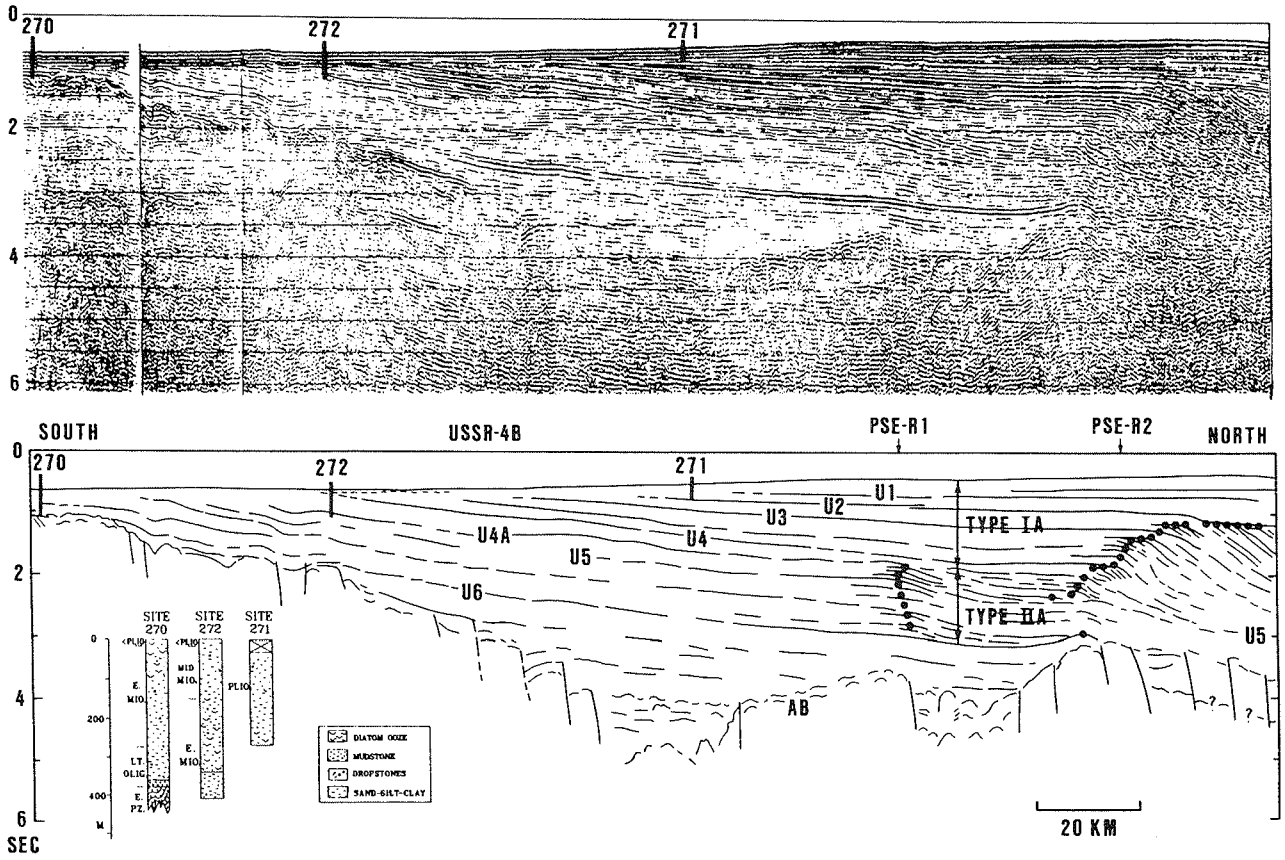

Fig 4.4.3 Seismic data and line drawing showing Cenozoic type IA and IIA sequencies in the eastern Ross Sea. Cooper et al. (1991) suggest that the transition from IA to IIA sequencies indicates a major early Miocene change in glacial depositional environments at the paleo-shelf edge. Type IIA sequences may result from distal grounded ice sheets on a normal depth shelf and type IA from ice sheets grounded out to the shelf edge on an overdeepened shelf. From Cooper et al. (1991).

(Larter & Cunningham, 1993). The lower continental slope is characterised by channel/levee deposits, contourite drifts and contourite deposits formed by the complex interaction of turbidity flows and strong bottom currents (Prydz Bay: Kuvaas & Leitchenkov, 1992; Weddell Sea: Kuvaas & Kristoffersen, 1991; Antarctic Peninsula: Larter & Cunnigham, 1992; McGinnis & Hayes, 1994; Rebesco et al., 1994).

4.5 Seismic Stratigraphy and Terminology of the Weddell Sea Sediments

Hinz & Krause (1982), Hinz & Kristoffersen (1987) and Miller et al. (1988) have laid the foundations of the seismic stratigraphy of the Eastern Weddell Sea.

Hinz & Krause (1982) identified two major units, separated by the "Weddell Sea continental margin unconformity". The upper sedimentary unit could be subdivided into four depositional sequences: WS-1, WS-2, WS-3A and WS-3B. The lower unit, WS-4 consists of a succession of oceanward dipping reflectors called the Explora Wedge, thought to be a Middle/Late Jurassic volcanic sequence. Since at that time no drill hole existed in the Weddell Sea, the regional unconformities separating the sedimentary units were tentatively correlated with major paleoceanographic and paleoclimatic changes.

Hinz & Kristoffersen (1987) developed a circum-Antarctic Stratigraphic concept that combined MCS data with drilling results and correlated regional unconformities to major plate tectonic and paleoceanographic events. They defined nine regional seismic unconformities, U1 to U9.

During ODP Leg 113, several sites were drilled in the Weddell Sea providing borehole control on the seismic sequences. From this new information, Miller et al. (1988) defined a series of depositional sequences. The profile ANT V/4-22 which passes over ODP Site 693, forms part of a seismic network connecting the drillsites (Fig. 4.5.1), and was used as a seismostratigraphic stratotype section. The depositional sequences were named W1 to W7, that included both the sequences and their basal unconformities (Fig. 4.5.2).

W1: The basal unconformity corresponds to the "Weddell Sea Continental Margin Unconformity". It is the U9 unconformity of Hinz & Kristoffersen (1987) and the boundary between the WS-4 and WS-3A units according to the terminology of Hinz & Krause (1982). The sequence W1 consists of landward onlapping reflectors, suggesting deposition on a subsiding base. It is characterised by some low-frequency events in the basal interval and by distinct but discontinuous reflectors in the upper part of the sequence.

W2: Sequence W2 is a stack of continuous, sub-parallel reflectors, affected by faulting in the vicinity of the "outer high", the apparently structureless wall bordering the plateau at the Explora Escarpment. Its basal boundary, W2, is an erosional unconformity. The sequence wedges out in a landward diverging configuration against the back of outer high. This pattern suggest that the layer

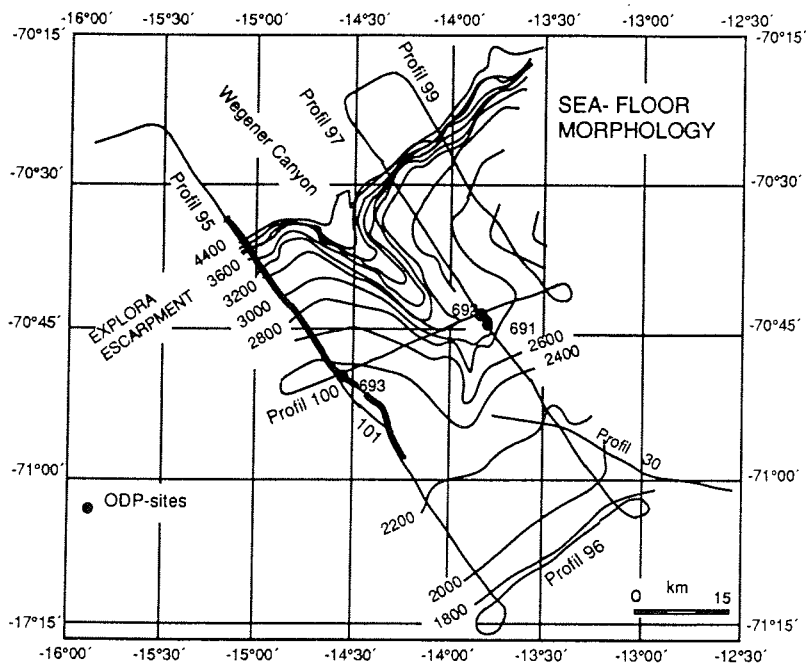

Fig 4.5.1 Bathymetric map of the Wegener Canyon showing the location of ODP Sites 692 and 693 and the seismic stratigrapic stratotype profile, ANT V/4-22 (indicated as PROFIL 95). From Miller et al. (1988).

displacement was contemporaneous with a rotational uplift of the outer high.

W3: The sequence is characterised by hummocky reflections with numerous diffraction hyperbolae, and with the relative absence of continuous reflectors at Site 693. The basal reflector W3 is a clearly defined erosional unconformity. The top interval of W3 was found to be of Aptian to Albian age at Site 693. The lower interval drilled at Site 692, about 150 m above W3, showed possible age associations ranging between Late Tithonian and Late Hauterivian depending on the studied fossil assemblage. The deposits recovered from this section were organic-rich mudstones and claystones.

W4: The deposits of sequence W4 show a draping configuration. The whole sequence looks rather noisy, with many diffractions and weakly defined subparallel discontinuous reflectors. Slumping has been reported from the corresponding section of Hole 693B. The sequence consists of nannofossil bearing clayey mud and diatomaceous silty to clayey mud. Its age is from Early-Late Oligocene to Early-Middle Miocene. The basal reflection W4 is very

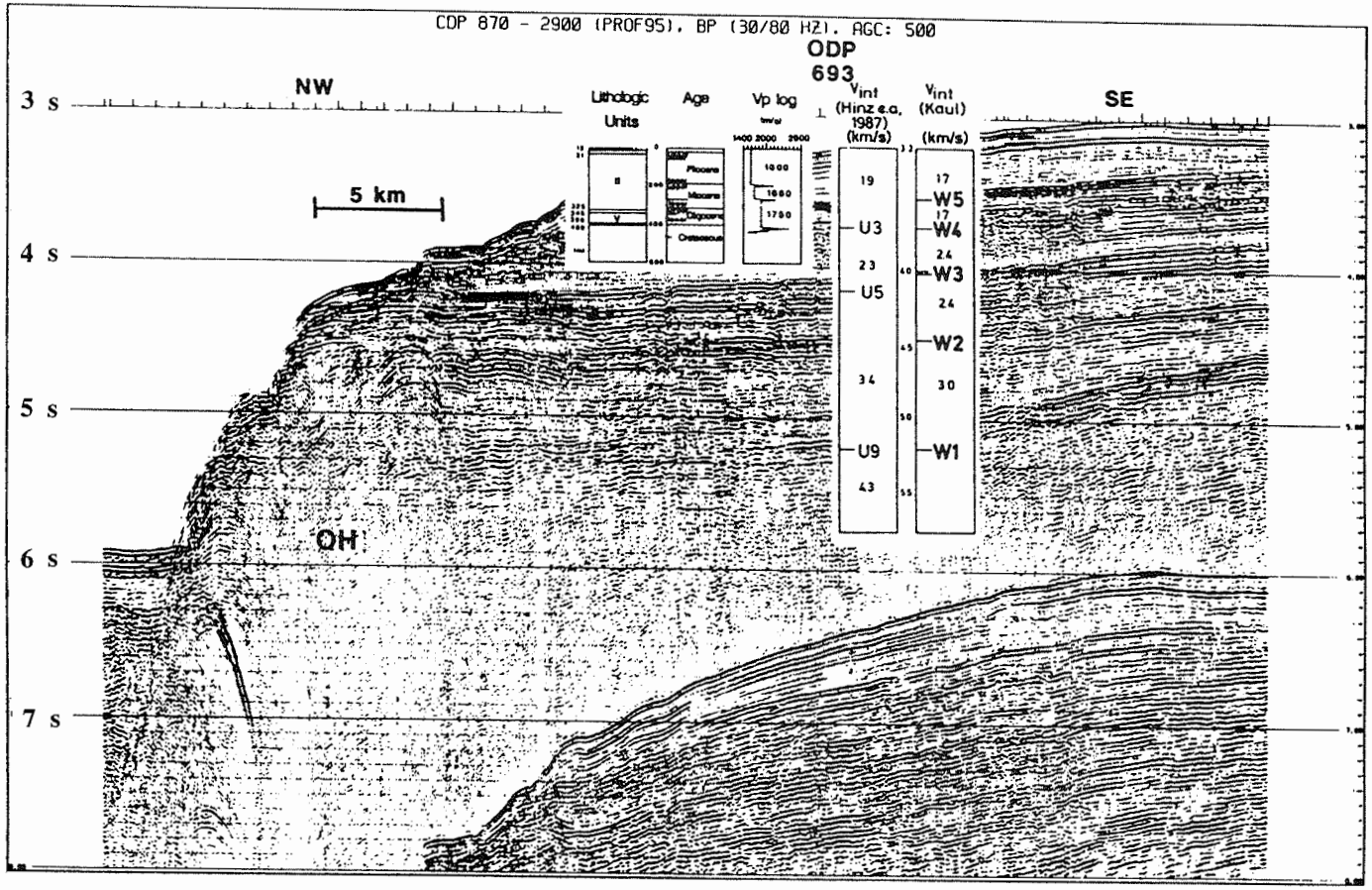

Fig. 4.5.2 Processed seismic stratigraphic stratotype profile (ANT V/4-22) across ODP Site 693 together with litho- and chronostratigraphic logs and velocity models. OH: "Outer High". Profile location in Fig. 4.5.1. From Miller et al. (1988).

weak and discontinuous, but it represents a local hiatus of about 60 Ma.

W5: This reflector corresponds to a minor hiatus in hole 693 where most of the Middle Miocene is lacking. Horizon W5 signals a dramatic change in seismic facies: all units above it display a regular, thin bedded pattern of parallel, continuous reflections, only disturbed downslope by some incipient slumping. This change in seismic facies apparently reflects the increased role played by glacial marine sedimentation related to the renewed cooling and major expansion of the East Antarctic Ice Sheet starting in Middle Miocene times. Late Miocene silty and clayey mud was recovered from this sequence.

W6: The acoustic characteristics and the composition of this sequence are similar to unit W5. The unconformity W6 is marked by a well defined reflector, possibly related to the jump observed in the p-wave velocity log in Hole 693. The sequence W6 consists of lower Pliocene deposits.

W7: The basal unconformity W7 truncates W5 and W6 further upslope. The depositional sequence W7 forms a continuous cover over these units. The sequence consists of late Pliocene and Pleistocene sediments with composition and acoustic characteristics similar to the underlying unit.

Haugland et al. (1985), Anderson et al. (1986) and Miller et al. (1988) posited the existence of a submarine fan in the Weddell Sea. Kuvaas & Kristoffersen (1991) established the overall stratigraphy and architecture of the fan. Several piston core studies have been carried out to investigate the lithology and the distribution of the near surface sediments (Anderson et al., 1986; Fütterer & Melles, 1990; Solheim 1990; Melles & Kuhn, 1993; Kuhn & Weber, 1993).

Continental shelf Surface sediments in front of the Filchner Shelf (Fig. 4.6.1) consist mainly of pebbly and sandy muds of glaciomarine origin. The Crary Trough acts as a sedimentary basin trapping fine-grained material winnowed from the shelf and from ice rafted debris (IRD). This is supported by glaciomarine sediments that are up to about a meter thick in the trough's axis and only 20 cm or less on its flanks (Fütterer & Melles, 1990). The onset of glaciomarine sedimentation is assumed to have taken place very soon after the peak of the last glacial around 18 ka BP (Fütterer & Melles, 1990). Sedimentation rates derived from this age are 1-6 cm/kyr for the present interglacial.

Stiff, overconsolidated glacial diamicton was found beneath the soft, glaciomarine sediments. The diamicton is low in water content and biogenic component, but high in IRD (Fütterer & Melles, 1990). Radiocarbon dated shells date the top of the overconsolidated sediments at 31 ka BP (Solheim, 1990). The existence of the overconsolidated diamicton indicates that the Filchner Ice-Shelf was probably grounded in the Crary Trough during the last glacial period (Solheim, 1990; Fütterer & Melles, 1990).

Reflection seismic data revealed details of the deeper structure of the Filchner Shelf. Haugland et al. (1985) reported that acoustic basement, probably representing the East Antarctic craton, was exposed in a 50-100 km wide swath along the ice barrier between 78°S and 75.5°S on the eastern side of the Crary Trough. They found the entire sediment section overlying the acoustic basement was undisturbed by faulting and folding. The undisturbed character of the sediments indicates that the uplift of the Trans-Antarctic Mountains and the relative motion of East Antarctica had little effect on the area north of the Filchner Shelf and east of 41°W.

Seismic profiles crossing the shelf edge north of the Crary Trough showed a succession of prograding sequences (Haugland et al., 1985; Miller et al., 1988). The prograding sequences were interpreted as a submarine fan complex, the Crary Fan, developed in the Southeastern Weddell Sea Embayment. By using analogies from the Ross Sea, Haugland et al. (1985) suggested that the

substantial buildup of the Crary Fan had taken place after the onset of glaciation.

Continental slope and rise. Oceanward convex bathymetric contours outline the lateral extent of the trough-mouth fan located in front of the Crary Trough (Fig. 4.6.1). Based on MCS studies Kuvaas & Kristoffersen (1991) described the fan as the superposition of three major channel/levee complexes designated I, II and III (Fig. 4.6.1).

The individual channel/levee systems of the complexes are often asymmetric (Fig. 3.3) with a better developed levee on their western side and a less pronounced, often missing one on their eastern side (Kuvaas & Kristoffersen, 1991).

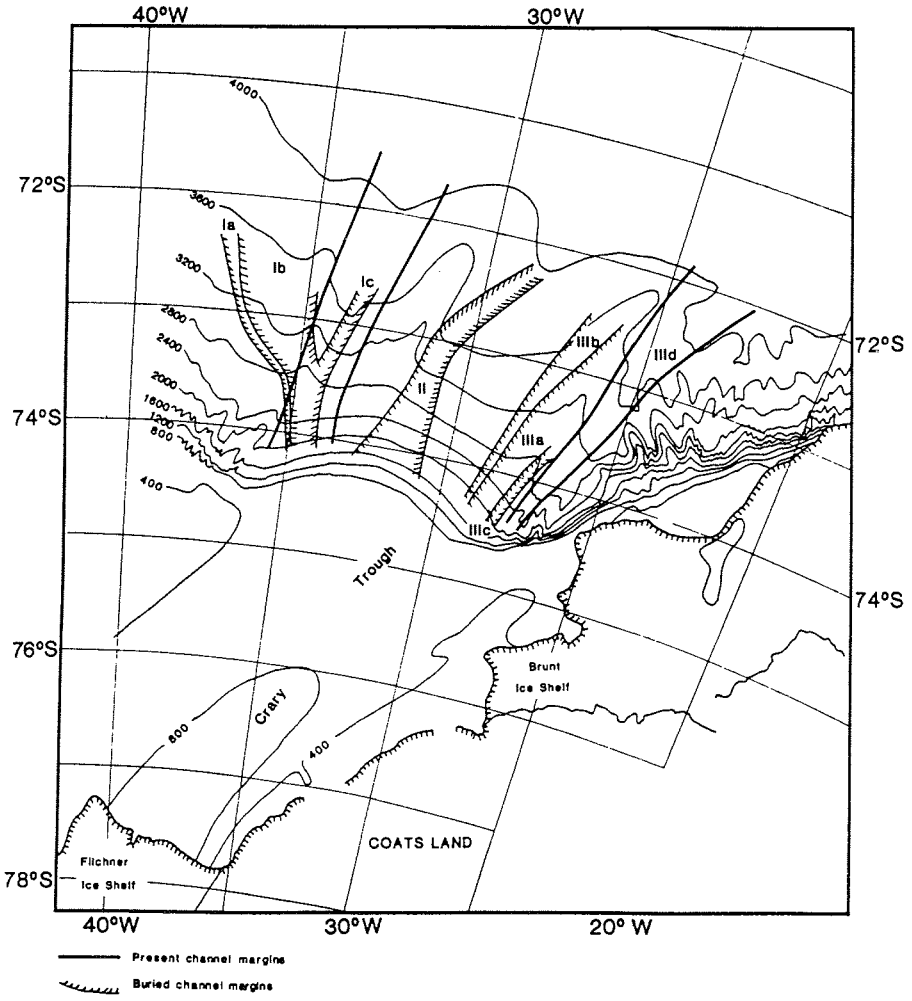

Fig. 4.6.1 Present and buried channels on the Crary TMF after Kuvaas & Kristoffersen (1991).

The growth of the fan is characterised by an eastward migration of the channel/levee complexes. The youngest complex (III) partly overlies complex II, which in turn partly overlies the oldest complex I. Complex III is not buried by sediments. One of its channel/levee systems is presently active, as manifested by the Deutschland Canyon/Channel (Kuhn & Weber, 1993).

Large growth faults are often observed within levee deposits. Sediment fluidization and slumping phenomena occur at the footwall of some major listric faults. These features suggest rapid deposition of fine grained material, resulting in overpressured-undercompacted conditions (Miller et al., 1988).

Several piston cores sampled channel facies. These cores encountered coarse grained sediments composed of sand and gravel (Anderson et al., 1986; Kuhn & Weber, 1993).

Anderson et al. (1986) described piston cores from levee facies as interbedded hemipelagic sediments and fine grained turbidites. Kuhn & Weber (1993) suggested a different interpretation: laminated clay and silt recovered from levee deposits were proposed to be contourites. These contourites contain some better sorted, cross-bedded layers analysed as spill-over turbidites. But according to the authors turbidites represents only 1/10 of the levee deposits. The laminated sediments are glacial deposits. High sedimentation rates of more than 2 m/kyr were measured on the levees for the last glacial. Kuhn & Weber (1993) described thinner layers of non-stratified, bioturbated distal hemipelagic sediments interbedding the contourite/turbidite deposits. The hemipelagic sediments were formed during interglacials. Sedimentation rates of 10 to 15 cm/ka were derived for the last interglacial (Fütterer & Melles, 1990).

In the uppermost part of the fan sequence, in front of the Crary Trough, Kuvaas & Kristoffersen (1991) described lens-shaped sediment packages on a line running parallel to the shelf edge. The unit is several hundred ms (TWT) thick and reaches its maximum vertical extent in front of the Crary Trough´s axis. It comprises a stack of numerous small, lens-shaped bodies.

In the same position, Kuhn & Weber (1993) described large areas of discontinuous echoes separating acoustically transparent, wedge-shaped sediment bodies. On the high resolution "Parasound", profiles, these sediment bodies show a small lateral extension parallel to the isobaths and a greater downslope extension reaching thicknesses of up to 30 m. The lens-shaped sediments of Kuvaas & Kristoffersen (1991) and the "wedging subbottoms" of Kuhn & Weber (1993) describe the same sediment facies. The different acoustic characteristic of this body is due to the difference in resolution between the "Parasound" records and the conventional seismic survey. The acoustic characteristics and the piston core

studies show that this sediment unit consists of slumps and proximal debris flow deposits (Melles & Kuhn, 1993; Kuhn & Weber, 1993). Homogeneous sediments were recovered from the proposed debris flows with high pebble content. Sand and clay components were high whereas silt fraction was low in comparison to nearby sediments.

Fan development Several authors have suggested different sedimentational processes that may control the buildup of the fan.

Kuvaas & Kristoffersen (1991) argue that during glacial periods meltwater streams, from a wet-based ice sheet grounded at the shelf edge, supplied sediment directly to the channels. Slumping of rapidly deposited sediments at the grounding line generated the mass flow and turbidite sedimentation that appears as lens-shaped deposits in front of the Crary Trough. During interglacial periods, sediment supply to the fan was greatly reduced. Vigorous downslope currents of dense Ice Shelf Water eroded the shelf and slope. Small amounts of sediments may have been supplied by winnowing from the shelf area and by the flow of Ice Shelf Water. The authors suggested that the eastward shift of sedimentation between channel/levee complexes was associated with major climatic changes. The shift from complex II to III was correlated with the Middle Miocene expansion of the East Antarctic Ice Sheet. The basal unconformity of the fan deposits was correlated with the W4 unconformity of ODP Site 693 by Miller et al. (1988). Consequently, Kuvaas & Kristoffersen (1991) proposed, that the fan was largely composed of glacial sediments deposited since the Early Oligocene.

Kuhn & Weber (1993) interpreted the channel/levee complexes as drainage systems for bottom water currents. They argued that current controlled sedimentation caused the buildup of the fan. During glacial times, thermohaline currents, and to a lesser extent, turbidity currents controlled the sedimentation on the asymmetric channel/ridge systems. Current velocities and the frequency of turbidity currents were higher during glacial times. The Crary Fan with its fronting debris flows also supplied sediments to channel/levee systems. The debris flow deposits covered a large sector of the lower fan filling some of the channels. The age of these debris flow deposits was assumed to be younger than the channels of this area.

Bart et al. (1994) described chaotic seismic facies having large areal extent. They interpreted the chaotic units as debris flows from the collapse of large, shelf-edge deltas on the upper slope, and proposed a genetic process for the formation of the Crary Fan. Large shelf-edge deltas were formed by ice sheets during extended glacial periods. The glacial detritus slid from the slope to the basin after

the ice-sheet had retreated, during the isostatic rebound of the continental shelf. The last major collapse of shelf edge deltas created the Deutschland Canyon and the smaller tributaries on the adjacent slope. The channel system was formed and partly filled by debris flows. The fan strata represents a uniform deposition by smaller-scale mass movements from the slope. The large debris flows of Bart et al. (1994) and the stack of smaller ones described by Kuhn & Weber (1993) are located in different areas and in different stratigraphic positions.

Anderson et al. (1986) concluded from the analysis of mineralogical composition of turbidity sands from the slope and abyssal plain that the primary development of the Weddell Fan occurred before the formation of the glacially overdeepened shelf geometry. They also suggested that the fan developed under a temperate glacial setting that included glacial outwash streams and beaches.

Most authors interpreting the fan complex have addressed the question of the asymmetry of the channel/levee systems. They have suggested two mechanisms for the development of a more pronounced western levee. One is that the Coriolis force deflects northward moving currents towards the west on the southern hemisphere and causes a preferential levee development on the western side. The other is that the contour following currents of the Weddell Gyre washed away suspension mode sediments transported by turbidity or thermohaline currents and deposited them preferentially on the western levee.

5. Drilling In the Weddell Sea From Glaciomarine and Tectonic Perspective

ODP leg 113 was devoted to the study of the tectonic and glacial development of the Weddell Sea region (Fig. 5.1). Sites 689 to 694 drilled in the Southern Weddell Sea sampled three contrasting environments: open-ocean pelagic sedimentation on Maud Rise (Sites 689 and 690), hemipelagic and terrigenous sediments on the East Antarctic Continental Margin (Sites 691-693) and a turbiditic sequence in the deep Weddell Basin (Site 694). Gondwana reconstructions show that East Antarctica, the Falkland Plateau and the Mozambique Ridge were joined till Late Jurassic times. The DSDP's results provide constraints on the continental or oceanic origin and on the geologic history of these areas (Fig. 5.1).

ODP Sites 689 and 690 (Fig. 5.1) are located on the Maud Rise, which is an aseismic ridge of oceanic basement. It is presumed to have been formed by the interaction of a spreading ridge with a hot-spot (Barker et al., 1988). The two sites are at a water depth of 2080 and 2914 m, respectively, on an isolated high rising 2000 m above its surroundings approximately 700 km off East Antarctica. The elevated position of the two holes protected them from strongly erosive bottom currents and from terrigenous sediment transport except for wind-blown and ice rafted components. They were also above the carbonate compensation depth during the deposition of most of the sediment section. Thus, they contain calcareous fossils.

The sampled deposits consists of almost pure siliceous and calcareous oozes to chalk (Barker et al., 1988) which, in the lower part of the section at Site 690, was mixed with terrigenous sediments. The sedimentary sequence ranges in age from Campanian (75 Ma) to Quaternary with some brief hiatuses or highly condensed sections. Sediment and microfossil diversity and assemblages clearly reflect a sequential cooling of the Antarctic water mass, probably related to Antarctica's glacial development. Siliceous biogenic facies progressively replaced the carbonate facies during the Cenozoic: initial siliceous sedimentation begins near the base of the Neogene; an exclusively siliceous sedimentation appears from the upper Miocene. The rate of sediment accumulation was always low ranging from 4 m/Ma to 8 m/Ma. The more or less continuous pelagic section obtained was of pioneering importance in the Antarctic biostratigraphy and oxygen stratigraphy and also provides a valuable record of Antarctica's palaeoceanography and glacial history. Site 690 penetrated 1.7 m into the acoustic basement. Oceanic alcali basalt was found with a composition similar to that in seamounts and oceanic islands.

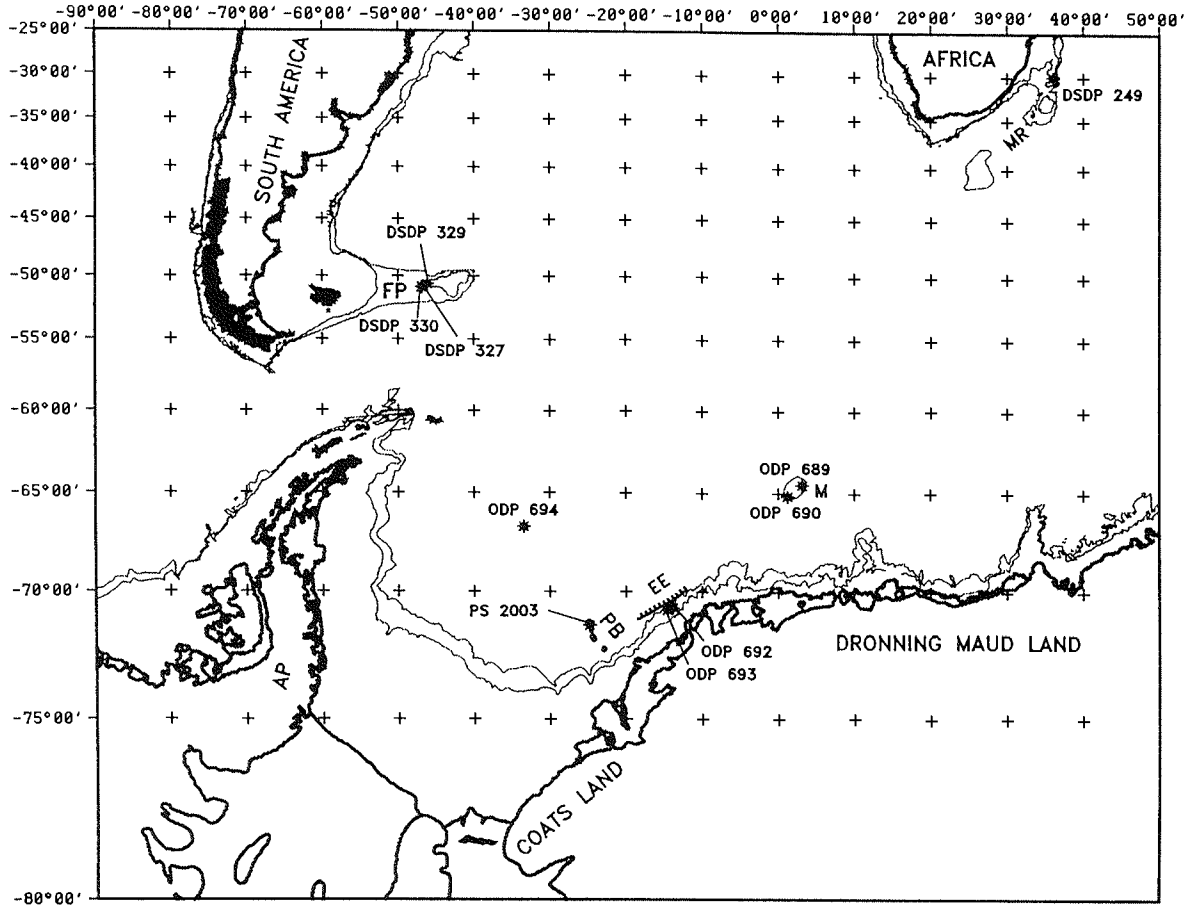

Fig. 5.1 ODP, DSDP and piston core sites referred to in this section. FP: Falkland Plateau; MR: Mozambique Ridge; PB: Polarstern Bank; EE: Explora Escarpment; M: Maud Rise; AP: Antarctic Peninsula.

The importance of these two ODP Sites for the present study stems from the remarkable similarity of their paleoenvironmental setting and geologic history to that inferred for the Polarstern Bank (§ 7.2.1).

ODP Sites 691-693 (Fig. 5.1) are located on the midslope bench landward of the Explora Escarpment. Site 691 lies within the Wegener Canyon, at a water depth of 3030 m. Site 692 is higher on the Canyon shoulder at a depth of 2870 m, Site 693 is about 10 km southwest of the outer rim of the canyon at 2359 m water depth. From the planned 1000 m section at Site 691, only 12.7 m could be drilled and 0.05 m recovered; therefore this site is not considered any further.

At site 692 three lithostratigraphic units were recognised (Barker et al., 1988) :
Unit I, at 0-30.4 m below the sea floor (mbsf), silty and clayey mud with non recovered coarse fraction, from the Miocene to Upper Pleistocene.
Unit II, at 30.4-53.2 mbsf, a "gravel bed" of pebbles, cobbles and probably a fine fraction which was not recovered, of unknown age.
Unit III, at 53.2-97.9 mbsf, nannofossil claystone with marcofossils, volcanic ash lenses, and laminae, and organic rich claystone interbeds, from the Lower Cretaceous.

The penetrated sediment section limits the age of the Wegener Canyon (Barker et al., 1988). Diatom assemblages of unit I are *in situ*. Their presence above the gravel bed of unit II suggests that by the Late Miocene or before, the canyon had cut down to the present shoulder, leaving behind a coarse gravel lag. In a subsequent rejuvenation of the canyon, perhaps after it had breached the outer high of Explora Wedge, the steeper inner canyon formed. The physical properties suggest that 250-300 m of overburden were eroded at this site, implying a simple original continuity of the parallel bedded reflectors of the canyon walls (Barker et al., 1988).

The Lower Cretaceous claystones of Unit III resemble sediments from the Falkland Plateau of a similar age. They were deposited under anoxic conditions at a maximum water depth of 500-1000 m at middle latitudes (43°±5° S). The estimated paleo-water depth indicate a subsidence of 1800-2300 m since the Early Cretaceous.

Site 693 is located approximately 30 km from Site 692, away from the rim of the Wegener Canyon where the thickness of the assumed Cenozoic section is greatest. Its core consists of 398 m Pleistocene to Oligocene hemipelagic muds and 86 m of Lower Cretaceous

claystones, mudstones, diatomite and limestones. Glacial dropstones are abundant down to the Middle Miocene, and present but less common through the Oligocene. Illite is the dominant clay in the Cenozoic section, reflecting a physical nature of the erosion whereas smectite is the most abundant clay mineral in the Cretaceous section. The biogenic component is almost entirely siliceous indicating that the site was below the CCD for all but a few brief periods.

Analysis of the core indicates that sedimentation rates were less than 10 m/Ma in the Pleistocene, 21-46 m/Ma in the Pliocene and Late Miocene and 7 m/Ma in the Early Miocene and Oligocene. The estimated, maximum erosion in the Oligocene-Lower Cretaceous hiatus was 300 m, which implies an average sedimentation rate of 5 m/Ma. The rate is similar in the Miocene/Oligocene. Assuming a Middle/Late Jurassic age for the basement, the long term average sedimentation rate in the Jurassic and early Cretaceous was 20-40 m/Ma. In general, between roughly 100 and 12 Ma this location was a starved margin, but before and since it had and has had sedimentation rates that were and have been much higher. Correlation with seismic profiles show that about 90% of the sediments around this site are pre-Upper Cretaceous. The similarity of the sedimentation rates of the Lower Cretaceous and Oligocene suggests that the hiatus did not result from a fundamental change in the rate of sediment supply. More probably, it was caused by the increased vigour of deep and intermediate water circulation, such as generally associated with the onset of bottom water formation at high latitudes at the Eocene/Oligocene boundary (Barker et al., 1988).

Benthic diatoms recovered suggest areas of shallow water depth (50 m) lacking permanent shelf-ice cover upslope of Site 693 during Oligocene to Early Miocene times.

ODP Sites 692 and 693 are located on seismic lines that form part of the extensive MCS network covering the southeastern Weddell Sea margin and are the only boreholes so connected. They provide the first opportunity to correlate the seismic sequences with lithologic units and chronostratigraphic boundaries. That correlation and its terminology are described in detail in § 4.5.

ODP Site 694 (Barker et al., 1988) is located in 4653 m of water on the northern part of the Weddell Basin abyssal plain (Fig. 5.1). The site is about 900 km north of East Antarctica and about 900 km east of the Antarctic Peninsula. The hole penetrated 391 m of sediments mostly terrigenous in origin with a minor biosiliceous component and a fluctuating abundance of ice-rafted material. Calcareous material is not present because the hole lies well below

the CCD. The sequence ranges in age from Middle Miocene to Quatenary. Almost all the sediments are interpreted as hemipelagic silts, clays and turbidites. The dominance of sedimentary rocks in the lithic material of the turbidites and the glacial material suggest that the principal source area is the Antarctic Peninsula and the present-day region of the Filchner-Ronne ice shelf rather than East Antarctica. Long term, average sedimentation rates are 30-40 m/Ma with some conspicuous peaks. Deposition of a thick (90 m) sandy turbidity sequence was extremely quick (about 180 m/Ma) during an interval of 0.5 Ma or less in the earliest Pliocene, before 4.8 Ma. Afterwards, sedimentation rates drastically decreased: the Lower Pliocene to Quaternary is represented by only 21 m sediments, a sedimentation rate of about 4 m/Ma.

Site 694 suggests frequent, high energy turbidity current activity on the Antarctic Peninsula and/or on the Filchner-Ronne Ice Shelf margin from the Middle Miocene to Lower Pliocene. Since then, the turbidity sedimentation has ceased. This prominent change should appear in the seismic profiles covering the continental slope in front of the Filchner Shelf.

DSDP Leg 36 (Harris & Sliter, 1977) drilled three successful sites on the Falkland Plateau (327, 329 and 330). Before the separation of the continents, these sites lay close to the present day East Antarctic margin. Since no older sediments than Early Cretaceous / Latest Jurassic were drilled on the Weddell Sea margin, the sites on the Falkland Plateau can help predict the nature of the pre-Cretaceous deposits in the Weddell Sea.

The recovered basement rocks confirmed the continental nature of the crust underlying the easternmost part of the Falkland Plateau. The samples are broadly comparable in age (535±66 Ma) as well as in lithology to the exposed basement rocks of the adjoining areas of the African and South American continents (Harris & Sliter, 1977). The Middle to Upper Jurassic sediments overlying the basement are characteristic of swampy, possibly deltaic, coastal plain environment. Marine transgression occurred during the Upper Jurassic (Oxfordian) as evidenced by the beach sand which is overlain by marine silts and clays representing a shelf environment and a water depth of 100-400 m. The Late Jurassic and early Cretaceous (late Aptian) sediments were formed under stagnant bottom conditions resulting in the deposition of sapropelic sediments characterised by abundant pyrite and organic carbon concentrations. Starting in the early Albian, open-marine conditions developed at Site 330 accompanied by a distinct improvement in oxygenation. Subsidence to their present depth occurred during the Late Cretaceous to Paleogene.

Early Cretaceous claystones of ODP Site 692 were deposited under anoxic conditions at shallow depths and show similarities to the Late Jurassic to Early Cretaceous sapropelic claystones found on the Falkland Plateau. By induction, the 1200 m sediment sequence not drilled at Site 692, for which a Late Jurassic / Early Cretaceous age was assumed (Barker et al., 1988), probably consists of sapropelic claystones to sandstones deposited in shallow marine, anoxic environment overlying a marine transgressional sequence of sandstones and fluviatile deposits. Long term average sedimentation rates at Site 692 are about a factor four higher than at Site 330 which probably reflects a higher terrigenous input on the Weddell Sea margin.

DSDP Site 249 (Simpson et al., 1974) located on the Mozambique Ridge at 2088 m water depth was intended to decide whether the ridge was oceanic or continental in origin. At 408 mbsf 3 meters of glassy basalt, weathered on top was recovered. Geochemical analysis showed that the basalt samples are similar in composition to the mid-ocean ridge abyssal tholeiites (Erlank & Reid, 1974). The analysis, however, could not determine if the basement was continental or oceanic.

Dark grey, almost black Cenomanian/Neocomian siltstones and claystones overlie the weathered basaltic basement at Site 249. The dark colour of the 121 m thick unit is probably due to the presence of free carbon and iron sulphides suggesting an anoxic depositional environment similar to that which prevailed on the Falkland Plateau and the Weddell Sea margin at the same time.

A large number of piston cores sampled the upper few meters of sediment in the Weddell Sea. Only one of these cores, PS 2003 (Kuhn et al., 1992), is described here in detail, because it was taken from the top of the Polarstern Bank (§ 7.2.1).

The core is 920 cm long and was taken at 3718 m water depth. Paleomagnetic measurements date the bottom of the core to 4 Ma (Gersonde, personal communication) implying an average sedimentation rate of 2.3 m/Ma. The core shows a homogeneous structural pattern, bedding is very rare and lamination is invisible. Its sediments are moderately bioturbated, the amount of IRD and terrigenous sand is more or less constant. No signs of current activity or hiatuses have been detected. The upper 230 cm of the core contains planctonic foraminifera within the sediments. The foraminifera content decreases downcore; only traces of biogenic components appear between 230 and 610 cm. In the lower part of the core (610 to 920 cm), siliceous microfossils are common.

The study of the piston core PS 2003 confirms that the top of the Polarstern Bank forms an ideal location for drilling due to its

elevated position. A condensed, but relatively continuous sediment sequence can be expected that will contain a record of the paleoceanographic, biostratigraphic and glacial history of the Weddell Sea.

6. A New Synthesis of the Glaciomarine Sedimentation in the Weddell Sea: A Seismic Stratigraphic Approach

In this chapter, a Cenozoic glaciomarine depositional history is synthesised for the Weddell Sea from acoustic stratigraphy, drilling and sea bottom sampling. The results of earlier seismic surveys by the BGR, the NARE and the AWI are compiled and reinterpreted together with new data collected by the AWI in 1990 and 1992 (Fig. 6.1).

Only glacial deposits are considered in this chapter. A prominent unconformity, the W4 (§ 4.5), forms the base of the Cenozoic glaciomarine sequence in the Weddell Sea (Miller et al., 1988). This erosional unconformity is marked by a strong reflector. The unconformity separates a unit of low frequency, subparallel, continuous reflectors from the overlying acoustically thin-bedded or transparent seismic sequences. The reflector can be followed on all seismic lines over the continental rise, and with some effort and uncertainty, over the middle and upper slope. Glacial deposits lie above this horizon.

In the first part of this chapter, a set of seismic facies are defined. These seismic facies are then used to introduce the schematic architecture of the southeastern Weddell Sea margin. This is followed by a detailed description of the formation of the individual facies. Finally, a general model is proposed for the glaciomarine depositional history of the Weddell Sea.

6.1 Seismic Facies

Several distinct seismic facies can be identified and traced over large distances on the seismic lines in the Weddell Sea (Fig. 6.2). The acoustic characteristics, the unit's external geometry, the sedimentary environment and the relative position to other facies were used to define the seismic facies. The different units were correlated with drilling and coring results, where such data were available, to determine the lithology and depositional history. For the lack of geologic samples - which was often the case - analogies were drown from areas with better constrained sedimentational processes.

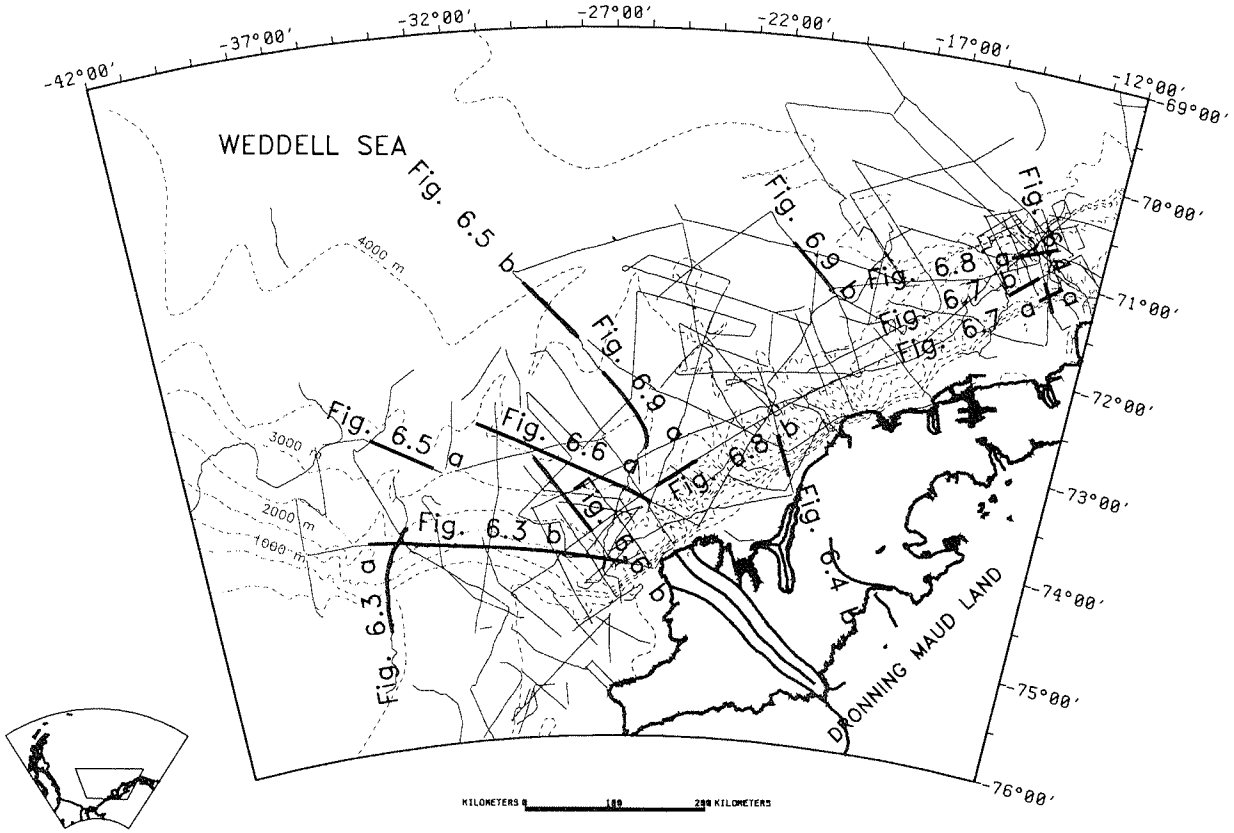

Fig. 6.1 Location of the seismic profiles shown in figures 6.3-6.9.

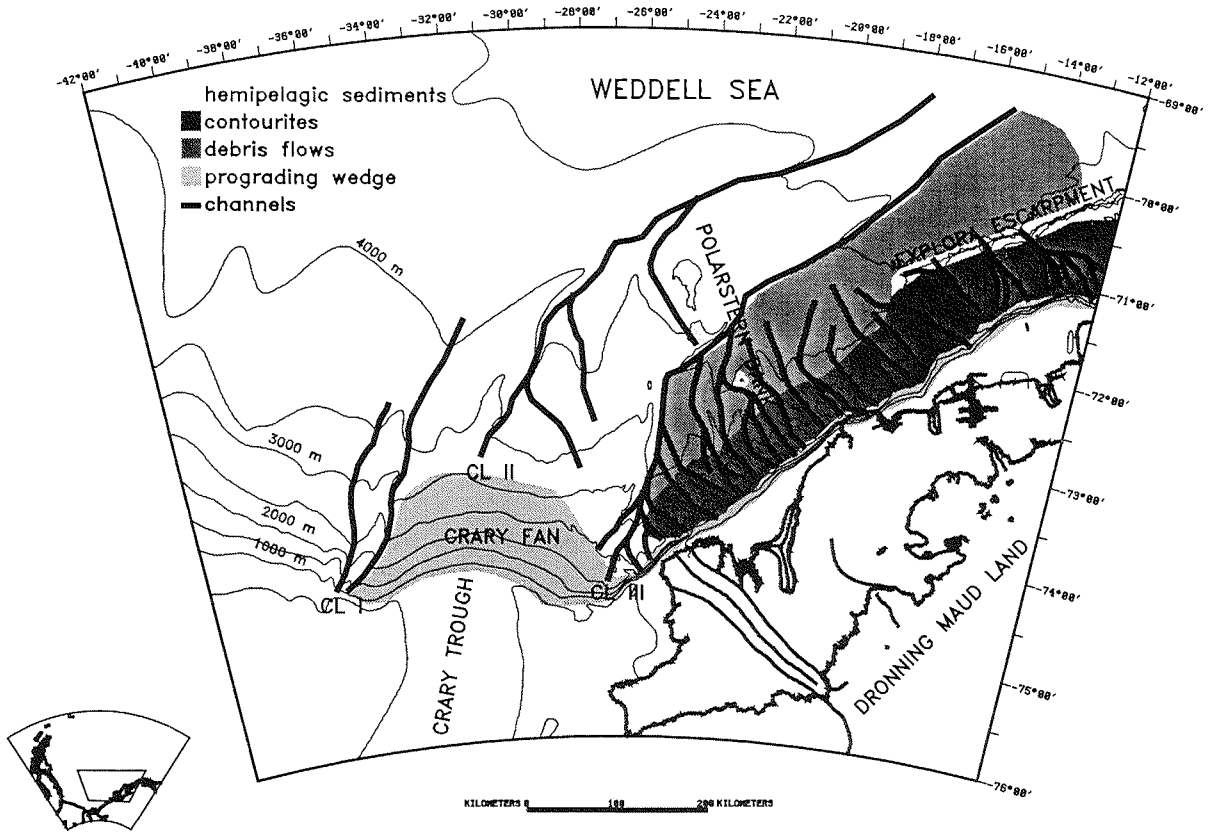

Fig. 6.2 Seismic facies on or directly beneath the seafloor: the prograding wedge, the contourite, the debris flow and the hemipelagic drape facies. Channel axes are indicated by black lines; the bathymetric contours outline their associated levees. CL I-III denote channel/levee complexes.

Prograding Wedge Facies The upper slope of the Crary Fan and the Dronning Maud Land Margin is dominated by a seismic facies of strongly prograding reflectors with steeper dip than that of the underlying unit. The upper surface of this *prograding wedge* (Fig. 6.2) inclines about 1.5° on the Crary Fan and 15° on the margin east of it (c.f. Fig. 6.3a, Fig. 6.4a). Reflectors of this facies downlap onto its basal unconformity and generally show a truncational termination on the continental shelf. Thin topset beds on the shelf can sometimes be observed with transparent or chaotic reflectors and high seismic velocities. Overcompaction caused by a grounded ice sheet was detected on sediment cores of topset facies (Fütterer & Melles, 1990; Solheim, 1990; § 4.6). Piston cores that sampled foreset beds on the slope recovered homogeneous glacial sediments deposited by small-scale debris flows (Melles & Kuhn, 1993). In slope direction, this seismic facies shows up as a stack of thin (50-100 ms, TWT) lens or wedge-shaped bodies (Fig. 6.3a, Fig. 6.4a). The individual units consist of chaotic reflectors or are transparent. These acoustic characteristics also suggests the sediment body was deposited by small-scale debris flows. Along slope, the facies as a whole appears wedge-shaped tapering downwards (Fig. 6.3a). Along strike, the unit is lens-shaped with a maximum observed thickness of 1000 ms, TWT (Fig. 6.3b). The sediment body generally reaches its greatest thickness and forms a bulge in the bathymetry in front of glacially eroded troughs. The smooth upper slope of the Weddell Sea is formed by this facies (Fig. 6.2).

In the model proposed here, the *prograding wedge* seismic facies is a glacial sediment sequence deposited from a grounded ice sheet as it episodically advanced to the shelf edge. Slope failures initiated small-scale debris flows and caused the redeposition of the diamict further downslope. Similar deposits can be found on all Antarctic margins and were termed IA sequences by Cooper et al. (1991, § 4.4). Their interpretation is consistent with the interpretation just given.

Channel/levee facies The bathymetric map (Fig. 6.2) outlines three main channels branching out into numerous tributaries on the continental slope. Channels are bounded by levees which are often better developed on the western side of the channel (Fig. 6.5 and 6.6). On the seismic profiles channel facies are characterised by high amplitude, low continuity reflectors with channel fill external geometry. Piston cores recovered lag deposits from the channel floor composed of sand and gravel (Anderson et al., 1986). Levees appear as continuous, low amplitude, acoustically thin bedded reflectors converging away from the channel axis (Fig. 6.5). Sediment cores from levee deposits consist of laminated clay and

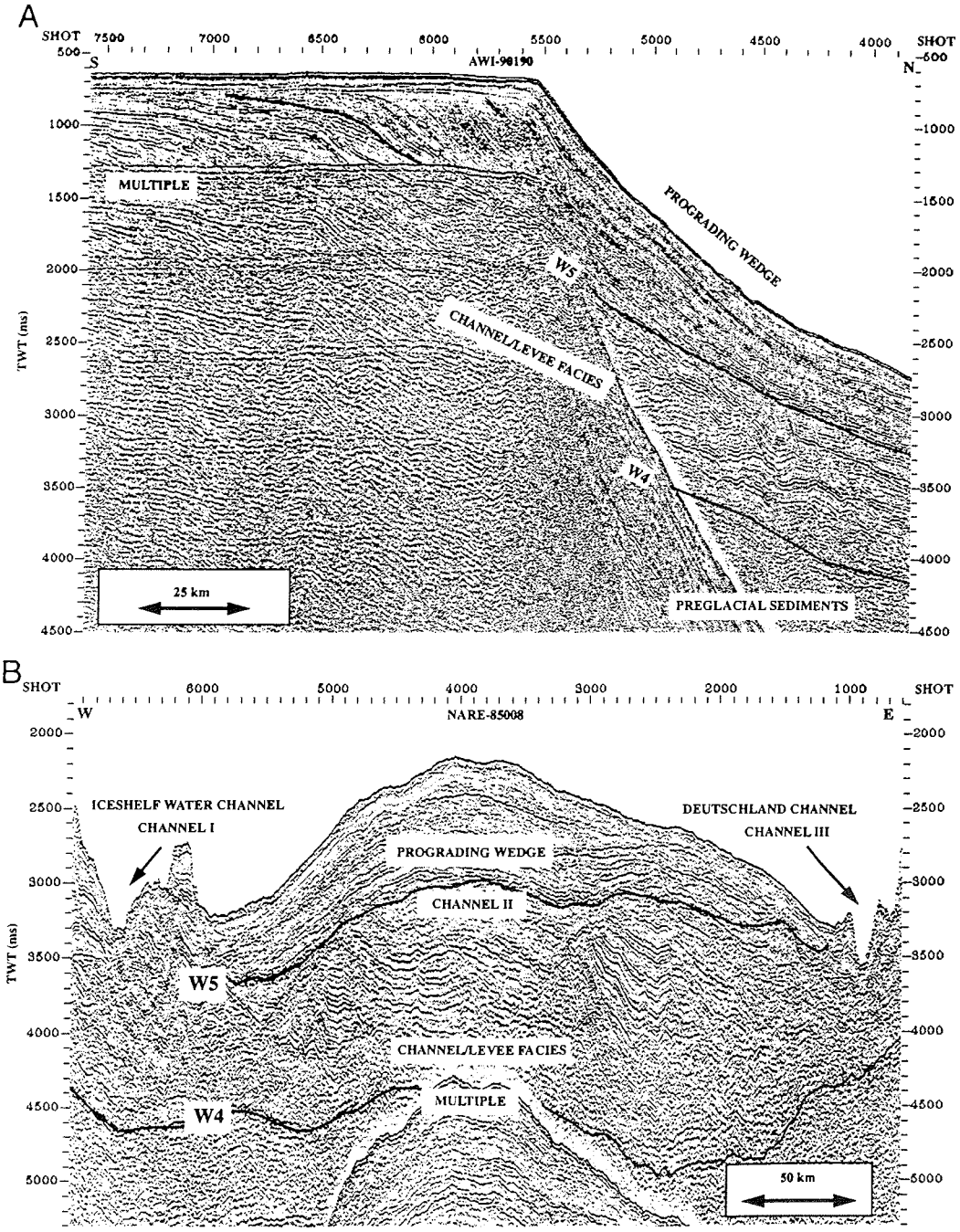

Fig. 6.3 **A)** On the Crary Fan in the slope direction, the prograding wedge facies tapers off downwards and downlaps onto the underlying sequence. **B)** Along strike, the prograding wedge forms a lens-shaped cover over the channel/levee facies. The W5 unconformity signals a distinct change from an aggradational/progradational build-up to a strictly progradational one. Profile location in Fig. 6.1.

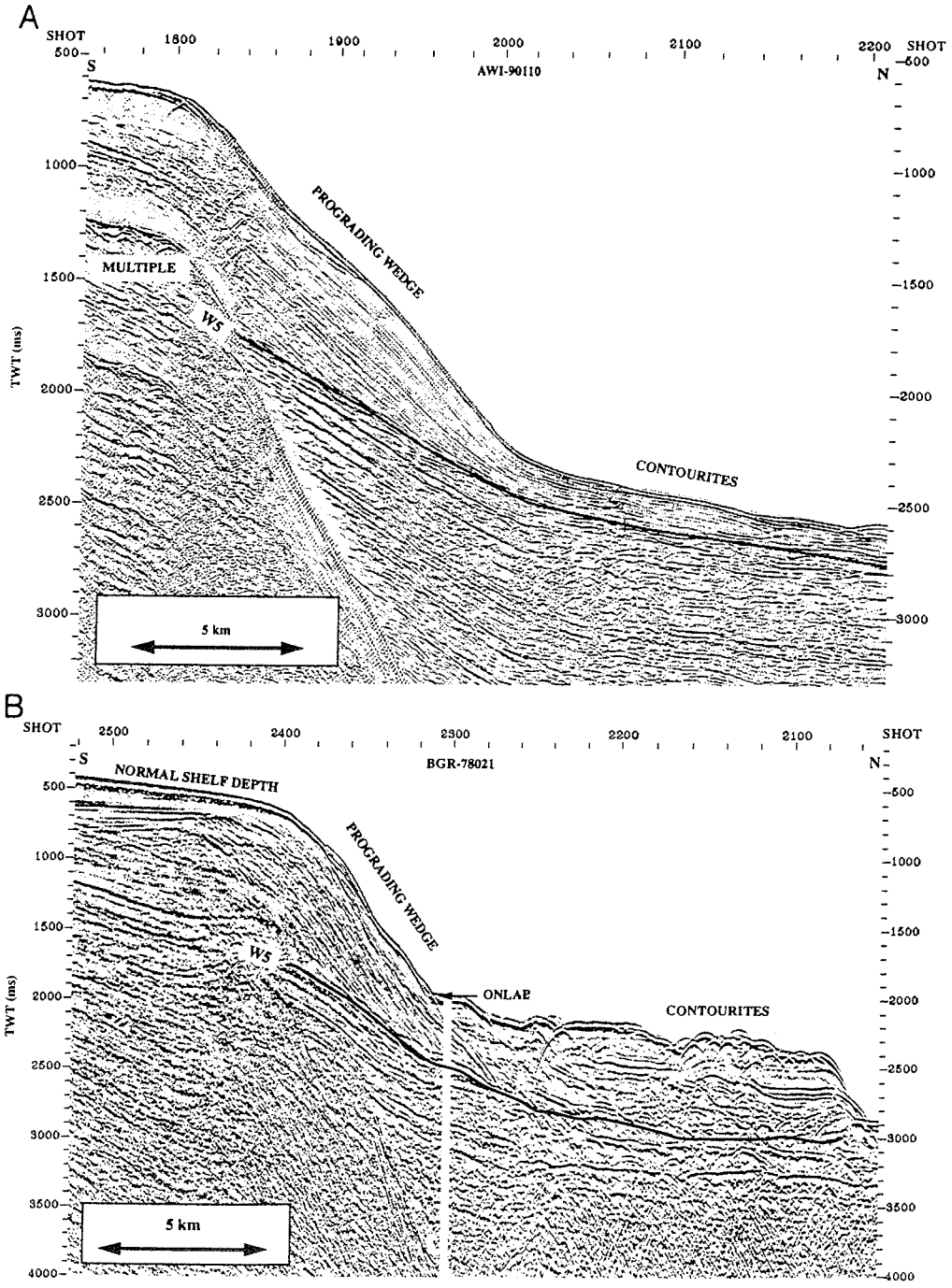

Fig. 6.4 Seismic profiles showing the relation between the prograding wedge and the contourite facies. **A)** At 13°W, the shelf is overdeepened. The prograding wedge can be correlated with the contourite facies. **B)** At 22°W, the shelf has a normal depth. The contourites onlap onto the prograding wedge. Compared to the Crary Fan, a distinct steepening of the upper slope can be observed. Profile location in Fig 6.1.

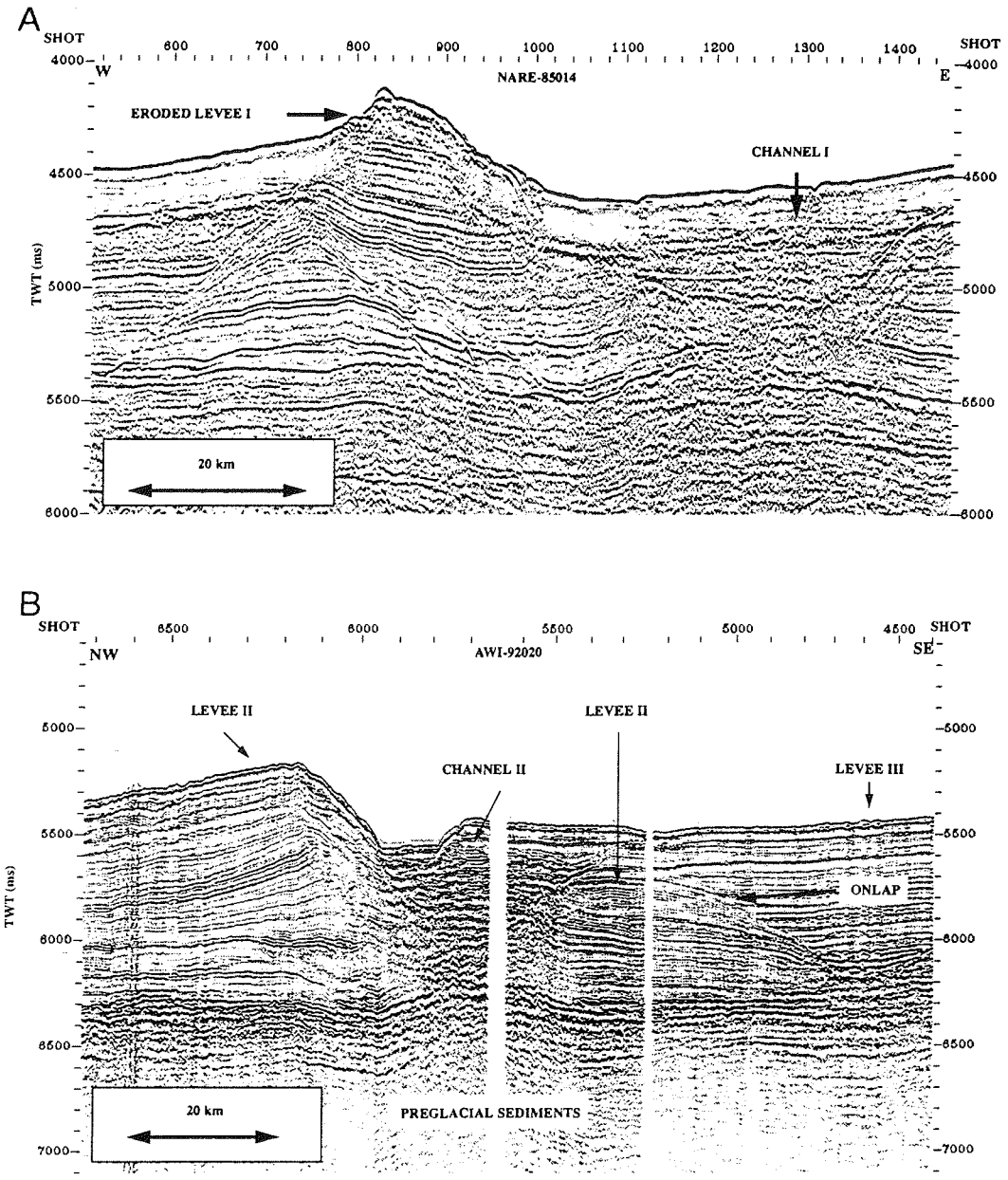

Fig. 6.5 A) Channel/levee complex I is strongly eroded and partly buried by sediments which show the channel is inactive. **B**) Channel/levee complex II is strongly asymmetric, well developed and active. The levee of complex III onlaps on the flank of complex II. The glacial-preglacial transition is represented by a sharp change in the acoustic characteristics at about 6500 ms. Profile location in Fig. 6.1.

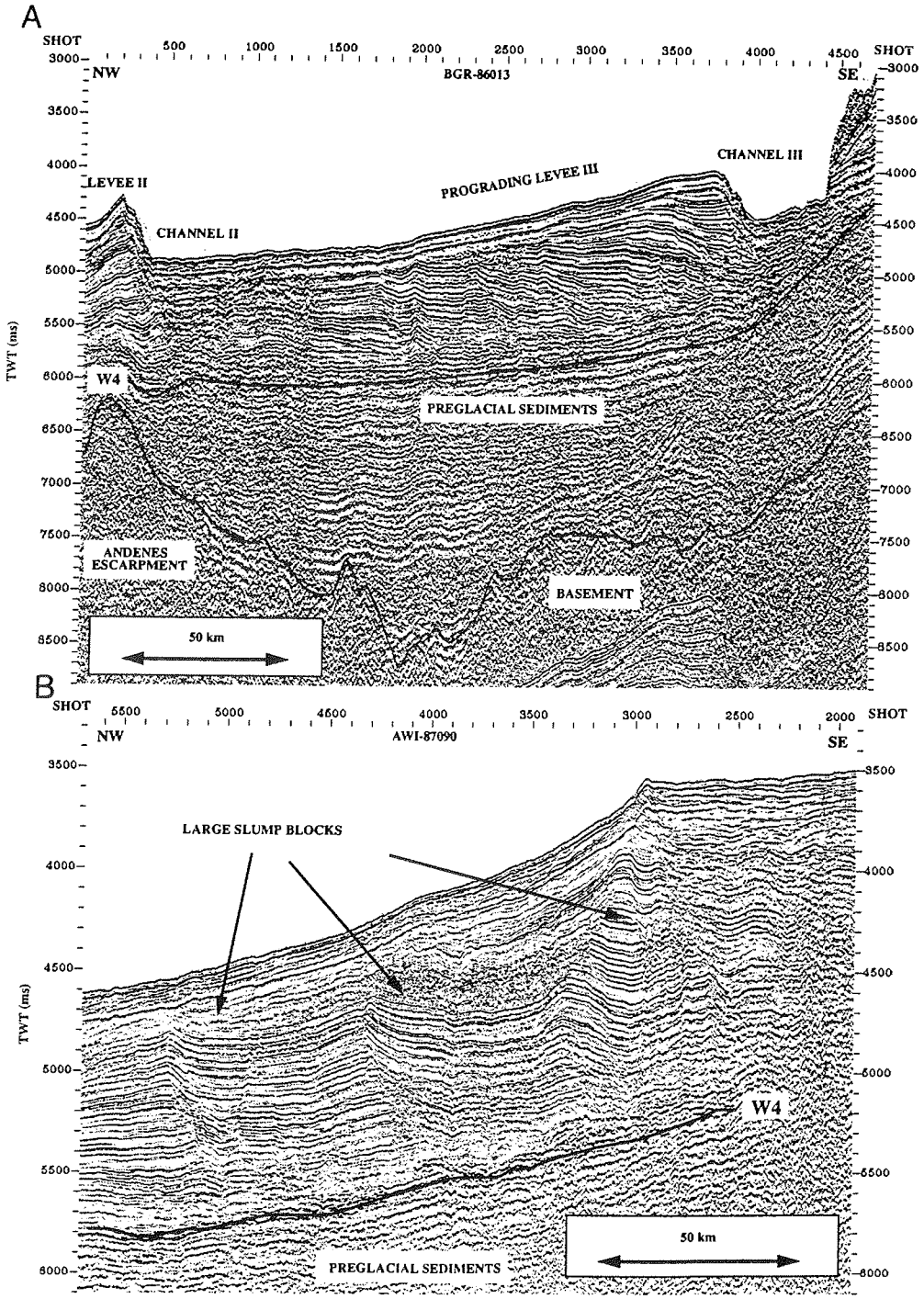

Fig. 6.6 **A)** Seismic section showing the more than 100 km progradation of channel/levee complex III. The position of channel II coincides with the Andenes Escarpment indicating that the trends of the channels are basement controlled. **B)** Large slump blocks can be observed in levee III. Profile location in Fig. 6.1.

silt, formed as overbank deposits interbedded by hemipelagic sediments (Anderson et al., 1986; Kuhn & Weber, 1993; § 4.6).

In the proposed model, the prevailing process responsible for the formation of the *channel/levee* system is turbidity sedimentation and, to a lesser extent, winnowing and deposition by thermohaline currents (Anderson et al., 1986; Kuhn & Weber, 1993; Kuvaas & Kristoffersen, 1991). Seismic units buried by sediments, but having the acoustic characteristics described above, are also interpreted as channel/levee facies.

Current controlled sediment facies The upper sediment package of the middle and lower slope area on the Dronning Maud Land margin (Fig. 6.2) shows dramatically different acoustic characteristics than that of the underlying unit. It appears as low amplitude, highly continuous, thin layered reflectors that drape over the basal unconformity of the sequence. The unit is up to 200-300 ms thick and tapers off upwards. The small, branching tributaries of the Wegener Canyon appear as v-shaped valleys within this sediment body (W5, Fig. 6.7a and 6.7b). These gullies are bordered by continuous, converging reflectors. ODP site 693 penetrated this sediment facies (Barker et al., 1988). Its basal unconformity correlates with the Middle Miocene hiatus, W5 (Miller et al., 1988), the unit itself consists of upper Miocene to Recent silty mud and clay (Fig. 6.8a).

The strong change in acoustic characteristics associated with this facies signals the increased role of contour currents during sedimentation (Barker et al., 1988). The invigoration of current activity was probably induced by the Late Miocene cooling and by the expansion of the East Antarctic Ice Sheet (Miller et al., 1988)

Debris flow facies Large reflection-free sediment facies are intercalated into channel/levee sequences on the Weddell Sea continental rise (Fig 6.9a). These reflection-free facies are also frequent on the lower continental slope of the Dronning Maud Land margin (Fig. 6.9b). The upper and lower unconformities bordering the acoustically-transparent sediment bodies are generally strong, rugged reflectors. On seismic profiles crossing the channel, these transparent units typically appear as channel fill deposits, strongly eroding the sides and the base of the channel (Fig. 6.9a). Along slope, the unit as a whole appears lens-shaped with a thickness of up to 300 ms (TWT) and a length of tens of kilometres.

At present, no direct geologic information is available concerning the nature of these sediments. But according to Bouma et al. (1983) and Sangree & Widmier (1977), the acoustic

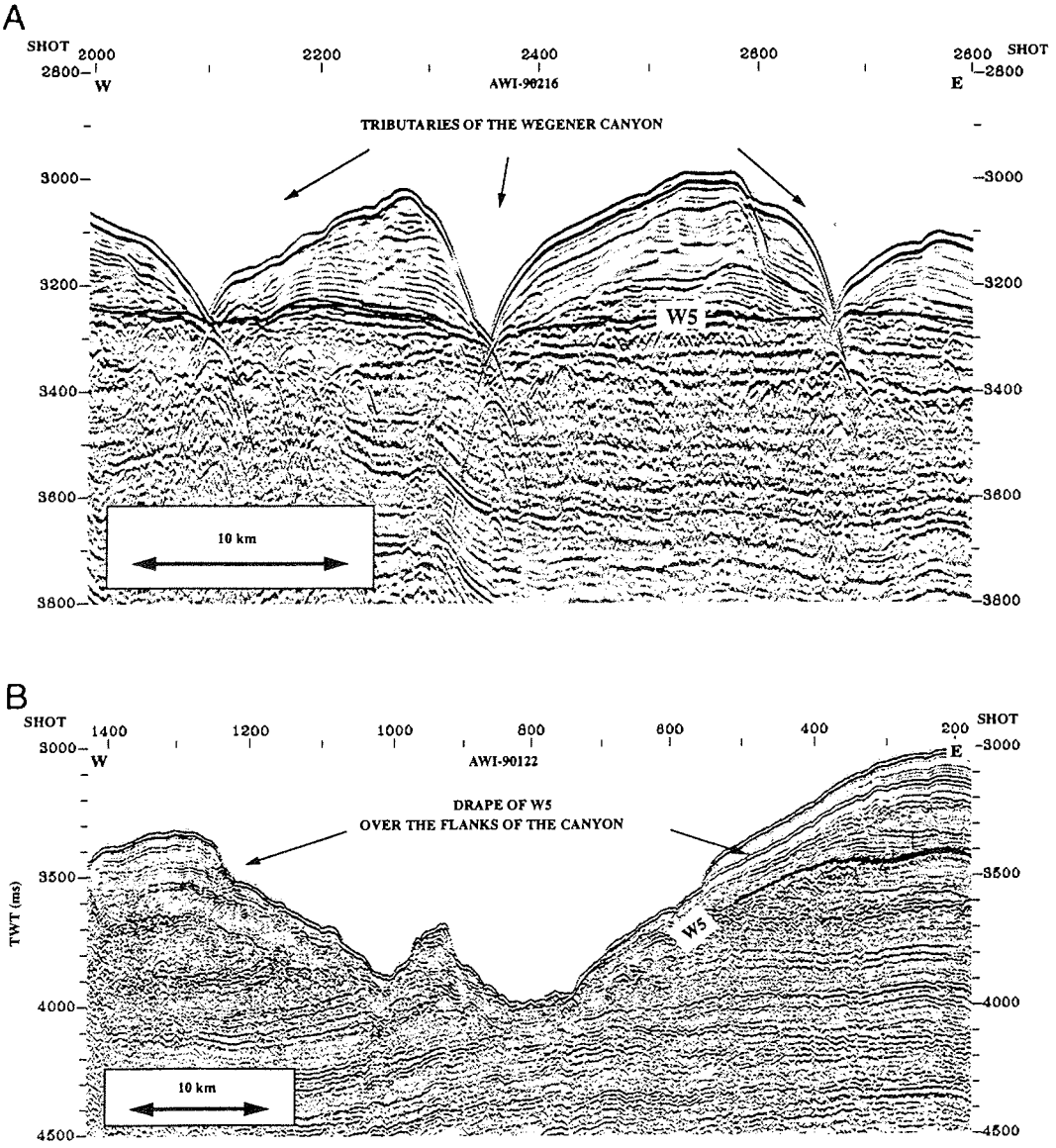

Fig 6.7 Seismic sections documenting two phases of canyon formation. **A)** The small tributaries of the Wegener Canyon have been formed since the onset of the deposition of the contourites, the W5 sequence. **B)** At greater water depths the drape of W5 over the flanks of the canyons indicates an earlier phase of canyon cutting. Profile location in Fig. 6.1.

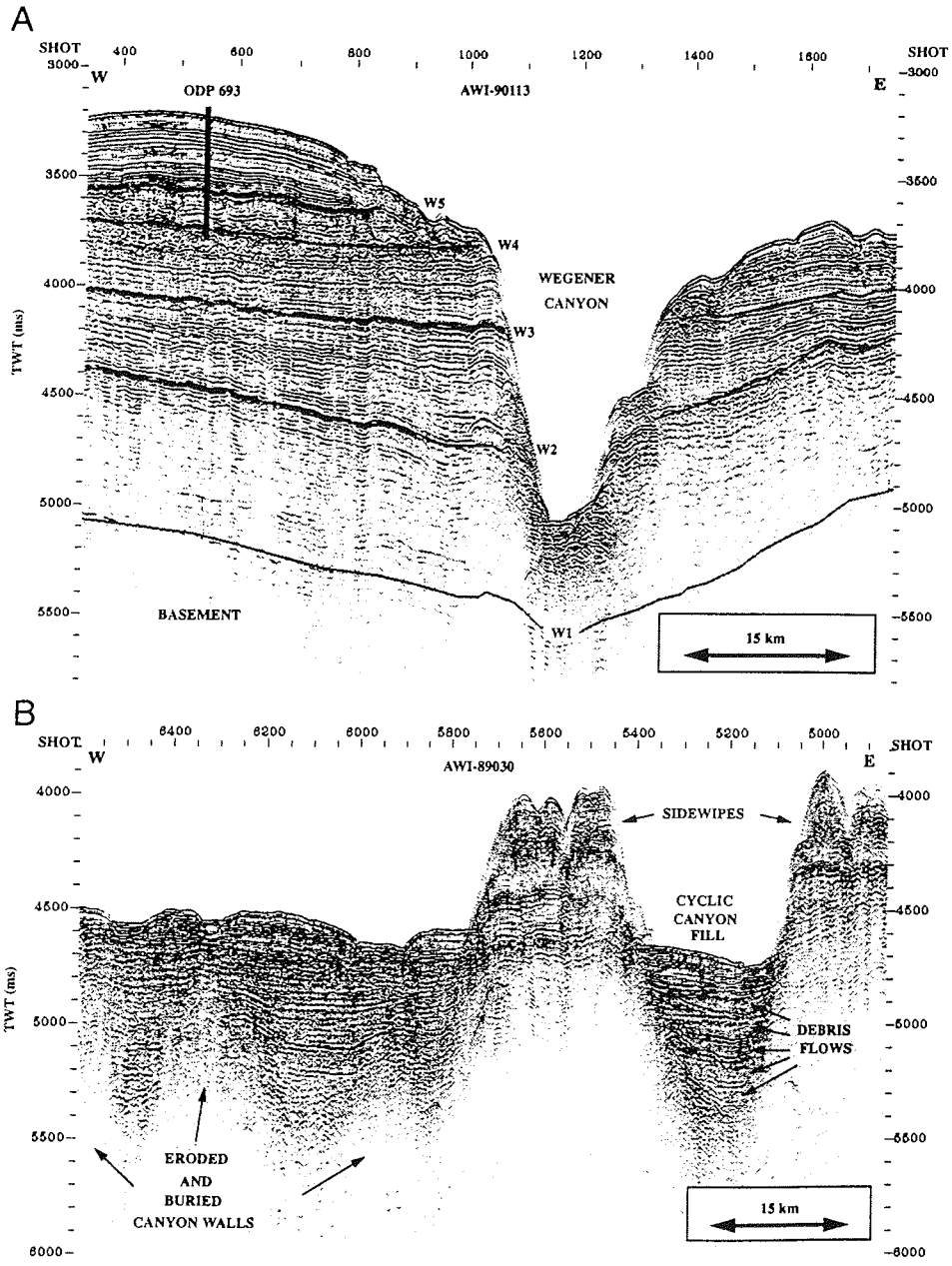

Fig. 6.8 **A)** Seismic profile showing the seismic sequences W1-W5 and ODP Site 693. The continuity of the reflectors of W1-W3 sequences across the Wegener Canyon indicates that canyon cutting postdates the formation of W3. **B)** In the vicinity of the Crary Fan, a seismic section documents eroded canyon walls and canyon infill formed as channel/levee complex III migrated eastward, eroded and partly closed the outlets of these canyons. Profile location in Fig. 6.1.

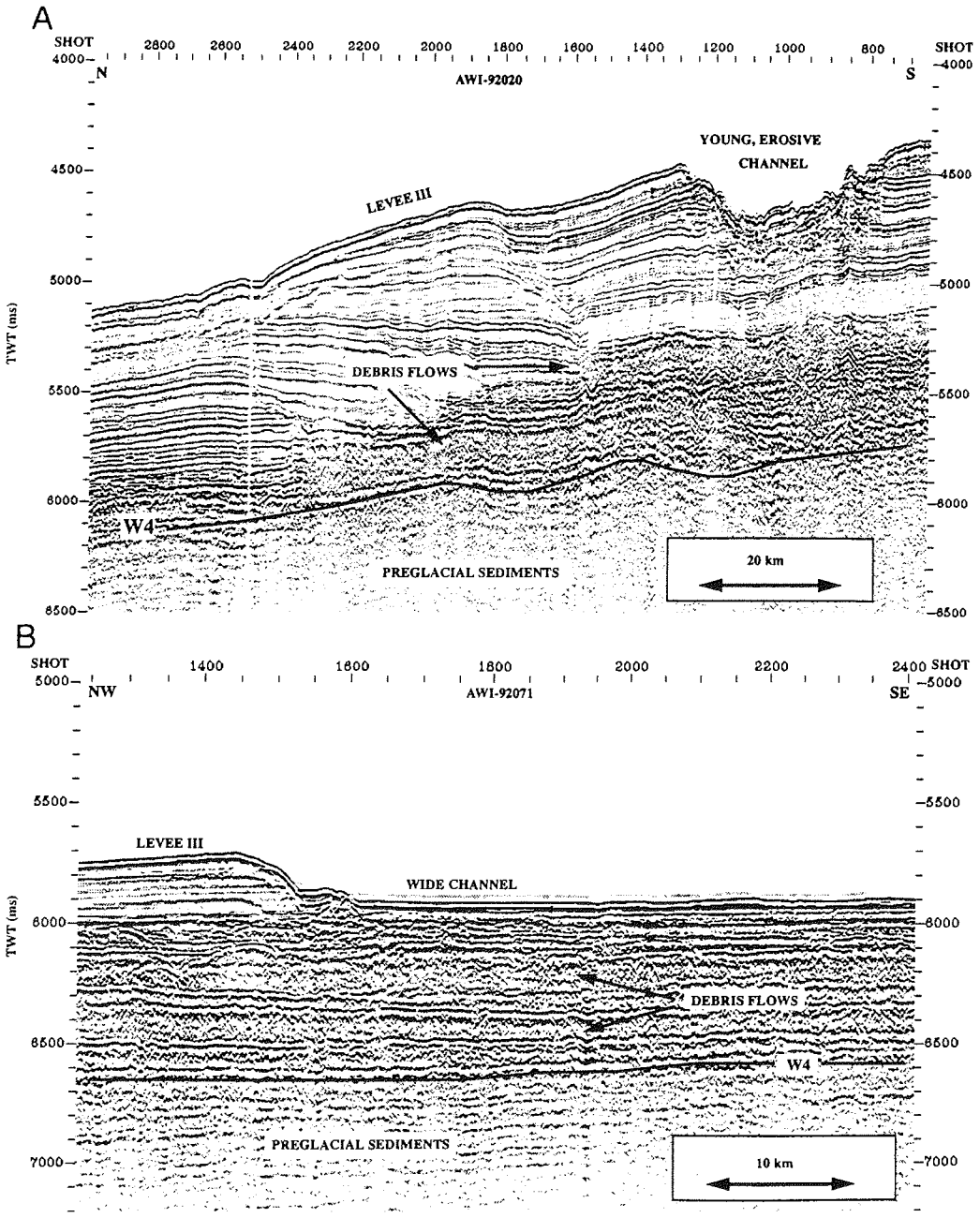

Fig. 6.9 **A)** Seismic section showing that debris flows interfinger with channel/ levee facies. **B)** In easterly direction, the importance of channel/levee sedimentation decreases and debris flows become dominant. Profile location in Fig. 6.1.

characteristics of these facies indicate debris flow deposits or slumped bodies. Bart et al. (1994) have interpreted this facies in a similar manner (§ 4.6).

These acoustic characteristics are also consistent with a different depositional process. At the base of large growth faults, sediment fluidization and slumping occur (Fig. 6.6b) marked by chaotic to undulating seismic bodies (Miller et al., 1988; § 4.6). These units can appear very similar to those described above. Hence, the internal reflection pattern alone is not sufficient to identify the debris flow facies. The depositional environment (channel fill or within-levee position) often helps to distinguish between these possibilities.

The small-scale debris flows of the prograding wedge and the vast debris flows described above occur in different stratigraphic positions (cf. Fig. 6.3, Fig. 6.9) and dominate in different water depths (Fig 6.2). Hereafter, *debris flow facies* will mean the large, chaotic, transparent bodies on the continental rise.

Hemipelagic drape facies On the flat top of the Polarstern Bank, uniform sedimentation is observed (Fig. 6.2). Highly continuous, subparallel reflectors build up a sheet-drape external geometry. Piston cores recovered hemipelagic sediments from these facies showing low sedimentation rates and no sign of current-controlled deposition (Gersonde, pers. comm.; § 5).

6.2 The Architecture of the Glacial Sediments From Seismic Facies

On the upper slope of the Crary Fan, channel/levee systems are covered by the prograding wedge facies. As this cover tapers off downslope, channel/levee facies emerge from it and can be followed through hundreds of kilometres on the Weddell Sea continental rise (Fig. 6.2). The base of the channel/levee facies was tentatively correlated with the W4 unconformity (Fig. 6.8a) of ODP Site 693 (Miller et al., 1988). The correlation indicates that the fan development started by the Early Oligocene.

The Dronning Maud Land continental slope is also covered by the prograding wedge facies. This sediment body forms a narrow and steeply dipping stripe here (Fig. 6.2). Reflectors of the prograding wedge facies downlap onto its basal unconformity. This downlap surface can be correlated with the W5 unconformity on seismic lines located in the vicinity of the ODP Site (Fig. 6.4a). The W5 unconformity forms the lower boundary of the acoustically laminated, current controlled sediments or contourites at the ODP Site 693 (Fig. 6.8a). The correlation of the base of the current controlled sediments and the prograding wedge indicates simultaneous deposition of these facies started by the Late Miocene. Numerous canyons cut deeply into the preglacial deposits downslope of the prograding wedge (Fig. 6.2). On the continental rise, debris flow facies interfinger with the channel/levee facies (Fig. 6.9a) partly by infilling the channels and partly by eroding the levee deposits.

Between 25° W and 22° W on the Dronning Maud Land margin, the continental shelf has a depth of 200-300 m and a gentle slope of 3° (Fig. 3.3). Canyons can be followed up to the shelf edge and do not terminate in the middle slope as it is common in the adjacent areas. Here the prograding wedge facies is completely missing and acoustically thin bedded, current controlled deposits cover the entire slope. These observations suggest that this part of the margin was not effected by glacial erosion and deposition. At worst, the shelf may have been covered by a thin, stagnant grounded ice sheet that caused little erosion or sedimentation.

6.3 Depositional History of the Seismic Facies

6.3.1 The Channel/Levee (CL) Facies

Three major channels and their associated levees form the main architecture of the Crary Fan (Kuvaas & Kristoffersen, 1991). This structure is also reflected in the topography of the lower slope and continental rise (Fig. 6.2). The CL complexes are designated I, II and III, numbered from west to east. Each individual CL complex comprises several stacked CL systems, representing the different growth phases of the CL complex.

Below the cover of the prograding wedge, the reflectors of the CL complexes can be traced up to the shelf. They prograde and aggrade the shelf in contrast to the dominating progradation of the covering facies (Fig. 6.3a). CL facies constitute a more gentle dip than the overlying reflectors. The extrapolation of the basal unconformity of the CL facies to the shelf indicates that the shelf edge must have been advanced about 70-80 km since the onset of the deposition of this sequence (Kuvaas & Kristoffersen, 1991). The base of the fan was correlated with the W4 unconformity of ODP Site 693. It gives an Early Oligocene age for the onset of the fan growth (§ 4.6).

All three CL complexes turn gradually eastward, downslope, until they run parallel to the Dronning Maud Land coast. This general eastward turning is probably controlled by the basement topography (Fig. 6.6a). Channels are bordered on the west by the basement ridge of the Andenes Escarpment, and on the east by the continental margin. They are deflected eastward by the crustal depression caused by the load of the Polarstern Bank.

CL complex I was interpreted by Kuvaas & Kristoffersen (1991) to be the oldest of the three complexes. This structure is only partly covered by the prograding wedge. It is located at the margin of the bathymetric bulge (Fig. 6.2) where the lens-shaped body of the prograding wedge becomes thinner. The available seismic and bathymetric data are insufficient for a detailed study of this CL complex. This complex consists of several CL systems, and probably had a complicated history. The major ridge of this complex is strongly eroded (Fig. 6.5a). Its channel seems to be covered by sediments of the prograding wedge suggesting that the CL system is inactive at present. West of this ridge, younger, active channels can be observed. The lack of pronounced levees indicates erosional rather than depositional features. These younger channels may have conducted the Ice Shelf Water flow, a strong thermohaline

current that has been observed in this area (Foldvik et al., 1985; § 4.2).

CL complex II has a simpler history than complex I. It consists of a single channel that has been stable for a long time (Fig. 6.5b). This channel is younger than CL complex I (Kuvaas & Kristoffersen, 1991). Later, deposits of the prograding wedge gradually covered CL complex II on the upper slope. This new sediment source reactivated the channel. It became wide at the foot of the prograding wedge, and narrowed quickly downslope (cf. Fig. 6.5b, Fig 6.6a). Probably turbidity currents fed and eroded the channel in this second growth phase. They were generated by small-scale debris flows and slumps rising in the prograding wedge.

CL complex III is younger than complex II (Kuvaas & Kristoffersen, 1991) as evidenced by the onlap of levee III reflectors on levee II (Fig. 6.5b). The progradation of the levee deposits and the existence of high amplitude, discontinuous channel facies below the entire CL complex III shows the gradual eastward migration of the channel (Fig. 6.6a) over a distance of 100 km. Originally, channel II and III merged into one channel at the northern tip of Polarstern Bank (Fig. 6.2). Later, however, channel III changed its bed. It cut between the two southern seamounts of the Polarstern Bank to form what it is at present: a slope-base channel. The reason for the change of the channel bed was probably the eastward migration of the complex. It caused a narrowing of the channel between Polarstern Bank and its well developed western levee. A slump of the levee or a bigger debris flow then closed this narrow gorge, forcing the channel to turn sharply eastward.

At least three major debris flows interfinger with the CL deposits of complex III (Fig. 6.9a). These deposits can be correlated with channel fill facies on the Dronning Maud Land margin (Fig. 6.8b).

With the commencement of the deposition of the prograding wedge the sediment input decreased from the Crary Fan direction to the continental rise. The numerous, smaller tributaries of the Dronning Maud Land margin became the main sediment source of CL complex III. The presently active Deutschland Canyon (Fig. 6.3b) reflects this phase of channel development. The cover of the prograding wedge explains why no continuation of the channel can be found on the upper slope in the present morphology of the fan (Fig. 6.2).

Large growth faults and slumping can be observed in all the levee sediments, but are best developed on complex III (Fig. 6.6b). These phenomena can be attributed to the rapid deposition of fine grained

material resulting in overpressured/undercompacted conditions (Miller et al., 1988; Kuvaas & Kristoffersen, 1991).

Asymmetric build-up is common in channel/levee complexes with a better developed levee on their western side and a less pronounced, often missing one on their eastern side (Fig. 6.5b). The Coriolis force deflects northward flowing currents towards the west. Thus, it may cause preferential western levee development (Kuvaas & Kristoffersen, 1991; Kuhn & Weber, 1993; Andersen et al., 1986). Another possibility is offered by the Weddell Gyre. It flows towards the west in this area, and may wash away suspended sediments and cause higher sedimentation rates on the western levees (Bart et al., 1994; Kuvaas & Kristoffersen, 1991).

On the continental rise in the vicinity of the Polarstern Bank, CL systems are strongly asymmetric. Long term current measurements found that flow velocities of the Weddell Gyre in this area were negligible, the annual averages were less than 1 cm/s (Fahrbach et al., 1994; § 4.2). Current controlled sedimentation requires several times higher velocities. The assumption of a paleo-current system that would have had average velocities much higher than at present, seems unlikely. Sediment cores from Polarstern Bank show no sign of strong currents during the last 4 Ma (Gersonde, pers. comm.; § 5). The lack of strong bottom currents and the observed asymmetry of the CL systems in this area suggest that the prevailing effect causing the asymmetric levee build-up is the Coriolis force rather than the Weddell Gyre.

6.3.2 The Prograding Wedge and the Current Controlled Sediments

Despite the general structural similarity between the prograding wedge facies of the Crary Fan and the Dronning Maud Land margin, several drastic differences can be observed. The average slope of the Crary Fan is about 1.5° as opposed to the approximately 15° inclination of the upper continental slope east of it. The upper slope of the Crary Fan reaches below 3000 m. On the Dronning Maud Land margin, it terminates above 2000 m with a distinct change in inclination. As a result of these differences, the width of the prograding wedge on the Crary Fan exceeds 100 km, whereas the Dronning Maud Land upper slope is only about 10 km wide (Fig. 6.2). Since the formation of the prograding wedge facies started, the Crary Fan shelf break advanced at least 30 km (Fig. 6.3a) in contrast to the approximately 10 km progradation of the eastern steeper slope (Fig. 6.4a). On the Dronning Maud Land upper slope, the foot of the prograding wedge facies turns into current controlled, acoustically thin bedded facies (Fig. 6.4a). The

prograding wedge of the Crary Fan continues into the channel facies of complex III, feeding it with debris flows and turbidites.

These distinct differences may be attributed to two basic factors influencing the sedimentation: the amount of sediment input and the flow velocity of the Antarctic Coastal Current.

The Crary Fan has a huge drainage area compared to its relatively narrow inlet. The Dronning Maud Land margin has a smaller drainage area which feeds a long coastline (§ 4.1). The sediments, alone, carved out from the Filchner Shelf have a vast volume, orders of magnitude greater than those removed from the smaller troughs of the Dronning Maud Land shelf. Thus, a much higher sediment input can be expected in front of the Crary Fan than on the adjacent areas.

The Antarctic Coastal Current (ACC) reaches relatively high average velocities of up to 16 cm/s on the eastern part of the margin (Fahrbach et al., 1994; § 4.2). At approximately 27° W, however, the ACC splits into two branches. The one following the Filchner Shelf edge has a lower mean speed of 6-7 cm/s (Foldvik et al., 1985a; § 4.2). The Coriolis force contributes to the erosional potential of the current. It deflects the current to the left against the slope. Due to the higher velocities and the larger N-S component of the current on the Dronning Maud Land margin, the Coriolis force has greater effect on the current in this area.

The strong current activity and the lower sediment input on the Dronning Maud Land margin may have caused an effective winnowing of glaciomarine diamicton on the upper slope. These badly sorted, sand-prone lag deposits allow very steep slopes. These sediments are responsible for the 15° dip of the upper slope. The winnowed, fine-grained material may have been sedimented contemporaneously further downslope. It could have formed the current controlled deposit facies, or it could have been transported to the Crary Fan realm.

On the Crary Fan, a higher sediment input and weaker currents prevented the formation of lag deposits. A significant portion of the prograding wedge covering this area was probably eroded from the Filchner Shelf during the formation of the Crary Trough. This implies redeposition of partly non-glacial sediments on the Crary Fan. This material having a fine-grained component could not form steep of slopes as the unsorted lag deposits on the Dronning Maud Land margin.

Close to the area of normal depth shelf and gently dipping slope, current controlled sediments onlap on the prograding wedge (Fig. 6.4b). This configuration differs from the relation of these facies at other places. Here, the formation of the prograding wedge had

ceased, but the deposition of current controlled sediments continued. It indicates that a grounded ice sheet advanced to the shelf edge and built up the prograding wedge during an earlier glaciation. Later, the ice advances may not have reached the shelf break, though the deposition of the current controlled sediments continued. This is not an unlikely scenario as the profile lies close to a shelf area that was unaffected by major glacial erosion.

A rough estimate of the volume of the sediments build-up in the prograding wedge and the sediments eroded from the Crary Trough has been computed and compared.

The Filchner Shelf topography was determined by the bathymetric map of Vaughan et al. (1994). It was assumed that the shelf had a typical depth of 200 m before the onset of glacial erosion. Complete isostatic rebound was also supposed which is plausible, since the last documented grounded ice advance onto the outer shelf occurred 31 ka BP (Solheim, 1990; § 4.1) and the time constant for isostatic recovery is about 3 ka (§ 4.1). The present Antarctic Ice Sheet can only account for a small portion of the depth of the trough. A terrestrial ice sheet with a thickness of 1800 m would produce a proglacial depression 155 m deep (Cooper et al., 1991). The Crary Trough is bounded by floating ice shelves and by grounded ice with an average thickness of 500-1000 m (Drewry, 1983). Thus, the isostatic effect of the present ice sheet is less than 10% of the 1500 m depth of the trough. This crustal depression caused by the present ice load was neglected. Seismic reflection profiles indicate that the depression was glacially eroded and not tectonically formed (Haugland et al., 1985).

Overcompaction due to ice grounding, decompaction during erosion and compaction after sedimentation were not considered. Only the volume of sediments eroded north of the southern tip of Berkner Island was taken into account. Because this is the site where the ice stream splits: one branch follows the Crary Trough, the other is located west of Berkner Island. Nor was the winnowing of sediments of the prograding wedge considered. This is reasonable, since sediment cores from this facies contain a fine grained fraction (§ 4.6) and since low current velocities were detected in this area (§ 4.2).

A simple model was used for the geometry of the trough. Its cross section was approximated by a sine curve with a constant maximum depth below the Filchner Ice Shelf and a shallowing sine-shape depth north of it. The volume of eroded sediments was estimated to be 24100 km^3 below the Filchner Ice Shelf and 22600 km^3 in front of it. This gives a total of 46700 km^3 excluding sediments eroded south of Berkner Island.

A chalet-roof geometry tapering downslope, truncated by a horizontal plain at the depth of the shelf break, was used in estimating the volume of the prograding wedge. This results in 13000 km^3 for the total volume of this sediment body.

Due to their simplifications, the estimates may have large errors. A brief accuracy analysis indicated, however, that the true values probably lay between one half and twice the given estimations. (Sediments eroded by ice upstream from Berkner Island could not be included in this analysis.) Even this level of accuracy allows us to draw some interesting conclusions.

It might be expected that the volume of the prograding wedge would be somewhat larger than the volume of sediments eroded from the shelf. This mass balance would mean that the grounding line was on the inner shelf, close to the coast before the ice sheet first reached the shelf edge. With the first prominent ice advance, the grounding line would have advanced across the shelf, reached the shelf edge and deposited the first layer of the prograding wedge. During later glaciations this cycle would have been repeated.

But the estimates clearly show that this was not the case. The volume of the sediments eroded by the Filchner Ice Shelf is more than three times the volume of the prograding wedge. Even the sediments eroded oceanward of the present Filchner Ice Shelf have a greater volume than that of the prograding wedge. Therefore, most of the sediments must have been removed from the Crary Trough before the onset of deposition of the prograding wedge. By that time, the trough must have extended to a position north of the present day Filchner Ice Shelf edge. This also means that most of the sediments eroded from the shelf are incorporated in the channel/levee facies, rather than in the prograding wedge facies.

A grounded ice sheet advanced to the shelf edge builds up prograding wedge facies as evidenced by the Prydz Bay drilling studies (Cooper et al., 1991; § 4.4) and by investigations of different glaciomarine sedimentary environments (Powell, 1984; § 4.3). Thus, it is improbable that the grounding line reached and long remained at the shelf edge during the deposition of the channel/levee facies. A plausible interpretation of these data is as follows. The grounding line of the ice sheet advanced several times across the shelf, eroding sediments and reaching a position between the edge of the present day Filchner Ice Shelf and the shelf break. During ice advances, probably the sub-ice topography determined the position of the grounding line. Ice congested and remained grounded in the narrow passage between Berkner Island and East Antarctica, but it became afloat as it reached the broad shelf in front of the island. Following a climatic deterioration, cold ice conditions were established, the ice sheet advanced to the shelf edge and the deposition of the prograding wedge commenced.

6.3.3 Canyons and Debris Flows

On the Dronning Maud Land margin, large canyons cut into the Explora Escarpment. These canyons are associated with the major glacial troughs carved into the continental shelf. Further to the west, numerous deeply incised canyons can be found without any observable relation to shelf structures (Fig. 3.3).

Some constraints on the onset of canyon cutting can be derived from seismic profiles. The sheet-drape configuration of the current controlled sediments covering the canyon walls indicates that the canyon started to form before the deposition of these facies (Fig. 6.7b), i.e. before the Late Miocene. This observation is further supported by the results of ODP Site 692 (§ 5). Further upslope, the formation of the small tributaries of the Wegener Canyon appears to be contemporaneous with the deposition of current controlled sediments (Fig. 6.7a). It suggests a second phase of canyon cutting. On seismic profiles crossing the Wegener Canyon, the reflectors of sequence W3 and of the underlying sequences can be correlated across the two sides of the canyon. They run approximately horizontally, lie at the same depth on both sides of the canyon and show sharp truncation at the canyon walls (Fig. 6.8a). This reflection configuration suggests that canyon cutting post-dates the deposition of these sediments, thus it occurred after the Albian/Aptian.

A cyclic fill can be observed in the canyons at the western part of the Dronning Maud Land margin (Fig. 6.8b), but it is missing from the canyons further to the east (Fig. 6.8a). Thicker, transparent seismic facies and units of high amplitude, discontinuous reflectors cover each-other in turn (Fig. 6.8b). Up to five such cycles can be detected. Some of the transparent units can be traced downslope and correlated with the debris flow deposits interfingering with sediments of channel/levee complex III (Fig. 6.9a). This correlation indicates that canyon cutting occurred before the deposition of channel/levee complex III. The eastward migration of this channel/levee complex is probably responsible for the initiation of the canyon fill. As the CL complex migrated, it gradually closed the narrow outlets of these canyons. Its vast western levee acted as a sill retaining sediments transported by the canyons. The lower part of the canyon walls were partly eroded and partly covered by the eastward migrating channel of CL complex III (Fig. 6.8b). Further to the east, the channel diverges from the lower termination of the canyons (Fig. 6.2), therefore it did not initiate canyon fill in this area (Fig. 6.8a).

In summary, canyon cutting must have started before the Late Miocene, but after the Aptian/Albian, a time span of some 100 Ma. The most prominent unconformity encountered at ODP Site 693 was the Lower Oligocene/Cretaceous hiatus (W4). About 300 m of sediments were removed by the erosional event causing this hiatus (Barker et al., 1988). The Eocene/Oligocene boundary coincides with widespread deep sea hiatuses (Kennett & Barker, 1990) and also with the commencement of the ice sheet growth in Antarctica. Therefore, the Eocene/Oligocene boundary is proposed as the time of the initiation of the canyon cutting on the Dronning Maud Land margin.

Before the deposition of the current controlled sediments, the prevailing sedimentation process on the Dronning Maud Land margin west of the Explora Escarpment was the generation of large debris flows. Seismic profiles crossing the lower continental slope show these lenticular, acoustically transparent bodies stacked onto each other (Fig. 6.9a). On the continental rise moving away from the Crary Fan, the importance of channel/levee deposition decreases and debris flows become dominant in front of the Explora Escarpment (Fig. 6.9b). Debris flow deposits interfinger with channel/levee complexes on the continental rise suggesting a contemporaneous deposition of these facies.

6.4 Glaciomarine Sedimentation in the Weddell Sea: A New Scenario

Due to climatic deterioration at the Eocene/Oligocene boundary, a continental scale ice sheet started to form on East Antarctica (Ehrmann, 1993, § 4.1). Freezing commenced at the Antarctic margin initiating bottom water formation and development of widespread marine hiatuses (Kennett & Barker, 1990). This erosional event formed the W4 unconformity at ODP site 693 by eroding some 300 m of sediments (Barker et al. 1988). Probably the same event is responsible for the onset of incision of the numerous canyons on the Dronning Maud Land margin.

From the Early Oligocene to the Late Miocene, the Antarctic Ice Sheet was temperate and wet based (§ 4.1) and did not have the polar character it has today. Vegetation existed in several areas of Antarctica (Kennett & Barker, 1990); and the main ice discharge mechanism was melting rather than iceberg calving. A grounded ice sheet episodically advanced to a position north of the northern tip of Berkner Island, but did not reach or stay long on the shelf break. The temperate ice sheet supported large amounts of suspended sediments in meltwater streams providing favourable conditions for rapid build-up of channel/levee systems. On the Dronning Maud Land margin, lower sediment input caused sediment starvation (Barker et al., 1988; § 5). Occasionally, vast debris flows occurred eroding and partly filling the canyons. These debris flows can be found interbedded with channel/levee sediments on the continental rise.

In the Late Miocene, renewed cooling caused the re-advance of the grounding line, the establishment of polar ice conditions (§ 4.1) and the invigoration of current activity (Kennett & Barker, 1990; § 4.2). The grounded ice sheet episodically reached the shelf break, and deposited sediments directly on the slope forming the prograding wedge. Sediment input increased on the Dronning Maud Land margin (§ 5). Intensification of bottom water formation and contour current activity (§ 4.2) resulted in current controlled sedimentation on the middle slope. The higher sediment input initiated the rejuvenation of the canyons. The dominant ablation process changed from melting to iceberg calving. The time of the maximum ice extent on Antarctica was the Late Miocene (Ehrmann, 1993; § 4.1). During this time, the ice sheet had reached areas that later were unaffected by ice sheet erosion. This may explain the onlapping of contourites on the prograding wedge facies in some

areas. Channel/levee systems of the Crary Fan were also reactivated. Channels acted as conduits for turbidity currents initiated by debris flows or small slumps of sediments building up the prograding wedge. Strong, erosive thermohaline currents could also use the pre-existing channels eroding and transporting sediments downslope.

Sea-level lowstands, alone, can cause ice sheet advances even under an unchanged climate (Huybrechts, 1992; § 4.1). The waning and waxing of continental ice-sheets probably account for most of the third-order cycles of the eustatic see-level fluctuations (Vail et al., 1977b). Therefore, it is reasonable to assume that major glacial advances and retreats can be correlated with eustatic sea-level changes (Moons et al., 1992).

During glacial periods since the late Miocene, large amounts of sediment have been transported directly to the continental slope by grounded ice sheets. During interglacials, the deep sea floor was sediment-starved, and only strongly erosive thermohaline currents caused some sedimentation or sediment redeposition (Kuvaas & Kristoffersen, 1991; Kuhn & Weber, 1993).

From the Oligocene to the Late Miocene, the difference between sediment input in glacials and interglacials may not have been that great. During both periods, meltwater streams could transport sediments to the continental slope and rise. During interglacials, however, the greater distance to sediment source and lower sediment input resulted in somewhat reduced sedimentation rates.

6.5 Alternative Sedimentation Models of the Weddell Sea

By and large, the model proposed for the channel/levee deposition corresponds to that of Kuvaas & Kristoffersen (1991) with two major differences: the debris flow facies were not part of their model and the deposition of the prograding wedge was thought to be contemporaneous with the formation of channel/levee system III. The area where debris flow deposition predominates lies mainly outside the seismic network used by these authors, which explains the absence of this facies in their model. Several observations detailed above, such as the smooth upper slope, sediment cover over channel/levee facies and the change of the dip of the slope suggest that the deposition of the prograding wedge and the channel/levee facies occurred in two distinct phases. This interpretation resolves the contradiction that the channel/levee facies would have been deposited from a grounded ice sheet that had advanced to the shelf break.

Bart et al. (1994) suggested large scale debris flows on the Crary Fan. They proposed that the deposition of these facies resulted from the collapses of large shelf edge deltas. The shelf edge deltas were deposited from a grounded ice sheet. They argued that the formation of the channel/levee systems, i.e. the fan development, is related to this process.

But the formation of an upper-slope diamictit apron, the prograding wedge, clearly post-dates the main deposition phase of the channel/levee facies. Furthermore, no major scar caused by large-scale slope failures can be observed on the present day slope morphology. These suggest that the process that formed the channel/levee facies was not related to major collapses of large shelf-edge deltas. However, the interpretation of these chaotic/transparent facies as debris flows was adopted from this model.

Anderson et al. (1986) suggested that the formation of the Crary Fan dates back to pre-glacial times. It seems reasonable that not only post-Eocene, but also previous sea-level lowstands caused fan growth in the Weddell Sea. But the correlation of the W4 unconformity with the base of the fan sequence (Miller et al., 1988), and the dramatic change in sedimentation due to the commencement of glaciation, suggest that the main period of fan growth occurred during glacial times.

Kuhn & Weber (1993) interpreted piston core data from levee facies as laminated, current controlled deposits and to a lesser extent as turbidites. They concluded that the prevailing sedimentation process that built up the channel/levee systems was current controlled deposition from thermohaline flows rising on the shelf or upper slope. The onset of bottom water formation at high latitudes dates back to Early Oligocene times (Kennett & Barker, 1990). Even if they were not as vigorous as at present, thermohaline currents already existed in the Early Oligocene.

But the shallow piston core data provide a high resolution record only of the last few glacial cycles. Thus, the sedimentation model proposed by Kuhn & Weber (1993) covers this time interval and may correspond to the development of the prograding wedge or to the intense glacial/interglacial cycles that began in the Late Pliocene. Seismic investigations indicate that the main phase of channel/levee development occurred earlier, thus it is probably not represented in the piston core data. The model proposed by these authors fits the seismic picture describing the formation of the prograding wedge.

The main phase of fan growth probably occurred under more temperate climatic conditions than those documented by the piston cores. During temperate ice conditions, thermohaline currents play a lesser role in sedimentation; partly, because sedimentation from meltwater streams carrying large amounts of suspended material dominates; and partly, because temperate ice conditions require temperatures above the freezing point at sea level for most of the year.

The intense glacial/interglacial cycles in the Weddell Sea starting at about 2.5 Ma ago (§ 4.1) were associated with glaciation in the northern hemisphere and with global sea level fluctuations (Ehrmann, 1993). These fluctuations should have induced a distinct change in sedimentation process of the Weddell Sea.

To incorporate this event into the sedimentation model, the timing of the horizons must be shifted. In this alternative model, the base of the prograding wedge would correspond to the onset of intense glacial/interglacial cycles at 2.5 Ma, since this horizon represents the latest prominent change in sedimentation process. The lower unconformity of the channel/levee system could be correlated with the Late Miocene ice growth. The frequent ice advances to the shelf edge would then be responsible for the build-up of the prograding wedge. From the Late Miocene to Upper Pliocene (2.5 Ma) the grounding line would have stayed mainly at an inner shelf position advancing only occasionally to the shelf edge. Sediments would have been transported across the shelf to the slope by water currents causing channel/levee build-up.

This model would explain the relatively high sedimentation rates of turbidites at ODP Site 694 from the Middle Miocene to Early Pliocene (§ 5). It would also explain the sharp decrease of sedimentation at this site starting in the Lower Pliocene as a result of the commencement of the build-up of the prograding wedge. With the wedge established, fan development would have ceased causing a decrease of turbidity sedimentation on the continental rise and abyssal plain.

The lack of fan sequences older than Late Miocene could be attributed to the low sedimentation rates (5 m/Ma) found at Site 693 between 100 Ma and 12 Ma (§ 5). At about 12 Ma, sedimentation rates drastically increased (21-46 m/Ma) at this site, and then decreased again in the Latest Pliocene (10 m/Ma). This would correspond to the onset of turbidity sedimentation and to the beginning of the formation of the prograding wedge, respectively.

But for this model to be true, the correlation of both W4 and W5 horizons must be wrong, and the Weddell Sea should have had a glacial history significantly different from that of the Ross Sea and Prydz Bay. It could be argued that the some tens of meters of Pliocene to Recent sediments (2.5 Ma x 10 m/Ma) found at ODP Site 693 are below the resolution of the conventional seismic measurements. This can be the reason for the lack of the Upper Pliocene unconformity in seismic sections. The turbidites of Site 694 may also have their origin on the Antarctic Peninsula margin instead of the Crary Fan.

6.6 Problems, Questions and Flaws - The Proposed Model Under a Magnifier

The lack of good constraints and dating anchor points is the major weakness of all geologic and tectonic models of the Weddell Sea. The only borehole control of the proposed model is from two closely located sites having a major Cretaceous/Early Oligocene hiatus spanning about 60 Ma. From there, the horizons had to be correlated over more than 600 km of seismic lines cutting numerous canyons and different sedimentary environments, in order to date the lower unconformity of the Crary Fan and the prograding wedge facies. Another approach to date the horizons was to correlate the probable sedimentary environments of the seismic facies with the known milestones of Antarctica's glacial history. Although, these different approaches give dates that are in excellent agreement, due to the lack of adequate borehole control the result should be considered tentative.

The model suggests that the onset of fan growth occurred in the Early Oligocene. The question arises, why did not the warm and humid climate and the eustatic sea-level changes initiate fan deposition before Oligocene times?

An another implicit assumption is that the seismic facies, e.g. the prograding wedge formed simultaneously along the entire margin. This is reasonable, if there is no other information, but it may not be true. It obviously fails, for example, at one place on the margin, where the current controlled sediments onlap on the prograding wedge, but correlate elsewhere. The same criticism applies to the main erosional events, for example the canyon cutting, which was also assumed to be contemporaneous along the entire margin.

A different, but similarly basic flaw of this model is that the whole interpretation of the debris flow facies is based only on its acoustic characteristic.

7. Basement Structures and Potential Field Data as Constraints on the Tectonic Evolution of the Weddell Sea

Gondwana, the southern supercontinent with East Antarctica at its center, began to fragment during Late Jurassic times which led to the separation of South America, Africa, India and Australia. The southeastern Weddell Sea came into existence when South America and Africa separated from the rest of Gondwanaland. In the last two decades most of the basic questions concerning the reconstruction and breakup history of Gondwana have been answered. However, the history of West Antarctica, especially the Weddell Sea Basin, is still an enigma.

Breakup models of the Weddell Sea encounter two major difficulties:
1) the continent-ocean boundary is poorly defined in the Weddell Sea Embayment and 2) in reconstruction models, the present shape of Antarctica results in an unacceptable overlap on undoubtedly continental crust of the Antarctic Peninsula and Falkland Plateau.

To clarify the questions concerning the formation of the Weddell Sea, the evolution and architecture of the affected crustal blocks is briefly outlined in the first part of this chapter. Next, new constraints are presented on the geodynamic evolution and structure of the Weddell Sea continental margin derived from marine seismic and potential field data. Different breakup models are then tested using the new findings. The morphology of the continental margin predicted by these models is compared to the interpreted tectonic units, and their similarities and differences are discussed in detail to give guidance for future modelling. Finally, a tentative breakup model is proposed and discussed.

7.1 Continents, Microcontinents, Aseismic Ridges and Rift Basins

The marine geophysical reconnaissance survey of the Weddell Sea started in the late 1970s. Several important structures were discovered and mapped such as the Explora Escarpment, the Andenes Escarpment and the Polarstern Bank (Fig. 7.1), but a few crucial questions remained such as the origin of the Orion Anomaly or the crustal structure of the Filchner-Ronne Shelf (Fig 7.1).

Most reconstructions juxtapose the continental margins of Africa, South America and the southeastern Weddell Sea. The African and South American continental margins are better surveyed, but some basic questions like the continental or oceanic nature of the Mozambique Ridge or the pre-breakup position of the Falkland Islands are still debated (Fig. 7.1). The following briefly summarises our present understanding of the evolution and architecture of these areas.

The Falkland Plateau

The Falkland Plateau is a submarine projection extending from the South American continental margin to 1800 km east of the Falkland Islands. It can be morphologically divided into three blocks (Lorenzo & Mutter, 1987): an elevated microcontinental block to the east, the Maurice Ewing Bank, a marginal fracture ridge to the north and a central basin up to 8.5 km deep (Fig 7.1).

The basement of the Falkland Islands proves its continental origin, the overlying sedimentary rocks can be correlated with rocks of comparable age from South Georgia and southern Africa (§ 5). During ODP Leg 36, drilling reached granitic continental basement on the Maurice Ewing Bank (Harris & Sliter, 1977; § 5). Geophysical data, however, show possible evidences of Middle-Late Jurassic oceanic crust under the central plateau based on 1) basement volcanic edifices in seismic reflection profiles, 2) seaward dipping sub-basement reflectors, 3) high free air gravity anomaly over the deepest part of the basement, 4) estimates of crustal stretching = 2.8 (Lorenzo & Mutter, 1987) and 5) sonobouy profiles (Ludwig, 1983).

Using the angular distance between M4 and the continental margin magnetic anomaly measured on the conjugate African margin, the continent-ocean boundary can be projected backward from anomaly M4 identified in the Georgia Basin. This projection places the continent-ocean boundary near the center of the Maurice Ewing Bank and suggests that the floor of the Falkland Plateau

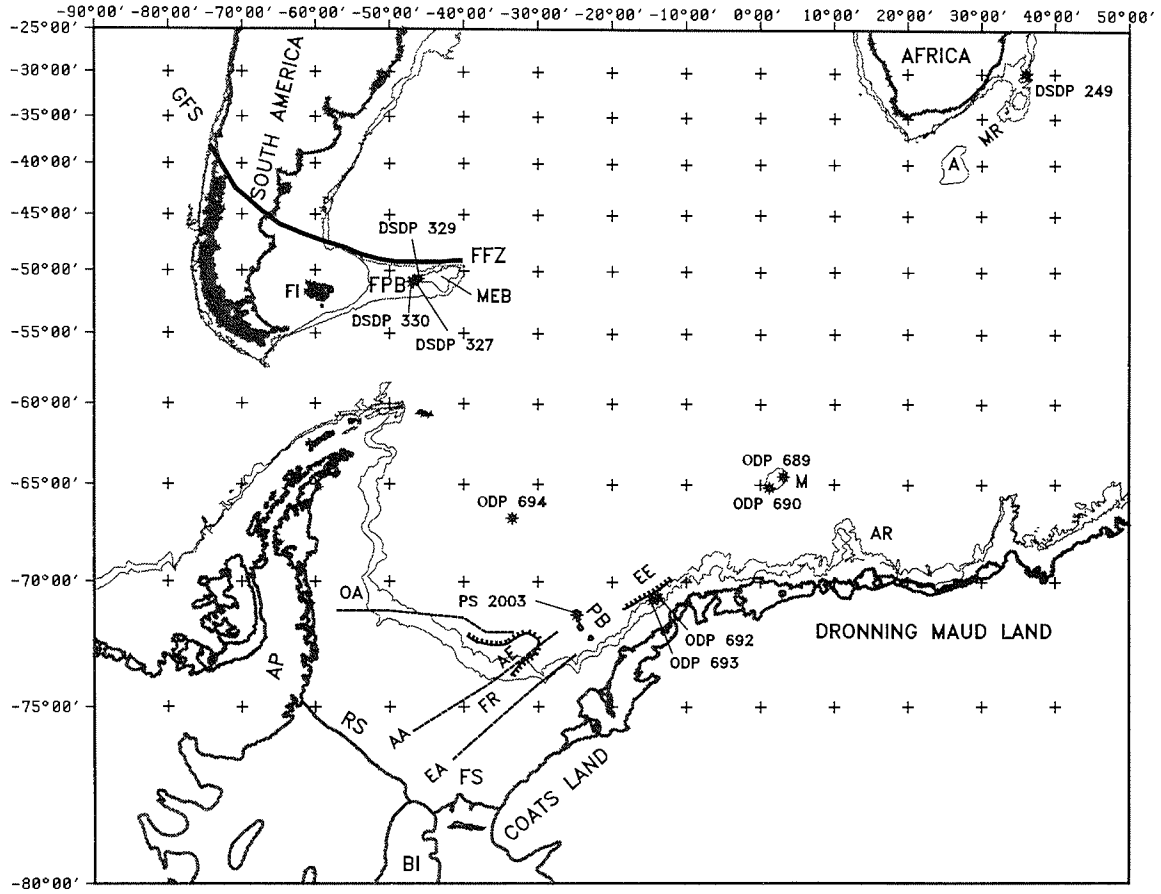

Fig. 7.1 Tectonic structures in the Weddell Sea sector: Agulhas Plateau (A), Mozambique Ridge (MR), Astrid Ridge (AR), Maud Rise (M), Gastre Fault System (GFS), Falkland Fracture Zone (FFZ), Falkland Islands (FI), Falkland Plateau Basin (FPB), Maurice Ewing Bank (MEB), Antarctic Peninsula (AP), Ronne Shelf (RS), Filchner Shelf (FS), Berkner Island (BI), Explora Anomaly (EA), Andenes Anomaly (AA), Orion Anomaly (OA), Andenes Escarpment (AE), Failed Rift (FR), Explora Escarpment (EE) and Polarstern Bank (PB).

Basin may have represented a zone of seafloor spreading during the early rifting of South America and Africa (Ludwig, 1983).

Paleomagnetic poles from Jurassic dykes in the Falkland Islands show a significant rotation (100°) occurred prior to the opening of the South Atlantic. This early rotation, if true, is not well dated. Most authors associate it with the early opening of the Weddell Sea (Marshall, 1994; Grunow et al., 1991).

Thus, it seems reasonable to keep the present shape of the Falkland Plateau in reconstructions during Cretaceous times. A possible minor stretching may have occurred as the Falkland Plateau separated from Africa. In the Middle-Late Jurassic, rifting and seafloor spreading changed the shape of the plateau. It may have been accompanied by microplate reorganisation. Though, the exact timing and magnitude of this process is not known, it was closely associated with the earliest opening of the Weddell Sea.

The Mozambique Ridge

The Mozambique Ridge is a north-south trending submarine plateau that runs parallel to the southeastern coast of Africa (Fig. 7.1). Predrift reconstructions suggest two possible paleo-positions for the plateau. Some propose an overlap of the present-day margins of Africa and East Antarctica at the Mozambique Ridge (Martin & Hartnady, 1986; Lawver & Scotese, 1987). They assume that the plateau formed later of oceanic crust; or alternatively, it is a continental fragment that drifted to its present position after the continental breakup (Fig. 7.2). Other reconstructions fit the Mozambique Ridge to the East Antarctic margin (Norton & Sclater, 1979; Lawver et al. 1991; Fig. 7.3). The eastern side of the plateau terminates in a cliff-like escarpment (>27°), called Mozambique Escarpment (Lawver et al., 1991). If the latter fit is correct (Fig. 7.3), then the Mozambique Escarpment was adjacent to the Explora Escarpment (Fig. 7.1) on the southeastern Weddell Sea margin and forms the conjugate pair of this transform margin (Lawver et al., 1991).

Fracture zones can be clearly traced on satellite gravity maps from the eastern side of the Mozambique Ridge to the western side of the Astrid Ridge, Antarctica (Fig. 7.4). At present, the Astrid Ridge (13° E) lies some 500 km from the Explora Escarpment (15° W). Transform movement or strongly oblique spreading on a scale required by the gravity data for juxtaposing the Mozambique and Explora Escarpments was not reported from the East Antarctic margin. Therefore, the Mozambique Escarpment is not considered to be the conjugate pair of the Explora Escarpment. Thus, Gondwana reconstructions of the first group (Fig. 7.2) will be applied in this thesis.

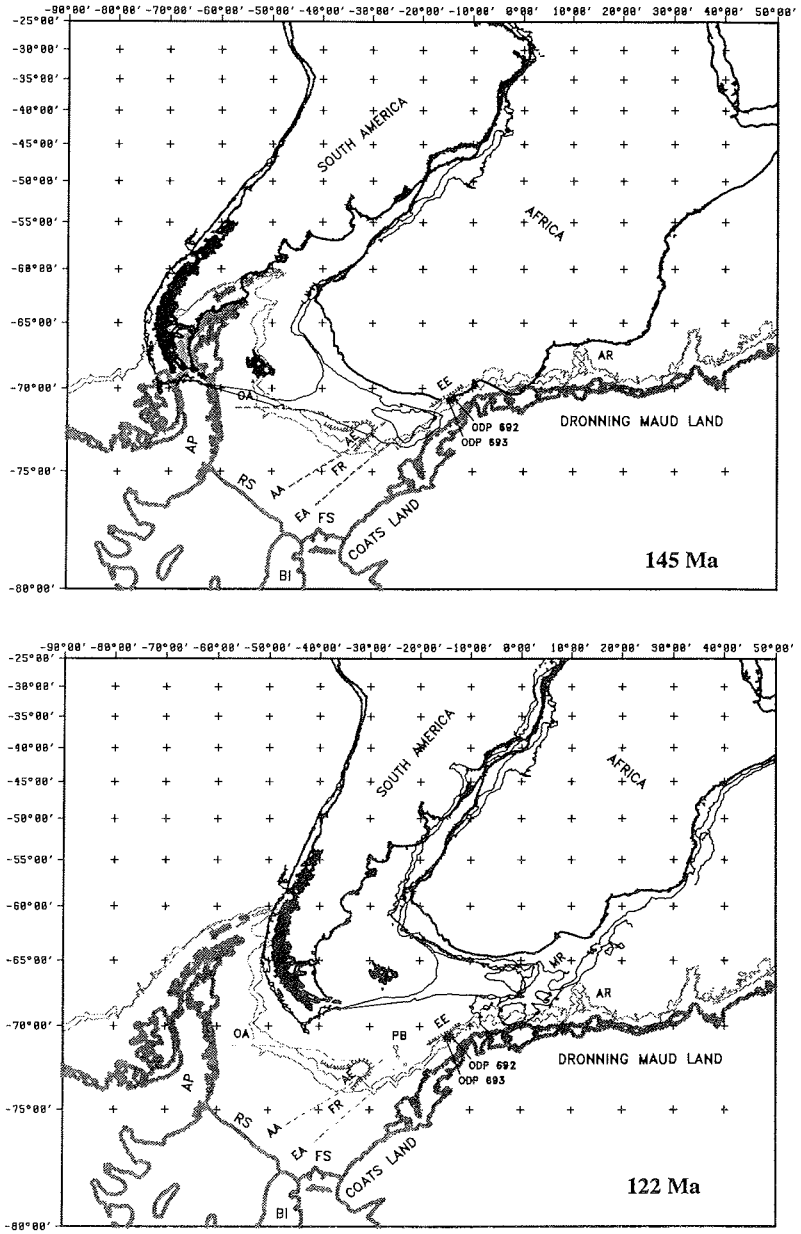

Fig. 7.2 Gondwana reconstruction (145 Ma) and the early opening of the Weddell Sea (122 Ma) after Martin & Hartnady (1991) with East Antarctica held fixed. Continents are outlined by the coastlines and by the 2000 m and 3000 m isobaths. Antarctica's crustal blocks are shown in their present positions; the symbols have the same meaning as those in Fig. 7.1. The reconstruction juxtaposes the East African Coast and the Explora Escarpment. The Mozambique Ridge is a later formed oceanic plateau in this reconstruction. The Mozambique Ridge and the Astrid Ridge are assumed to have been in a proximal position at 122 Ma. The model predicts strike-slip motion between Falkland Plateau-East Africa and the Explora Escarpment.

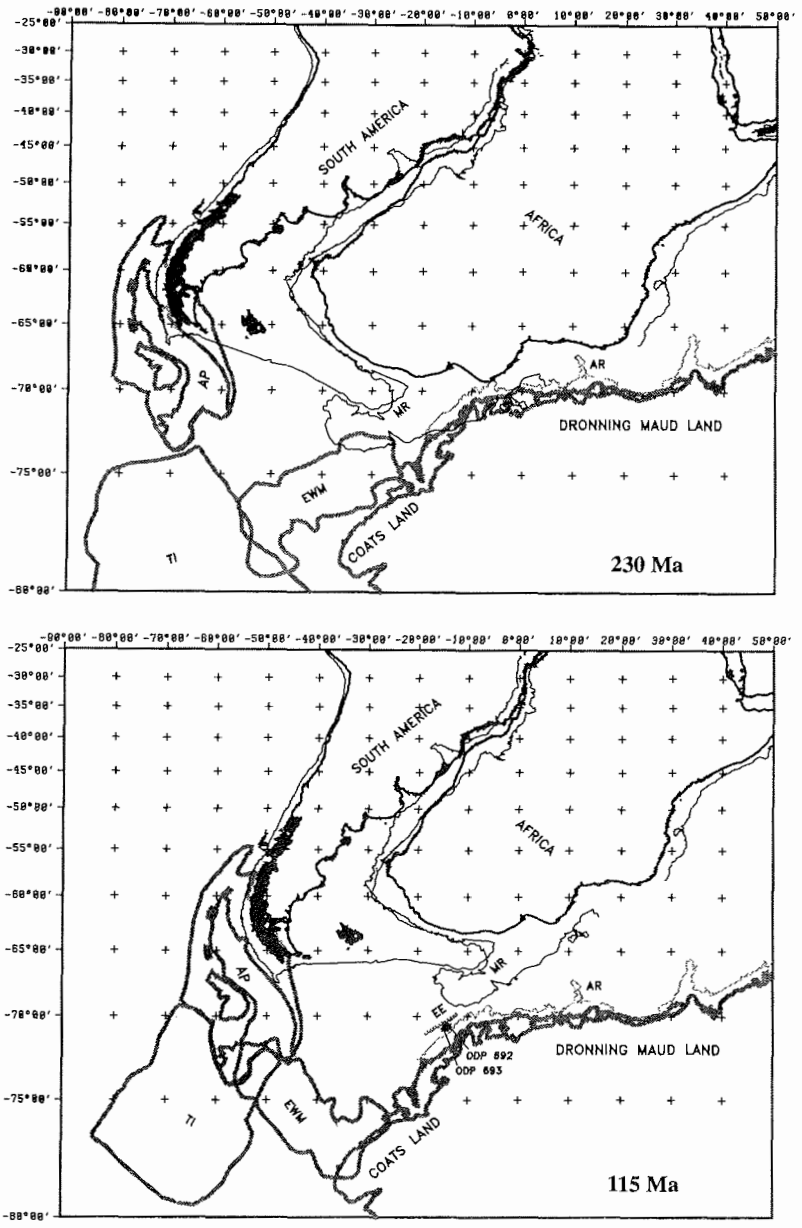

Fig. 7.3 Gondwana reconstruction of Grunow et al. (1991) with East Antarctica held fixed. The Norton & Sclater (1979) fit was used for the 230 Ma and 115 Ma paleopositions of South America and Africa (Grunow et al., 1991). Continents are outlined by the coastlines and by the 3000 m isobaths. AP: Antarctic Peninsula, TI: Thurston Island, EWM: Ellsworth Whitmore Mountains, MR: Mozambique Ridge, AR: Astrid Ridge, EE: Explora Escarpment. The reconstruction juxtaposes the Mozambique Ridge and the Explora Escarpment. At 115 Ma about 500 km oceanic crust separates the Mozambique Ridge and the Astrid Ridge. Strike-slip movement is predicted between the Mozambique Ridge and the Explora Escarpment.

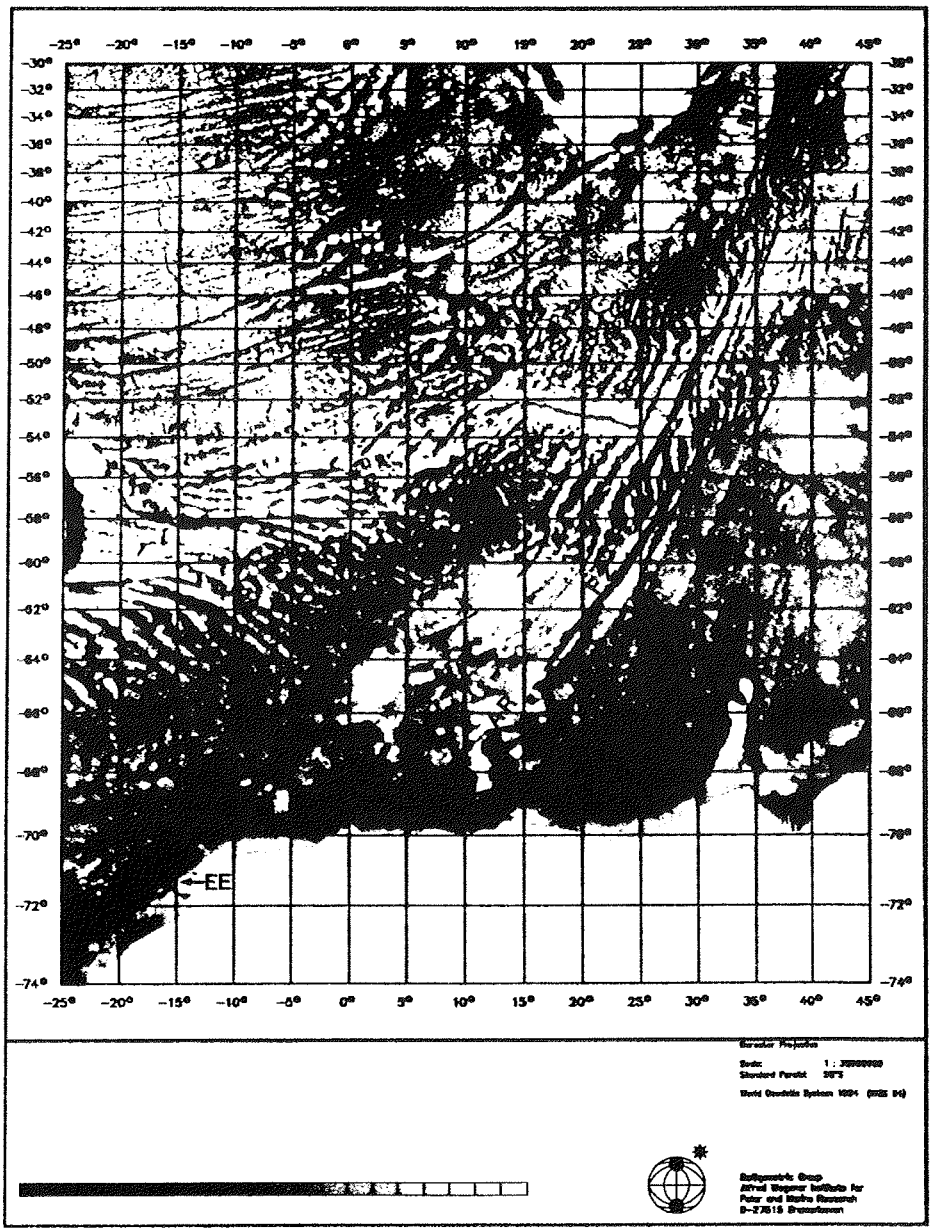

Fig. 7.4 Marine gravity anomalies from GEOSAT and ERS-1 (Schöne, unpublished map). Note the fracture zone (FZ) connecting the Astrid ridge (AR, 66°S 13°E) and the Mozambique Ridge (MR, 34°S 35°E). The map indicates that the Explora Escarpment (EE, 71°S 15°W) was probably not formed as the conjugate pair of the MR.

Agulhas Plateau-Maud Rise

Seismic refraction and reflection profiles indicate the Agulhas Plateau (Fig. 7.1) is a continental fragment that broke off the Falkland Plateau and was intruded by basaltic magmas during the early opening of the south Atlantic (Allen & Tucholke, 1981). Dredge hauls recovered low to high grade continental metamorphic rocks and basaltic igneous samples (Allen & Tucholke, 1981). The northern part of the plateau is assumed to be of oceanic crust formed during the separation of Falkland Plateau from southern Africa (Martin & Hartnady, 1986). Reconstruction models place the Agulhas Plateau south of Falkland Plateau. Thus, they probably formed a single microplate before the opening of the south Atlantic (LaBrecque & Hayes, 1979; Martin & Hartnady, 1986). These reconstructions also juxtapose the Agulhas Plateau and the Maud Rise.

Since the pre-rift size and position of the continental part of the Agulhas Plateau is uncertain, it will not be used in reconstructing the Weddell Sea. It must be noted, however, that a continental fragment, the Agulhas Plateau, lay south of the Falkland Plateau before the opening of the South Atlantic. Hence, the pre-drift shape of the Falkland Plateau was somewhat different from that shown in reconstructions (Fig. 7.2 - 7.3).

The continental mosaic of West Antarctica

West Antarctica was a mosaic of microcontinents during the Gondwana breakup compared to the structural unity of the East Antarctic Shield. That much is clear from the sub-ice topography, from the lack of continuity of related geologic units, and from the overlap of the Falkland Plateau and Antarctic Peninsula in rigid plate reconstructions (Dalziel & Elliot, 1982).

A deglaciated West Antarctica would be an archipelago with the main land masses separated by deep troughs and basins reaching depths of 2500 m. The troughs could be considered tectonically controlled boundaries or glacially-scoured structures (Storey, 1992).

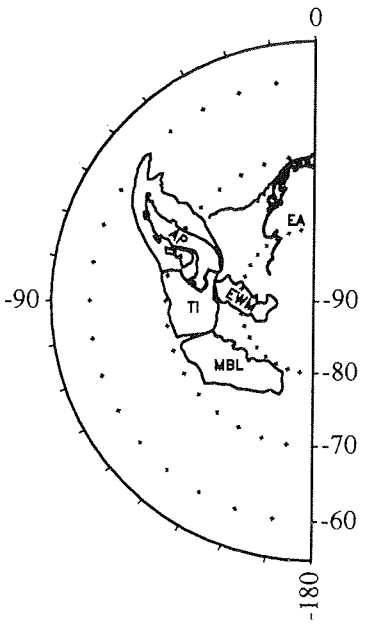

Fig. 7.5 West Antarctica's crustal blocks. Plate bounderies are from Lawver (pers. comm.), for legend see text.

Dalziel & Elliot (1982) subdivided West Antarctica into four morphologically and geologically related crustal blocks (Fig. 7.5): the Antarctic Peninsula (AP), the Thurston Island with part of the Eights Coast (TI), the Ellsworth Mountains including the ridge extending towards the Thiel Mountains (EWM) and the Marie Byrd Land (MBL) crustal blocks. Despite the general agreement about their existence, the areal extension and the relative movements of West Antarctica's crustal blocks are matters of considerable dispute (discussed later).

The geological history of the Antarctic Peninsula and the Ellsworth-Whitmore Mountains crustal blocks is closely related to the opening of the southeastern Weddell Sea, and so it is well worth examining.

The Antarctic Peninsula

An active Pacific margin of Gondwanaland existed from Permian times that included the present day Antarctic Peninsula crustal block (Dalziel & Elliot, 1982; Elliot, 1991; Fig 7.1). The presence of a magmatic-arc rocks indicates that the Antarctic Peninsula was part of the immediate Pacific Margin of Gondwana and excludes the possibility that the Peninsula overlapped on Falkland Plateau before breakup.

In the back-arc environment of the Early Jurassic, a well documented change occurred from a compressional regime, during which the Permo-Triassic Gondwanian fold belt formed, to an extensional regime forming the broad extensional provinces of West Antarctica and South America. Storey et al. (1992) suggested that this change might be linked to a change in subduction zone parameters. The compression followed by extension may be the result of a reduction in plate boundary forces and a change from a shallower to a steeply dipping subduction zone. The active margin tectonic setting may also indicate that during the early opening phase, the Weddell Sea was rifted as a part of a back-arc basin associated with the Middle-Late Jurassic back-arc spreading of southern South America (Lawver & Scotese, 1987).

Paleomagnetic data show that the Antarctic Peninsula was near its present position with respect to East Antarctica by 130 Ma (Grunow, 1993). Its motion between 230 Ma and 115 Ma derived from paleomagnetic poles is shown in Fig. 7.3 (Grunow et al., 1991). These published paleo-positions of the Antarctic Peninsula were strongly modified two years later in Grunow (1993) which suggests that the Peninsula's paleopoles are still subject to major uncertainties.

The Ellsworth-Whitmore Mountains

A thick Paleozoic sedimentary sequence of the Ellsworth Mountains is similar to the Gondwana craton cover exposed along the Transantarctic Mountains and the southern coast of Africa. Of particular note, is the occurrence of Paleozoic glacial deposits and Glossopteris-bearing Permian strata (Dalziel & Elliot, 1982). Glossopteris has not been found on West Antarctica outside the Ellsworth Mountains. This stratigraphic comparison, together with the isolation of the mountains and their anomalous structural grain led to the suggestion that the Ellsworth Mountains were originally between the Transantarctic Mountains and the Cape Mountains (Fig. 7.3).

The anomalous structural trend and the strong easterly vergence of folds in the Ellsworth Mountains as compared to the cratonward vergence of the related southern African and South American folds indicate a counter-clockwise rotation of the mountains (Dalziel & Elliot, 1982). Paleomagnetic data from lower Paleozoic rocks support a rotation of approximately 90° in this sense. An additional 175 Ma paleomagnetic pole of the Ellsworth-Whitmore mountains was published by Grunow et al. (1987).

Other authors have disputed the proposed movement of the Ellsworth-Whitmore Mountains on the basis of marine seismic data (Kristoffersen & Haugland, 1986; Hübscher, 1994; Jokat et al., submitted).

The Explora Wedge

Hinz & Krause (1982) identified the Weddell Sea Continental Margin Unconformity as the most distinct seismostratigraphic unconformity of the southeastern Weddell Sea margin. It is associated with a striking change in seismic velocities. It forms the upper boundary of extensive wedge shaped bodies comprising oceanward dipping reflectors, the Explora Wedge (§ 4.5). Analogies from other continental margins and ODP results led to the interpretation that these wedge-shaped units were emplaced by eruption of massive sequences of volcanic rocks onto highly distended continental crust in a subareal or shallow marine environment (Hinz, 1981). Hinz & Kristoffersen (1987) suggested that the formation of this unit was associated with the early rifting of Gondwana. They also identified similar sub-basement reflectors on the flanks of the Andenes Escarpment.

White & McKenzie (1989) introduced a general model which explains the formation of the Explora Wedge. It suggests a common origin for the extensive breakup related volcanism of southern Africa (Karoo flood basalts), the terrestrial volcanism of the Dronning Maud Land and the terrestrial/shallow marine volcanism of the Explora Wedge. The formation of these huge amounts of

igneous rocks is associated with breakup above a thermal anomaly caused by a hot spot. The thermal anomaly is responsible for the increased decompressional melting of hot asthenospheric mantle generating large igneous provinces. The postulated hot spot (Crozet hot spot) was located approximately below the Lebombo Monocline (22°S, 32°E, at its present position).

Breakup related volcanic rocks can provide time constraints on the initiation of continental drifting (White & McKenzie, 1989). Extensive Jurassic volcanism is documented in both Antarctica and southern Africa. East Antarctic basaltic rocks can be divided into two igneous provinces based on their geochemical composition. The northern province comprising the volcanic intrusions and extrusions of Coats Land and Dronning Maud Land shows affinities with the Karoo basalts, and was interpreted as breakup related volcanism (White & McKenzie, 1989). The boundary between the two coeval provinces lies between the Dufek intrusions related to the Transantarctic Mountains type (Ferrar group) and the Theron Mountains which belongs to the Dronning Maud Land province. Karoo igneous rocks were formed during two main periods of basalt flood production: 193±5 Ma and 178±5 Ma (White & McKenzie, 1989). The tholeitic basalts of Dronning Maud Land are dated as 179-162 Ma ±6 Ma (White & McKenzie, 1989). Hinz & Krause (1982) and the subsequent researchers used this volcanism, which corresponds to the second phase of Karoo extrusions, to date the formation of the Explora Wedge and the onset of seafloor spreading in the Weddell Sea.

The Explora Escarpment, Andenes Escarpment, Failed Rift and Polarstern Bank

Between 20°W and 10°W, the Weddell Sea continental slope descends to the abyssal plain in two steps forming the Explora Escarpment (Fig 7.1). On its landward side, sub-basement reflectors of the Explora Wedge terminate against a basement ridge (Hinz & Krause, 1982; Kristoffersen & Haugland, 1986). Continuing along the strike of the Explora Escarpment, a 15-30 km wide basement high, the Andenes Escarpment (Fig. 7.1), with a basement relief of 600-2000 m was found (Kristoffersen & Haugland, 1986). Sub-basement, dipping reflectors similar to that of the Explora Wedge are seen on both sides of the Andenes Escarpment (Kristoffersen & Haugland, 1986). The basement high is collinear with a pronounced positive magnetic anomaly, the Orion Anomaly (Fig. 7.1), that can be followed to the close vicinity of the Antarctic Peninsula. Kristoffersen & Haugland (1986) suggested that the Explora and Andenes Escarpments formed one continuous structure that represented the Antarctic plate boundary. According to this interpretation, the escarpments mark a rifted or obliquely rifted

plate boundary formed during the breakup of Gondwana. They speculated that the plate boundary follows the Orion Anomaly beyond the extent of the seismic network up to the Antarctic Peninsula.

Hinz & Kristoffersen (1987) described a basement depression located south of the Andenes Escarpment (Fig. 7.6). The basement structure is flanked on its landward side by the Explora Wedge and on its northern side by dipping sub-basement reflectors of the Andenes Escarpment. A positive free air gravity anomaly of about 50 mgal is associated with the basement depression. Gravity modelling shows a substantial crustal thinning accompanying the anomaly. The basement depression cuts the shelf edge at about 33°W. Hinz & Kristoffersen (1987) interpreted the depression as a rift that had generated a 40 km wide strip of oceanic crust.

Kristoffersen & Hinz (1991) introduced a model in which the initial opening of the Weddell Sea occurred in two phases. During the first phase, the basement depression and the volcanic wedges were formed as elements of a later failed rift. A second phase began with a change in the regional stress field resulting in a transtensional movement between Africa and East Antarctica. By this time, seafloor spreading ceased along the initial rift, and a new rift axis formed. This movement caused the formation of the Explora-Andenes Escarpment as a new plate boundary and led to the opening of the Weddell Sea by sea-floor spreading. In this model, the Explora-Andenes Escarpment represents the continent-ocean transition.

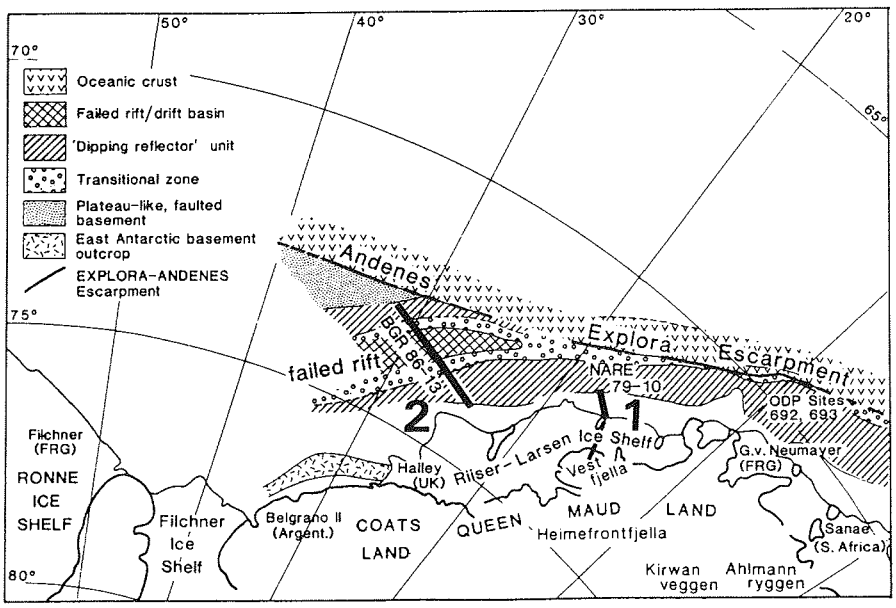

Fig. 7.6 Major geological structures of the survey area after Kristoffersen & Hinz (1991).

Miller et al. (1991) reported new seismic data from the area of the intersection of the failed rift and the Explora-Andenes Escarpment. They found no basement structure that could be interpreted as a link between the escarpments. They concluded that the Explora-Andenes Escarpment did not exist as a continuous structure. The Explora Escarpment represents the Antarctic plate boundary formed during the early opening of the Weddell Sea, the Andenes Escarpment probably has a different origin. Consequently, they suggested that the failed rift was not limited to the north by this boundary.

Henriet & Miller (1990) questioned the magmatic nature of the outer high of the Explora Escarpment. They proposed that the ridge is built up of stacked sedimentary rocks scraped off from oceanic crust in a compressive or transpressive deformational regime.

Johnson & Smith (1992) correlated the Explora Wedge with a magnetic high, the Explora Anomaly, which could be followed towards Berkner Island (Fig 7.1). On its western side, a prominent magnetic low is associated with the Explora Anomaly which was interpreted as the magnetic expression of the failed rift.

The seismic data reported by Miller et al. (1991) also revealed a basement structure located between the Explora Escarpment and Andenes Escarpment, the Polarstern Bank (Fig. 7.1), running approximately perpendicular to their trend. A distinct basement high of more than 2 km and a bathymetric rise of 400 m outlines this structure. A positive free-air gravity anomaly of 20 mgal is associated with the batymetric highs. Miller et al. (1991) described old, uplifted sediments on top of the Polarstern Bank. These uplifted sediments are onlapped on the flanks of the bank by younger deposits. The onlapped surface was correlated with the W4 unconformity giving a lower age limit of Late Cretaceous (Albian) for the development of the structure. Miller et al. (1991) interpreted the Polarstern Bank as a delayed crustal intrusion in the northern continuation of the failed rift axis.

Jokat et al. (in press) suggested a different interpretation. According to these authors, the Polarstern Bank is a seamount chain related to the volcanism of Vestfjella. They suggested that the onlap of old sediments on the western flank of the Polarstern Bank showed the structure was only slightly younger than the surrounding oceanic basement (about 150 Ma). A fracture zone or hot spot was assumed to be responsible for the development of the bank.

Filchner-Ronne Shelf

Reconstruction models placing the Ellsworth-Whitmore Mountains off Coats Land (Fig. 7.3) mostly propose or infer the presence of oceanic crust below the Filchner-Ronne Shelf (Grunow et al., 1991). The model of Hinz & Kristoffersen (1987) postulated stretched continental crust underlying the shelf with a narrow strip of oceanic crust represented by the failed rift. Russian deep seismic sounding seem to confirm this interpretation (Kudryavtzev et al., 1994). These seismic data also suggest the presence of a deep sedimentary basin beneath the Filchner-Ronne Shelf. Hübscher (1994) developed a similar model from seismic refraction profiles, in which a deep sedimentary basin (max. depth of 12 km) is underlain by stretched and underplated continental crust. Jokat et al. (in press) proposed that the continent-ocean boundary runs parallel to the isobaths of the continental slope of Coats Land and the Filchner-Ronne Shelf south of the Explora and Andenes Escarpments.

7.2 Compilation of the Marine Geophysical Data

An extensive marine seismic network was used to derive new constraints on the evolution and nature of the continental margin of the Weddell Sea (Fig. 7.7). A map of the acoustic basement was compiled from these data that outlines the boundaries and relations of the main tectonic units (Fig. 7.8). Details of the development of the mapped crustal blocks were deduced from seismic reflection profiles. Major basement structures were correlated with gravity (Fig. 7.9 and 7.10) and magnetic (Fig. 7.11) anomalies yielding further constraints on their nature. The correlation allows the mapped tectonic units to be followed beyond the extent of the seismic network. Results of these studies will be presented in this chapter.

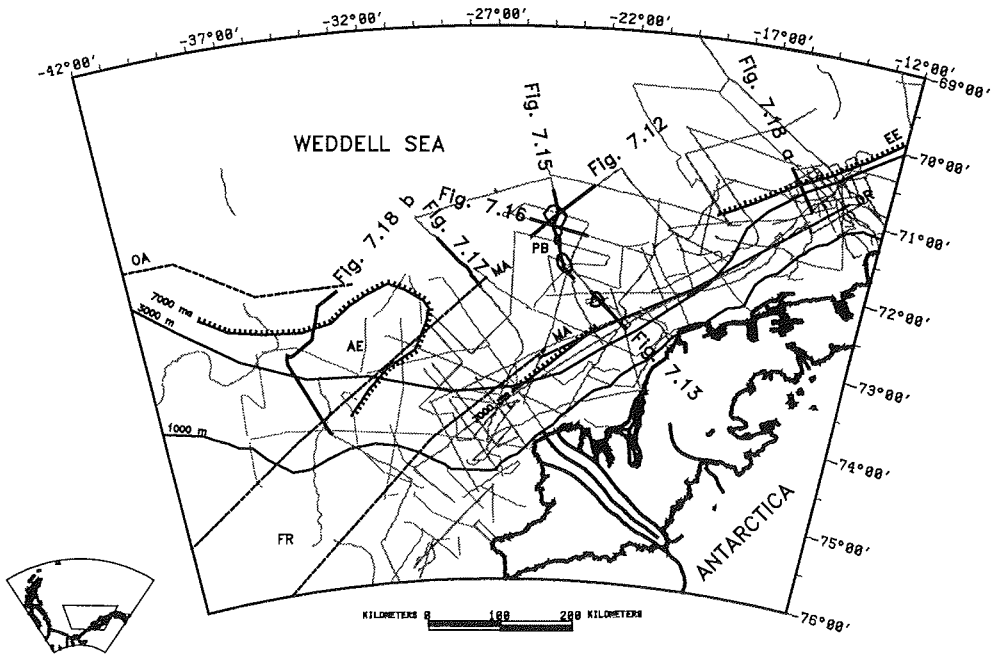

Fig. 7.7 Map showing the multichannel seismic network of the survey area. Black bars indicate locations of profile-segments illustrated in this chapter. The principal structural features are also shown: OA: Orion Anomaly, AE: Andenes Escarpment, EE: Explora Escarpment, PB: Polarstern Bank, FR: failed rift arm. DR: dipping reflectors of the Explora Wedge derived from seismic data, the unit forms a more than 50 km wide swath along the line. MA: magnetic lineations, c.f. Fig. 7.11. The 7000 ms isopach was digitized from the basement map. The 1000 m and 3000 m isobaths are also shown.

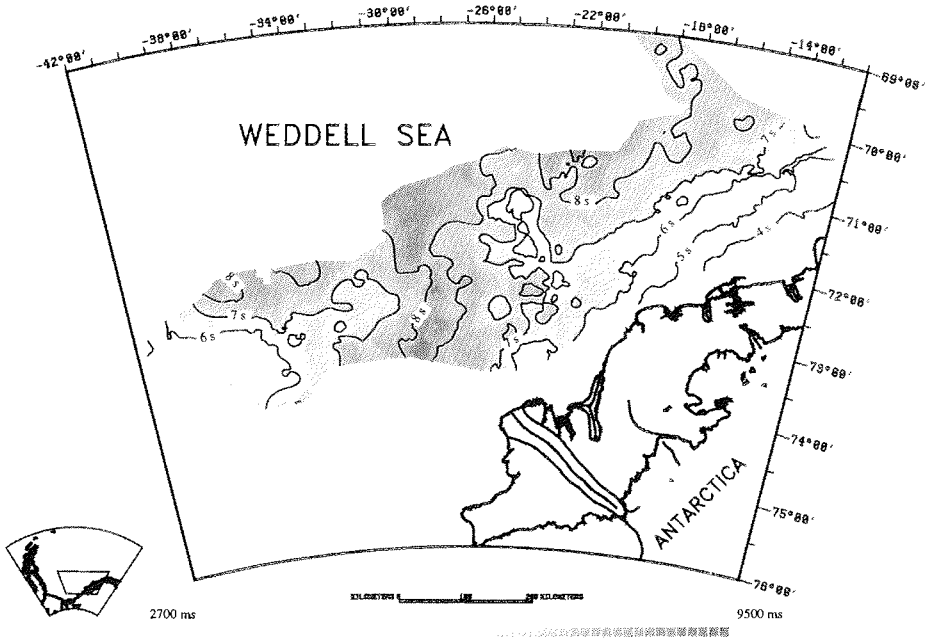

Fig. 7.8 Map of the acoustic basement derived from multichannel seismic data. Depths are in TWT.

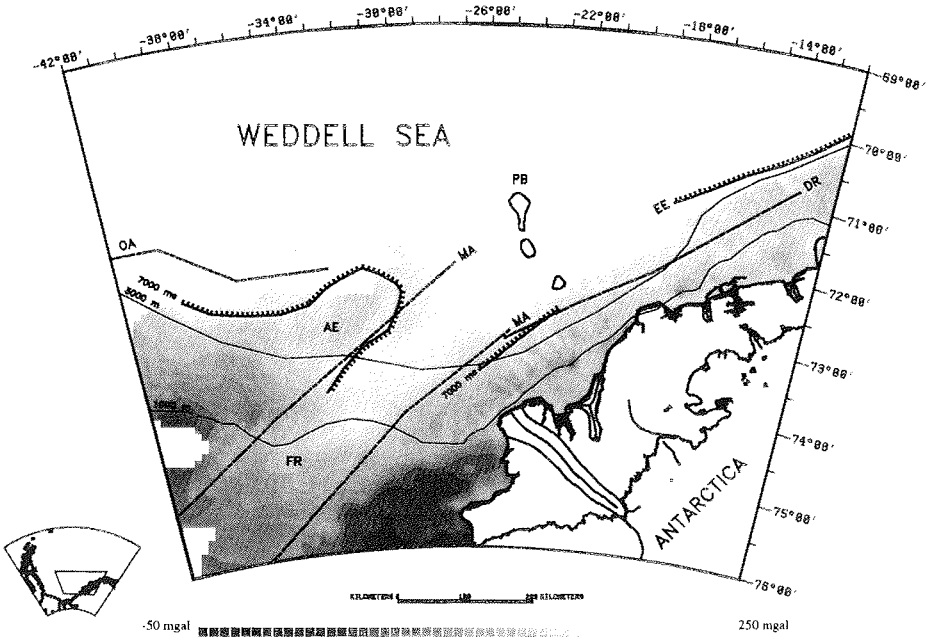

Fig. 7.9 Bouguer anomaly map (modified after Meyer, in press). OA: Orion Anomaly, AE: Andenes Escarpment, EE: Explora Escarpment, PB: Polarstern Bank, FR: failed rift arm. DR: center line of the dipping reflectors of the Explora Wedge. MA: magnetic lineations, c.f. Fig. 7.11. The 7000 ms isopach was digitized from the basement map. The 1000 m and 3000 m isobaths are also shown.

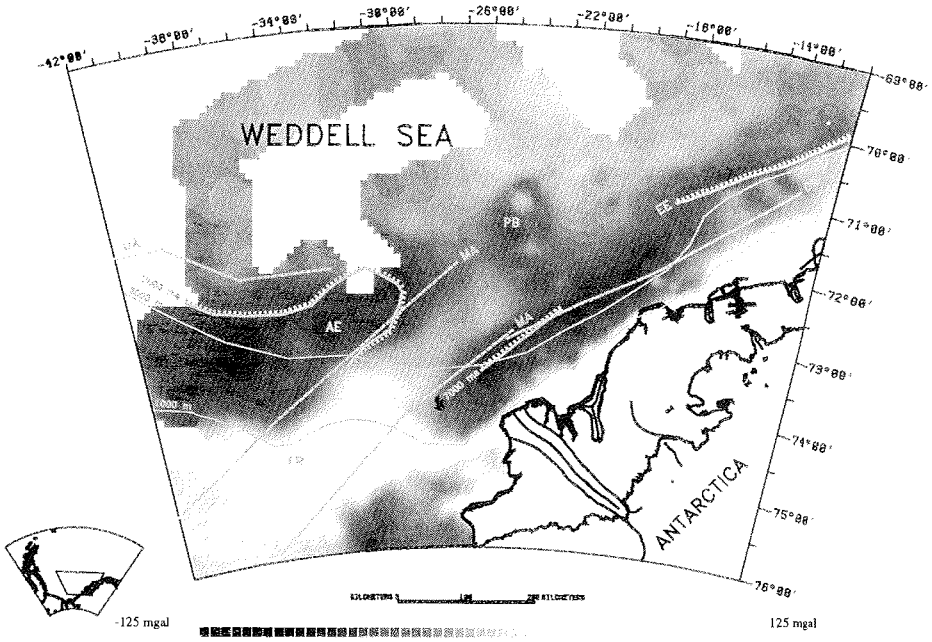

Fig. 7.10 Free-air gravity anomaly map (Meyer, in press). The symbols have the same meaning as those in Fig. 7.9.

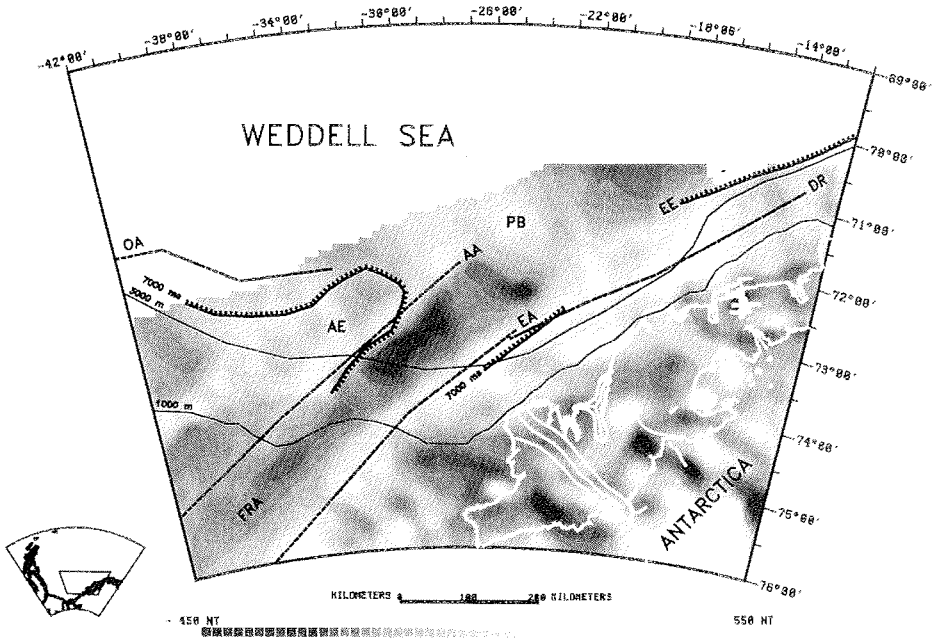

Fig. 7.11 Magnetic anomaly map (Johnson & Smith, 1992; modified). EA: Explora Anomaly, FRA: failed rift anomaly, AA: Andenes Anomaly. The symbols have the same meaning as those in Fig. 7.9 except the EA and the AA which are indicated as MA in other figures.

7.2.1 The Polarstern Bank

The Polarstern Bank is associated with a basement high of more than 2 sec TWT (Fig. 7.8) which produces no pronounced Bouguer anomaly (Fig. 7.9) but a distinct positive free air anomaly (Fig. 7.10) and a strong, positive magnetic anomaly (Fig. 7.11). Seismic reflection profiles crossing this structure show striking similarities to those crossing seamounts (Fig. 7.12). The major highs are surrounded by several smaller diapiric structures. These characteristics strongly support a volcanic origin for the Polarstern Bank as suggested by Miller et al. (1991) and Jokat et al. (1994).

North and west of the northern part of the Polarstern Bank, the basement has a hyperbolated, uneven appearance indicating oceanic crust. LaBrecque & Barker (1981) identified sea-floor spreading anomalies close to the northern tip of Polarstern Bank (M29) as further support for an oceanic basement. Oceanward dipping reflectors of the Explora Wedge abut the southernmost seamount on its landward side (Fig. 7.13). Depending on the interpretation of the Explora Wedge, this indicates the southernmost seamount lies either directly oceanward of the continent-ocean boundary or on transitional crust. Gravity modelling also suggests that the transition to oceanic crust lies close to the southernmost seamount (Meyer, in press).

The positive free-air gravity anomaly of the Polarstern Bank is associated with an approximately 20-30 km wide ring of negative anomaly enclosing the seamounts (Fig. 7.14). It is best developed on the northern side. The gravity low correlates with a basement depression of about 800 ms TWT. It contrasts with the elevated and block faulted basement connecting the seamounts (Fig. 7.15). The gravity low and basement depression probably result from the elastic bending of the lithosphere under the load of the seamounts. The 20-30 km width of the moat suggests that loading occurred on a relatively thin, and therefore young, oceanic lithosphere.

On the northern part of the Polarstern Bank, a flat, nearly horizontal unconformity cuts the steeply dipping reflectors beneath it (Fig. 7.12). It is covered by sediments showing parallel, continuous layering with a sheet-drape external geometry. The flat lying unconformity indicates subareal erosion. The draping reflectors are hemipelagic sediments that were deposited after the subsidence of the seamount below sea-level. The presence of hemipelagic sediments on the flat top of Polarstern Bank is further supported by

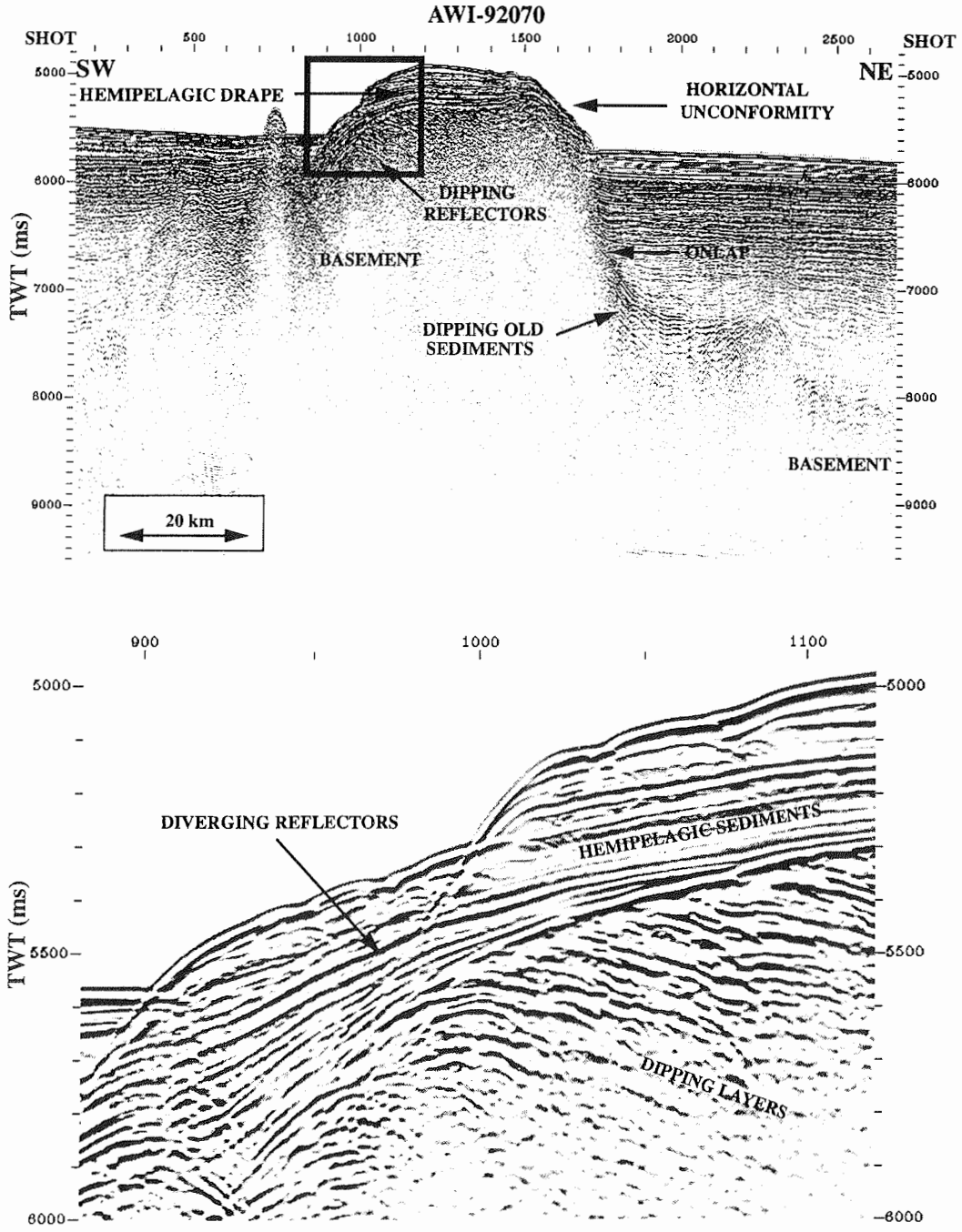

Fig. 7.12 Seismic section across the northern seamount. Profile location in Fig. 7.7.

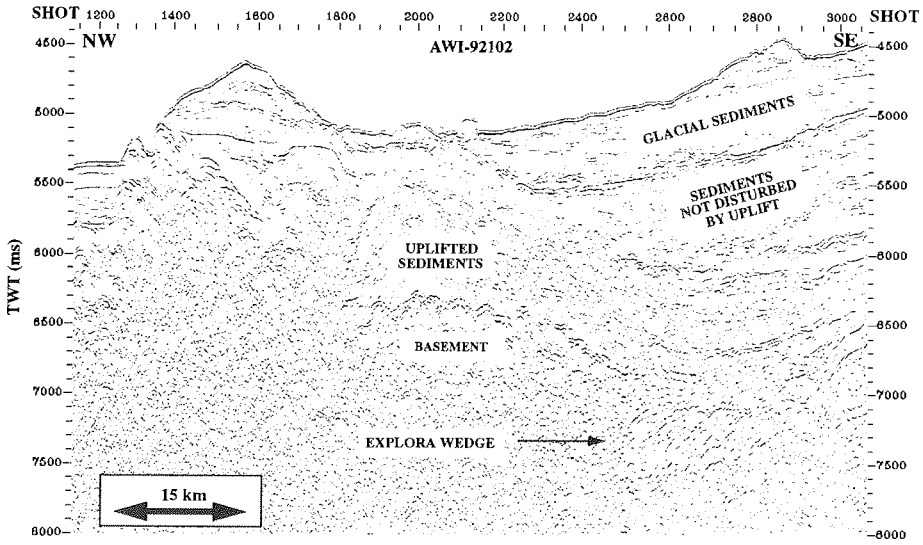

Fig. 7.13 Seismic section across the southern seamount. Profile location in Fig. 7.7.

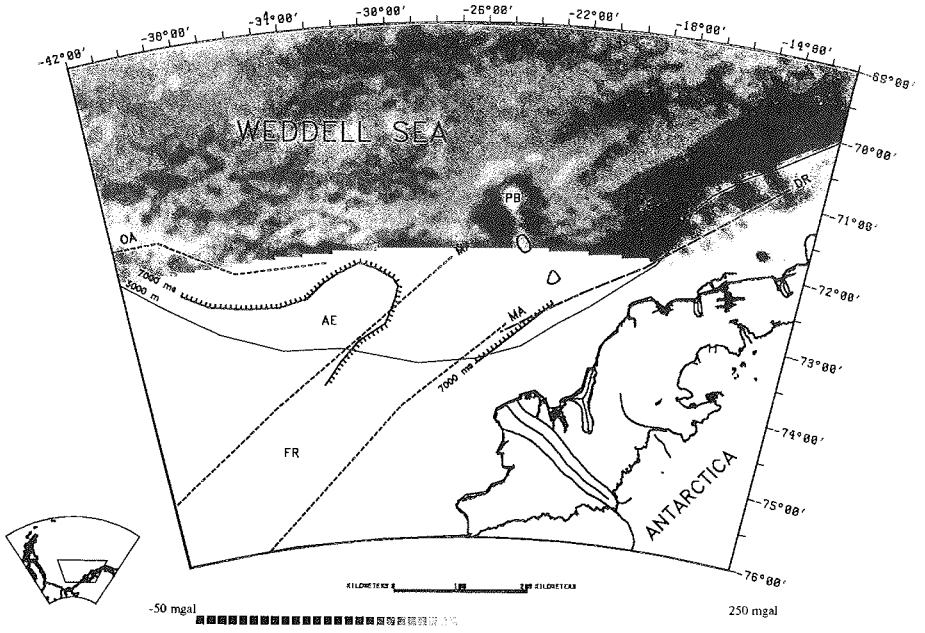

Fig. 7.14 Marine gravity anomalies from Geosat (Sandwell & McAdoo, 1988). OA: Orion Anomaly, AE: Andenes Escarpment, EE: Explora Escarpment, PB: Polarstern Bank, FR: failed rift arm. DR: dipping reflectors of the Exolora Wedge derived from seismic data, the unit forms a more than 50 km wide swath along the line. MA: magnetic lineations, c.f. Fig. 7.11. The 7000 ms isopach was digitized from the basement map. The 1000 m and 3000 m isobaths are also shown.

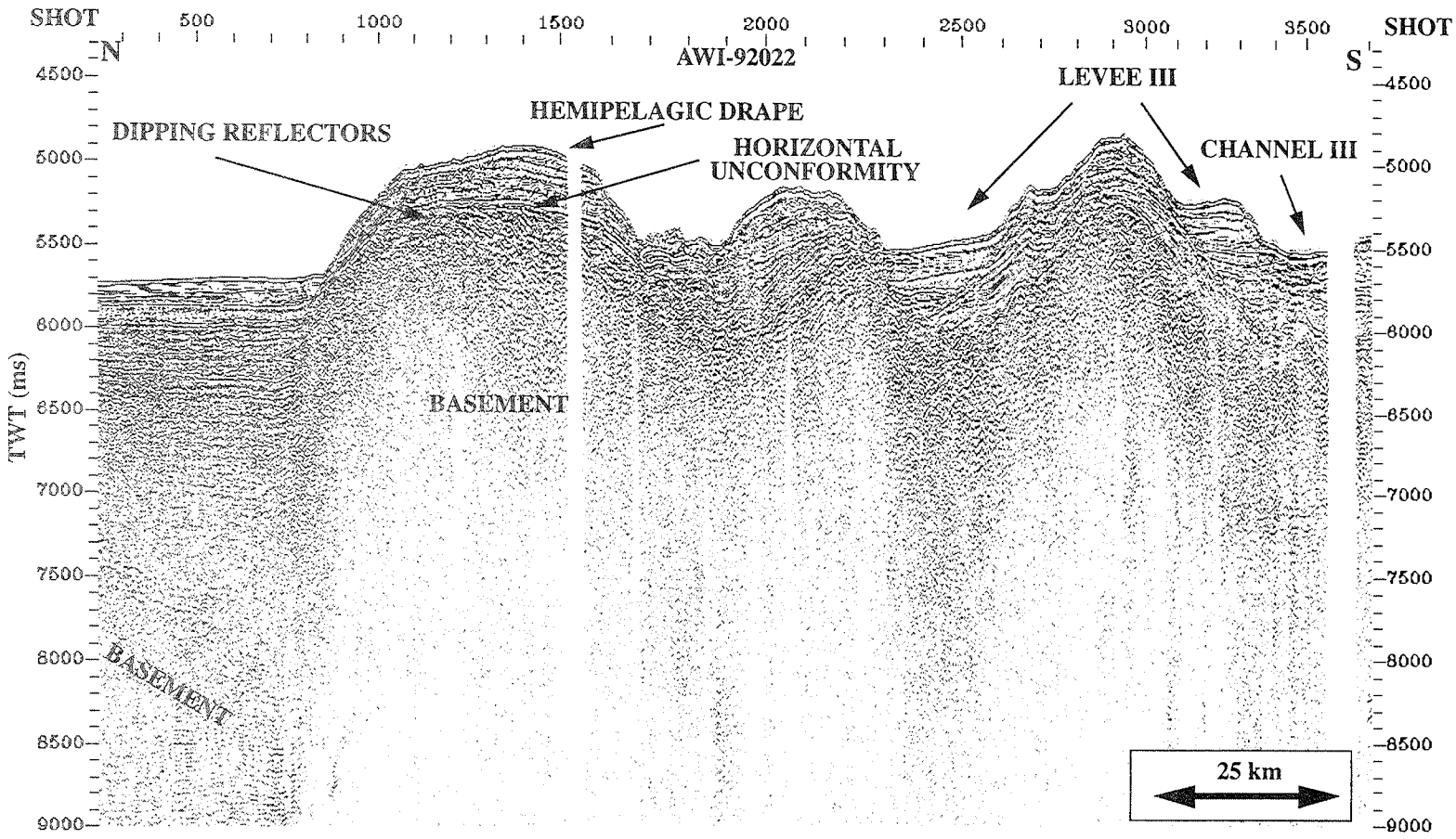

Fig. 7.15 Seismic section running parallel to the strike of the Polarstern Bank. Fig. 7.13 shows the southernmost seamount. Profile location in Fig. 7.7.

piston core data from the seamount and by analogies from the Maud Rise (§ 5).

The erosional surface has an elevation of more than 3500 m above the surrounding basement. Assuming that the subareally exposed top of the seamount was completely eroded, the paleo-water depth must have been about 3500 m in this area when the seamount formed. According to the depth-age relation curve of Parsons & Sclater (1977) the 3500 m water depth would correspond to an approximately 10 Ma old seafloor. But the southeastern Weddell Sea margin is a volcanic passive margin. In the early phase of its evolution a passive margin of this type is characterised by an anomalously shallow water depth and delayed subsidence compared to the non-volcanic type (White & McKenzie, 1989). Thus, this estimation indicates that a *minimum* of 10 Ma separated the formation of the northern part of the Polarstern Bank and the surrounding sea-floor. The time gap can also be considerably larger.

At the foot of the north-eastern part of the seamount, a sequence of seaward dipping reflectors terminates against the flank of the bank (Fig. 7.12). Their sigmoid geometry suggests that the source of these deposits was the top of the Polarstern Bank while exposed to subareal erosion. Alternatively, they could be a pile of old sediments deformed during the uplift of the seamount. The unit of dipping layers is only 400 ms (TWT) thick. The rest of the sediment sequence consists of flat lying reflectors onlapping the flank of the Polarstern Bank. Since most of the deposits are not affected by the buildup of the seamount, its northern part can not be significantly younger than the surrounding oceanic crust (Jokat et al., in press).

The southernmost seamount was uplifted with part of its original sediment cover (Fig. 7.13). This deformed and uplifted sequence correlates with an approximately 1 km thick pile of sediments overlying the Explora Wedge. The Explora Wedge is situated directly south of the structure. Thus, the development of the southern seamount post-dates the formation of the Explora Wedge at least by the time needed for the deposition of the 1 km deformed sediments. Sedimentation rates can be inferred from ODP Site 693. A rate of 20-40 m/Ma (§ 5) gives a time span of 50-25 Ma between formation of the Explora Wedge and the southern seamount.

For a tentative calculation it can be assumed that the northern tip of the Polarstern Bank is 10 Ma younger than the seafloor north of it. The 150 km oceanic crust between the northern and southern seamounts would be formed in 15 Ma by assuming a slow spreading of 1 cm/year (LaBrecque & Barker, 1981). If the

seamounts were built up by a single magmatic event, then the southernmost one would be (10 Ma + 15 Ma) 25 Ma younger than the oceanic crust adjacent to the Explora Wedge. This would correspond to the time span derived from the tentative southern seamount sedimentation rates.

On the flanks of the northern seamount, hemipelagic sediment facies showing subparallel, continuous acoustic bedding are underlain by a sequence of diverging, continuous reflectors (Fig. 7.12, Fig. 7.16). These sediments could be formed while part of the seamount was above sea-level, and the eroded volcanic, and maybe sedimentary material was redeposited on the flanks of the seamount that lay below sea-level. Differential subsidence of adjoining parts of the seamount is well documented by these layers (Fig. 7.16). Higher subsidence rates at the rim of the flat top of the seamount compared to its central area probably also contributed to the formation of the wedge shaped units of divergent reflectors.

On the western part of the northern seamount, discontinuous, south-eastward dipping reflectors underlie a nearly horizontal unconformity (Fig. 7.12). Hemipelagic facies show velocities of 1500-1800 m/s as opposed to the 3800 m/s interval velocity of the dipping layers. The unconformity is associated with a strong impedance contrast having higher amplitudes than that of the sea-bottom reflections. The magnetic signature, velocities and acoustic characteristics indicate that the unconformity signals a major lithologic change. The dipping reflectors probably represent flood basalts extruded in subareal environment. To the east these dipping layers turn into flat lying ones at a poorly resolved transitional zone. Reflectors are more continuous on the east, with lower amplitudes. This unit may be the prolongation of the basaltic flows, but more probably it represents volcaniclastics or sediments eroded from the seamount itself and being deposited on its top below the sea-level of that time.

On the seamounts further to the south, the acoustic basement has an uneven, strongly disturbed character. It may be interpreted as the top of the basaltic basement, or that it represents uplifted and faulted old sediments (Fig. 7.13).

The interpretation proposed here is different from that of Miller et al. (1991). They suggested that the diverging reflector and overlying units (not the underlying ones) were old, uplifted sediments onlapped by younger deposits (Fig. 7.16). The onlap surface was correlated with the W4 unconformity indicating a lower age limit of Late Cretaceous for the formation of the Polarstern Bank. Here, a different explanation is favoured. Continuous sedimentation occurred on the seamounts since their subsidence

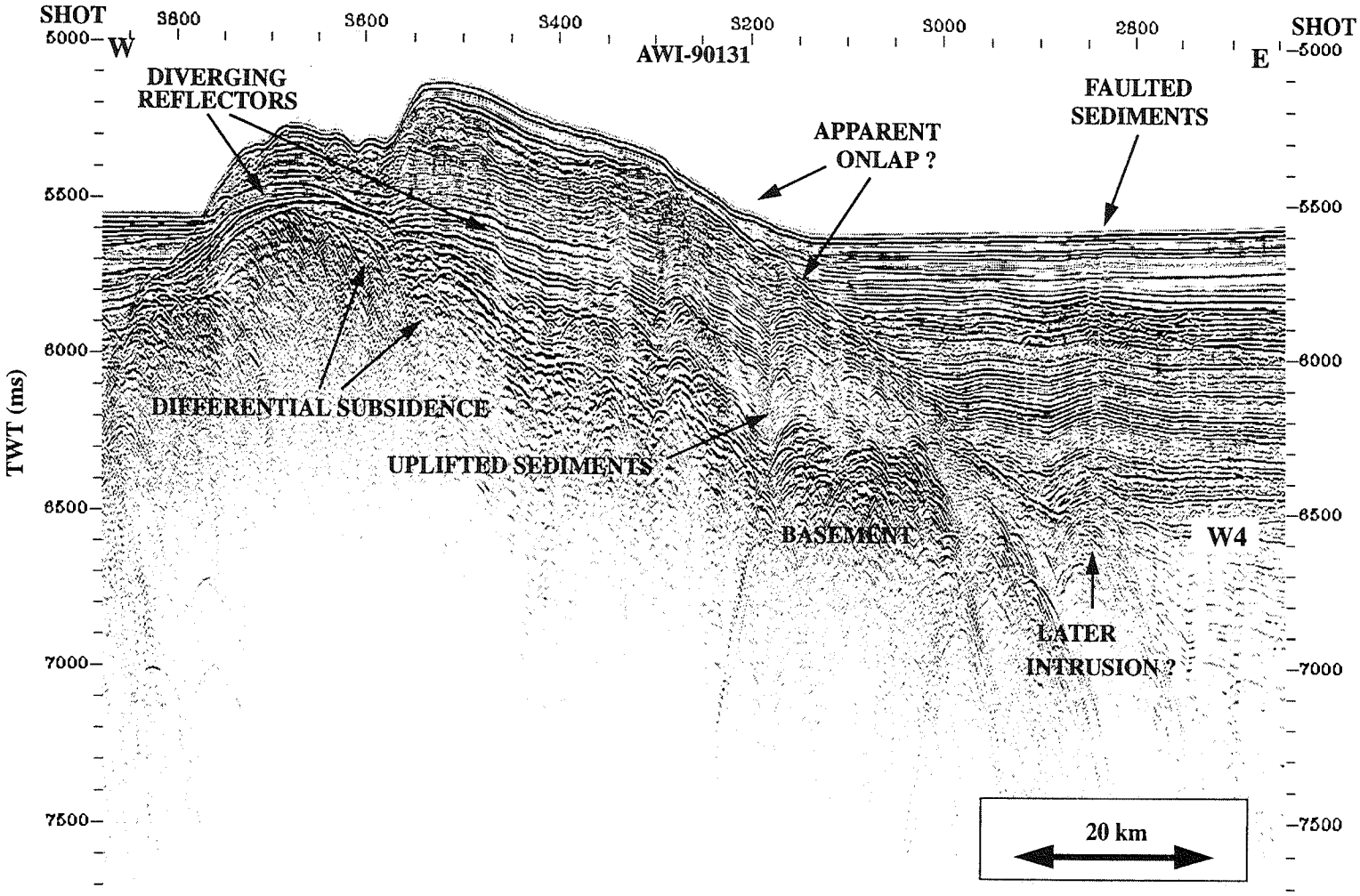

Fig. 7.16 Seismic section across the southern flank of the northern seamount. Profile location in Fig. 7.7.

below sea level. The onlap unconformity signals a dramatic change in depositional regime that accompanied the onset of the Crary Fan development. Levee deposits onlap on the flank of Polarstern Bank, but deposition was also continuous on its top and partly on its flanks at a reduced rate (Fig. 7.15). Thus, the proposed onlap surface, at least partly, only apparently onlaps due to resolution problems (Fig. 7.16). Therefore, it can not be used for dating.

Small scale diapiric structures were found in the vicinity of the seamounts. They caused deformation of the Cenozoic glacial sediments (Fig. 7.16). These diapirs may be intrusions from a later, but smaller magmatic event than the one that formed the seamount itself, though, the disturbed and faulted young layers could also originate from differential compaction of unconsolidated sediments above a buried diapir.

The map of the acoustic basement (Fig. 7.8) and the free air gravity field (Fig. 7.10) clearly show that the Polarstern Bank is isolated from both the Explora and Andenes Escarpments. Satellite altimetry and magnetic data (LaBrecque & Barker, 1981) indicate that the seamounts have no northward continuation (Fig. 7.14).

The proposed interpretation can be summarised as follows. The Polarstern Bank is a seamount chain formed by one or several volcanic events on oceanic crust. Age constraints on its development are poor. It post-dates the formation of the oceanic crust surrounding it (M29, 162 Ma, LaBrecque & Barker, 1981) by at least 10 Ma at the northern part of the seamount. Undisturbed, onlapping sediments indicate that the development of the structure occurred at an early phase of the basin's formation. Its linear trend and its termination at the continuation of the strike of the Andenes Escarpment suggest that the seamounts are associated with the early tectonic evolution of the area (Fig. 7.8, Fig. 7.14). They may have been formed by a delayed volcanism on a pre-existing major fault zone or fracture zone. The strike of the Explora Escarpment intersects the Polarstern Bank (Fig. 7.10). If the seamounts were older than the transform movement along the Explora Escarpment, the northern seamount would have been cut by this movement unless a spreading ridge existed between them.

7.2.2 The Andenes-Explora Escarpment (?) and the Failed Rift

On a map of acoustic basement, the Andenes Escarpment gradually vanishes eastward as a topographic feature. Several distinct highs can be observed on a broad basement elevation that becomes more and more subdued to the east (Fig. 7.8). Since the seismic lines obliquely cut the strike of the escarpment, these distinct elevations may be continuous along strike despite their separated appearance on the profiles. Though they become subdued and narrow towards the east, all seismic lines located west of the Polarstern Bank show a basement high of at least 1 s (TWT) and a minimum width of 30 km (Fig. 7.17) indicating the possible continuation of the structure.

The name 'escarpment' can be misleading. The acoustic basement gradually rises at the flanks of the escarpment interrupted at places by some step-like scarps. This contrasts with the cliff-like wall of the Explora Escarpment (Fig. 7.18). On seismic sections, the Andenes Escarpment appears as a basement ridge or plateau rather than an escarpment. Seismic characteristics and gravity modelling (Hinz & Kristoffersen, 1987; Meyer, in press) indicate that the basement northwest and southeast of the Andenes Escarpment is oceanic in origin.

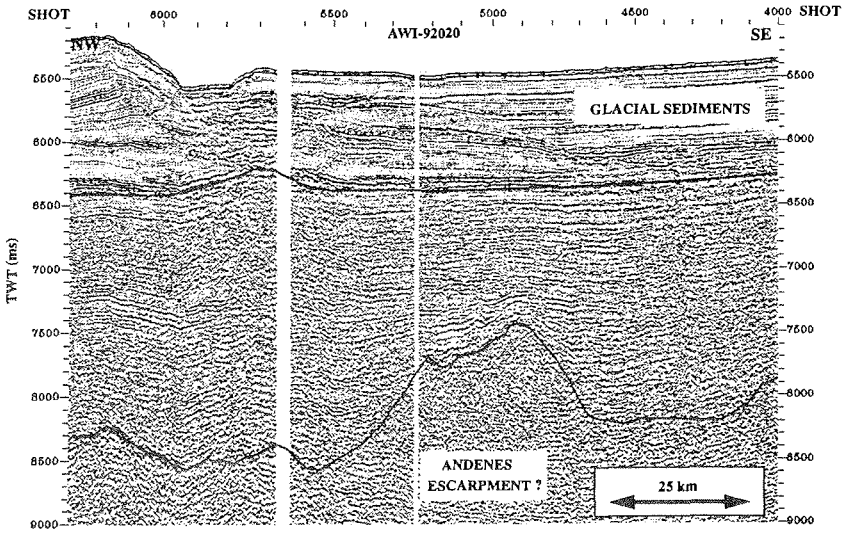

Fig. 7.17 Seismic section showing the possible continuation of the Andenes Escarpment. Profile location in Fig. 7.7.

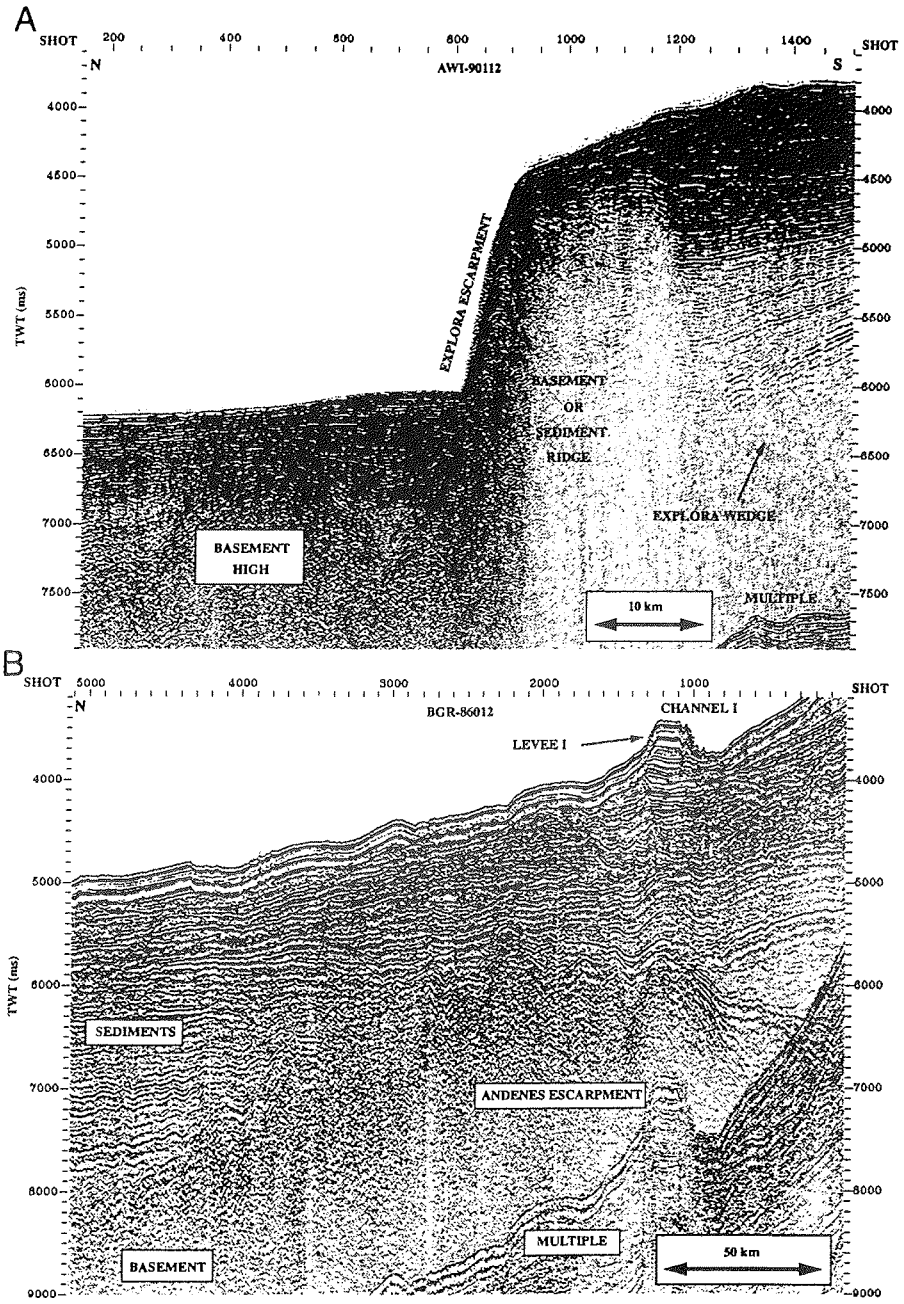

Fig. 7.18 Seismic sections across **A**) the Explora Escarpment, and **B**) the Andenes escarpment. The profiles show a prominent morphologic difference. The north side of the Explora Escarpment forms a cliff-like wall, whereas the Andenes Escarpment is characterised by a gradual basement rise. Profile locations in Fig. 7.7.

The Andenes Escarpment correlates with a pronounced gravity low that terminates against the shelf edge on the free-air anomaly map (Fig. 7.10). No such sharp boundary can be discerned on the Bouguer anomaly map (Fig. 7.9). The vanishing basement ridge and the northeastward fading Bouguer anomaly can be explained by the gradual thinning of the crust in this direction. The positive free-air anomaly at the shelf break, against which the negative anomaly of the Andenes Escarpment terminates, rises from the gravity effect of the sediments forming the continental shelf and slope.

The Explora Escarpment gradually diminishes westward; at about 18°W it disappears from the bathymetric map (Fig. 3.3). It can, however, be followed on the acoustic basement map almost to the Polarstern Bank (Fig. 7.8). Moving westward from 18°W, the prolongation of the escarpment becomes less and less pronounced and its steep slope becomes more gentle. Seismic sections show that the acoustic basement has an uneven character on the oceanward side of the Explora Escarpment (Fig. 7.18a). It is characterised by several smaller highs associated with a higher basement depth on their seaward side than on their landward side (Hübscher, 1994).

The oceanward dipping, sub-basement reflectors of the Explora Wedge lie close to the face of the escarpment on its landward side at 15°W (Fig. 7.18a). The strike of the escarpment and the trend of the Explora Wedge diverges in westerly direction (Fig. 7.10) indicating the different origin of the structures.

A pronounced, elongated magnetic high, the Explora Anomaly, correlates with the lineament of the Explora Wedge (Fig. 7.11). The similar trend and the good correlation of these lineaments support their common origin. The Explora Anomaly can be traced on the Filchner Shelf to Berkner Island (Fig. 7.11). To the north-west, a similar linear magnetic high coincides with the southern flank of the Andenes Escarpment. The anomaly runs parallel to the Explora Anomaly and crosses the bathymetric contours. The two magnetic lineaments border a magnetic low that gradually diminishes southward. The magnetic low coincides with a gravity high and a basement depression (Fig. 7.11). The gravity and magnetic anomalies can be followed across the shelf edge on the Filchner Shelf. The gravity high, the magnetic low, the sub-basement oceanward dipping reflectors and the basement depression can be interpreted as elements of a failed rift lying beneath the Filchner Shelf.

Seaward of the continental slope where the Andenes Escarpment diminishes or turns into a fracture zone, the failed rift is probably not bounded by continental crust to the north. After the failed rift formed, during a later phase of the Weddell Sea breakup,

the continental crust bordering this part of the failed rift drifted away. As it drifted, the continental block left behind an oceanic plateau, the Andenes Escarpment. The plateau probably formed on a fracture zone through intense igneous activity.

Under this interpretation, the Explora and Andenes Escarpments do not form a continuous plate boundary (cf. Kristoffersen & Hinz, 1991). The continent-ocean transition crosses the Andenes Escarpment by following the isobaths. Therefore, the term ´failed rift´ may be misleading for this northern part of the structure.

7.3 Gondwana Reconstructions in Light of the New Geophysical Data

The discovery that West Antarctica´s microcontinents moved relative to each other has inspired a number of different breakup models. One group of models assumes no large scale relative motion of the individual crustal blocks. The required change in the shape of West Antarctica is achieved by heterogeneous stretching and intracontinental deformation. These reconstructions abandon the exact fit of all available geologic information to get a rather simple and consistent model. Other models prioritise the exact fit of geological and geophysical data and obtain intense relative movements of the different microplates. The latter models while giving a good fit to those data, have severe problems with the driving forces of the motion and with evidence for generated, subducted and sheared crust.

In this section, the contrasting breakup models of Kristoffersen & Hinz (1991) and Grunow et al. (1991) will be compared to the new data. The Kristoffersen & Hinz (1991) model is ´static´, while Grunow et al.´s (1991) model involves intense microplate motions.

Fig. 7.19 shows that the movement of the Ellsworth-Whitmore Mountains can be used to check the consistency of Grunow´s model against the presented data. The different stages of the wandering of the Ellsworth-Whitmore Mountains are plotted over the geophysical data. Their 230 Ma, 175 Ma and 125 Ma positions cut every lineaments derived from gravity, magnetic and seismic surveys. This movement could only have occurred:

1) If the geophysically defined lineaments did not originate from continuous geologic structures, but from several smaller coinciding geologic units. The different structures show good continuity on all available geophysical data which strongly supports the presence of connected geologic units rather than an assembly of coinciding lineaments.

2) If the mapped geological structures are considerably younger than the movement of the Ellsworth-Whitmore Mountains. A basin formation that post-dates the Late Jurassic breakup allowing the 175 Ma and 125 Ma positions of the Ellsworth-Whitmore Mountains would result in a thick pile of disturbed and block faulted sediments on the Coats Land margin and on the Andenes Escarpment. No indication of such a thick sequence of disturbed sediments appears in the seismic data (Fig. 7.18b). A presumed younger age for the mapped structures would also contradict the dating of the Explora Anomaly and the associated

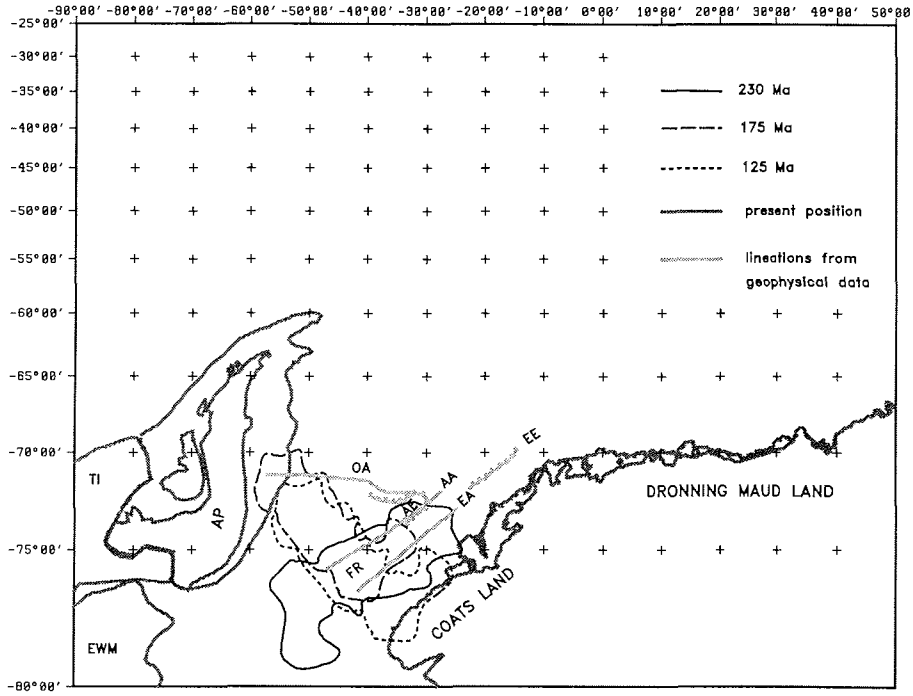

Fig. 7.19 The wandering of the Ellsworth-Withmore Mountains (EWM) after Grunow et al. (1991). Grey lines show Antarctica's crustal blocks including the EWM in their present positions. The reconstruction is superimposed on the lineations derived from geophysical data (cf. Fig. 7.8-Fig. 7.11). Crustal shortening is predicted on the Coast Land margin between 175 Ma and 125 Ma. Between the 125 Ma and the present position strike-slip motion is expected. Note the overlap of the paleo-positions of the EWM on the mapped lineaments. AP: Antarctic Peninsula, TI: Thurston Island, EA: Explora Anomaly, AA: Andenes Anomaly, OA: Orion Anomaly, AE: Andenes Escarpment, FR: Failed Rift, EE: Explora Escarpment.

Explora Wedge for which a Middle-Late Jurassic age was proposed (Hinz & Krause, 1982). The model predicts compression and strike slip motion on the Coats Land margin and oceanic crust beneath the Filchner-Ronne Shelf. Seismic refraction surveys indicate stretched continental crust beneath the Filchner-Ronne Shelf (§ 7.1). A Norwegian seismic line located directly north of the Filchner Ice Shelf (77.5°S, 40°W; 77.8°S, 35°W) shows no substantial basement faulting and no major faulting and folding of sediments. This suggests that the area was largely undisturbed by tectonic events following the breakup of Gondwana (Kristoffersen & Haugland, 1985). New seismic data close to the Norwegian line have been interpreted in a similar manner. Crustal stretching and subsidence has been documented rather than compression and transform movement (Jokat et al., submitted).

The 230 Ma position of the Ellsworth-Whitmore Mountains can not be excluded by the marine geophysical data, since the mapped structures are probably younger (170 Ma or less). Marine geophysical measurements suggest, however, that the Ellsworth-Whitmore Mountains crustal block moved away from the Filchner Shelf north of the ice shelf edge before the Weddell Sea opened. Either the Ellsworth-Whitmore Mountains did not cross the Filchner-Ronne Shelf or it crossed the present shelf earlier. In either case, the wandering of the Ellsworth-Whitmore Mountains crustal block need not be considered when reconstructing the breakup history of the Weddell Sea since 170 Ma.

The database used by Kristoffersen & Hinz (1991) to develop their breakup model also forms the core of the present study. New data are located in the area of the proposed connection of the Explora and Andenes Escarpments. Therefore, their proposed connection will now be discussed.

The model of Kristoffersen & Hinz (1991) predicts a major fracture zone bounding the old oceanic crust of the failed rift to the north (Fig. 7.6) and bordering the sheared continental margins of the Explora and Andenes escarpments. On the oceanic crust between the escarpments, the new data outline a basement high (Fig. 7.17). This could be the fracture zone predicted by the model of Kristoffersen & Hinz (1991). Though badly constrained, it is the most plausible interpretation of this structure independent of the above model.

However, detailed mapping indicates an offset of about 70 km between the strike of the Explora and Andenes escarpments. Consequently, they are probably not located on the same fracture zone.

The two stage model of Kristoffersen & Hinz (1991), provided the two stages were far apart in time, predicts that the sediment covered, old oceanic crust of the failed rift was juxtaposed against a young and elevated oceanic crust. The subsidence history on the two sides of the fracture zone should thus be strongly different. The seismic profiles do not show the presence of a major fault zone in the sediment sequence, nor discontinuity of horizons, nor disturbed sediments nor signs of differential subsidence on a scale predicted by the model (Fig. 7.17). Thus, it is probable that the two stages were not far apart in time, that actually they could have been active contemporaneously, forming a triple junction.

The pronounced difference between the shape of the north-western face of the two escarpments also needs explaining (Fig. 7.18). A linear plate boundary having a uniform geologic history during breakup times (Kristoffersen & Hinz, 1991) can not be reconciled with this morphologic difference.

This difference in shape could be explained by assuming that oblique spreading during the formation of the Andenes Escarpment became a transform/transpressional movement as transform motion continued along the Explora Escarpment. This model, however, can not account for the offset of the lineaments.

An alternative explanation could be that the Andenes Escarpment is similar to the Astrid Ridge (Bergh, 1987): it is an oceanic plateau that formed on a fracture zone in the vicinity of a hot spot or a triple junction or both. This would explain both the coinciding trends and the different architectures of the Andenes and Explora Escarpments. If the two escarpments are located on different fracture zones then the offset of their trends would follow.

7.4 A Tentative Breakup Model

By matching the bits and pieces discussed above, a tentative breakup model has been constructed (Fig. 7.20). It aims to give a self-consistent interpretation of the geophysical data and to highlight the main problems and the key areas on which future research could be focused.

In Early Jurassic times, a broad, subduction related extensional province characterised the Paleo-Pacific margin of Gondwanaland (Storey et al., 1992). This early rifting turned into seafloor spreading in the Falkland Plateau Basin, creating the Middle-Late Jurassic oceanic crust (Lorenzo & Mutter, 1987). This rift may have continued into the Ronne Shelf or terminated at a major fracture zone (Fig. 7.20). To the north, the Agulhas/Falkland Fracture Zone System and in its prolongation, the Gastre Fault System, bordered the new oceanic basin (Marshall, 1994). The Polarstern Bank seamounts are located in the approximate projection from the paleoposition of this fracture zone (Fig. 7.20). This may indicate that the fracture zone had a continuation towards the Southeast on which the Polarstern Bank may have been formed by a later magmatic event. Contemporaneously (?) with the rifting in the Falkland Plateau Basin, seafloor spreading commenced on the East Antarctic margin and formed the Weddell Rift as evidenced by the Explora Wedge, by the breakup related magmatism of the Dronning Maud Land and by the failed rift arm underlying the Filchner Shelf.

With the initiation of seafloor spreading in the Somali and Mozambique basins in late Middle Jurassic times, a major change occurred in the regional stress field and induced a substantial reorganisation of the seafloor spreading pattern. A new spreading axis formed between the Filchner-Ronne Shelf and the Falkland-Agulhas Plateau. Seafloor spreading probably ceased in the Falkland Plateau Basin at this time or shortly afterward (Fig. 7.20). A short-lived triple junction may have formed at the juxtaposition of the Weddell Rift and the new rift arm south of Falkland Plateau. As seafloor spreading ceased on the Weddell Rift, a transform/transpressive deformational regime formed along the present day Explora Escarpment. The new rifting event offers an alternative explanation for the formation the Polarstern Bank. The seamounts may have been located on the new axis of the initiation of seafloor spreading. The rift axis may have been offset by a fracture zone north of the present Polarstern Bank. During the strike-slip movement of East Antarctica and Africa, an oceanic

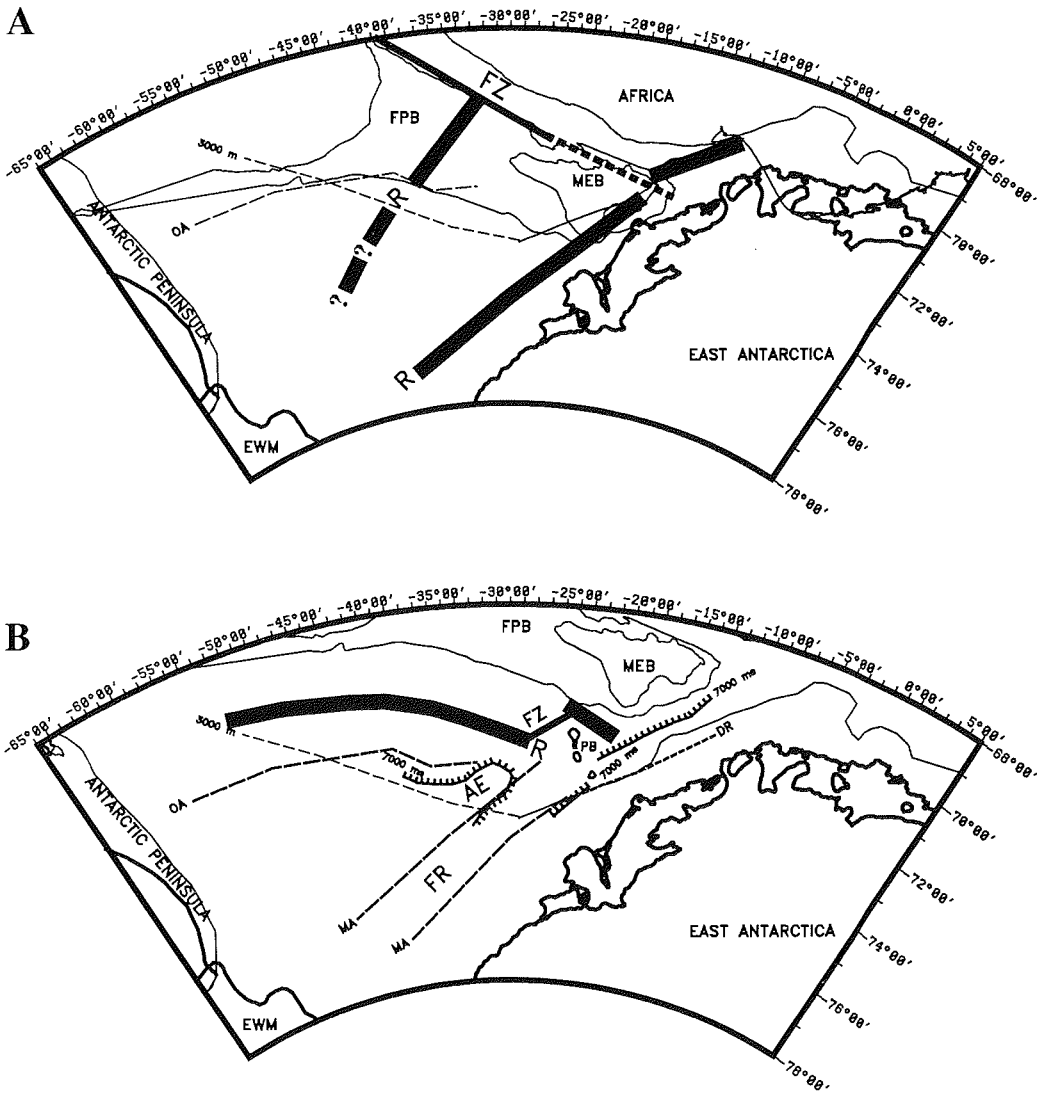

Fig. 7.20 The proposed breakup model. **A)** initial rift phase; **B)** the opening of the Weddell Sea. R: rift axis, FZ: fracture zone, OA: Orion Anomaly, AE: Andenes Escarpment, PB: Polarstern Bank, FR: failed rift arm, MEB: Maurice Ewing Bank, FPB: Falkland Plateau Basin. DR: dipping reflectors of the Explora Wedge derived from seismic data, the unit forms a more than 50 km wide swath along the line. MA: magnetic lineations, cf. Fig. 7.11. The 7000 ms isopach was digitized from the basement map. The 3000 m isobath is indicated by a dashed line in front of the Filchner Shelf and by a solid line east of it.

plateau, the Andenes Escarpment could have developed in this fracture zone due to the proximity of a triple junction or a mantle plume. The prolongation of this fracture zone probably does not coincide with the Explora Escarpment, but lies north of it. The position of the proposed fracture zone may be related to the pre-breakup position of the Agulhas Plateau-Maurice Ewing Bank microplates (Fig. 7.20).

East of the Polarstern Bank in the strike of the Andenes Escarpment, satellite altimetry data reveal a NE trending, lineated, positive gravity anomaly at about 70.5°S, 23°W (Fig. 7.14). Seismic profiles crossing the anomaly show an associated basement high. The gravity anomaly and the basement high may indicate the continuation of the proposed fracture zone; but the origin of the gravity anomaly as well as the nature of the continuation of the Andenes Escarpment should be justified by further seismic data.

Gravity anomaly trends northwest of the Explora Escarpment (Fig. 7.14), if interpreted as fracture zones, show that an early transform movement along the escarpment later changed into oblique spreading. Interpreted magnetic anomalies show a gradual, likewise change of the seafloor spreading direction (LaBrecque & Ghidella, 1994). This oblique spreading could have formed the basement highs oceanward of the Explora Escarpment (Fig. 7.18). This change in spreading direction, if it really occurred, could have been associated with the onset of rifting between South America and Africa.

7.5 Discussion of the Proposed Model

The initiation of continent drifting can be directly dated from the oldest seafloor spreading anomalies or its age can be inferred from breakup-related volcanism. The oldest seafloor in the Somali and Mozambique basins is thought to be 170 Ma old (Lawver & Scotese, 1991). Its counterpart on the Dronning Maud Land margin, dates the onset of seafloor spreading between 160 Ma and 166 Ma (Hinz et al., 1995). Breakup-related volcanism associated with the formation of the Explora Wedge occurred between 179-162 Ma ±6 Ma (White & McKenzie, 1989). A Middle-Late Jurassic age was suggested for the oceanic crust of the Falkland Plateau Basin and Late Jurassic age for the Rocas Verdes Basin.

As an alternative to the two-stage model described in § 7.4, the overlap of these ages can be interpreted such that seafloor spreading started simultaneously at about 170 Ma, in the Mozambique Basin, in the Somali Basin, on the Falkland Plateau and on the Dronning Maud Land margin. On the other hand, the scatter of these data allows two distinct phases that directly follow each other without the existence of an intermediate stage forming a triple junction. The presented geophysical data can not distinguish between these models. But whether it had one phase or two, a triple junction or not, the failed Weddell Rift below the Filchner Shelf was short lived and seafloor spreading in the Somali and Mozambique basins started not long afterwards.

The proposed breakup model infers the continent/ocean boundary runs south of the Explora-Andenes Escarpments. It is located just oceanward of the Explora Wedge on the Dronning Maud Land continental margin; it turns westward as it reaches the Filchner Shelf and then follows the isobaths (Jokat et al., in press). A strip of oceanic crust or strongly stretched continental crust may underlie the failed rift arm. The southern part of the Andenes Escarpment may be of stretched continental crust or of thickened oceanic crust. The northern part of this structure is probably of oceanic crust.

The continuous Antarctic plate boundary that connects the two escarpments can only exist if the two escarpments were located on the same fracture zone, which is not supported by the new results. But, the continuity of the failed rift and associated structures, alone, excludes the possibility of any large scale, lateral, post-breakup microplate movement in this area.

8. Conclusions

Seismic surveys supplemented with potential field and geologic data prove to be an effective tool for unravelling the formation of tectonic structures and glaciomarine sediments.

The sedimentary sequence on the Weddell Sea continental slope can be vertically divided into four distinct acoustic units, within the resolution of the seismic tool. The lowermost unconformity represents the acoustic basement. The next major change in acoustic characteristics is represented by a prominent reflector tentatively correlated with the W4 unconformity at ODP Site 693. This horizon signals the onset of ice growth on Antarctica during the Early Oligocene. The overlying glacial sediments add two significantly different stratigraphic sequences. Acoustic characteristics, drilling results, piston core data, analogies from other Antarctic continental margins and depositional models of different glacial regimes indicate that the boundary between the two glacial units signals a second, major climatic change during the Middle Miocene. What is known of the glacial history of the Southeastern Weddell Sea can be reconciled with the observations of acoustic stratigraphy as follows.

Due to climatic deterioration at the Eocene/Oligocene boundary, a continental scale ice sheet formed on East Antarctica. Freezing conditions were established at the Antarctic margin initiating bottom water formation and the development of widespread marine hiatuses. This led to the erosion of some 300 m of sediments at ODP Site 693 and formed the W4 unconformity. Probably the same event led to the first incision of the numerous canyons on the Dronning Maud Land margin.

From the Early Oligocene to Late Miocene, the Antarctic Ice Sheet was temperate and wet based and did not have the polar character it has today. Vegetation existed at several areas in Antarctica and ice ablated mainly through melting rather than iceberg calving. On the Filchner Shelf, a grounded ice sheet episodically advanced to a position north of the northern tip of Berkner Island, but did not reach or stay long on the shelf break. The temperate ice sheet discharged large amounts of suspended sediments to meltwater streams, providing favourable conditions for rapid build-up of channel/levee systems. On the Dronning Maud Land margin, lower sediment input caused sediment starvation. Occasionally, vast debris flows occurred that eroded and partly filled the canyons. These debris flows are interbedded with channel/levee sediments on the continental rise.

In the Middle Miocene, renewed cooling caused the advance of the grounding line, the establishment of polar ice conditions and the

invigoration of current activity. The dominant ablation process changed from melting to iceberg calving. The grounded ice sheet episodically reached the shelf break, and deposited sediments directly on the slope forming a diamict apron. On seismic lines, the diamict apron appears as a prograding wedge. Channel/levee systems of the Crary Fan were reactivated. The channels acted as conduits for turbidity currents initiated by slope failures on the prograding wedge. During interglacials, thermohaline currents may have flowed in the channels, eroding and transporting sediments downslope. On the Dronning Maud Land margin, sediment input increased as the grounded ice sheet extended to the shelf break. The intensification of bottom water formation and contour current activity resulted in current controlled sedimentation on the middle slope. The higher sediment input initiated the rejuvenation of the canyons.

Laterally, the upper continental slope of the survey area can be subdivided into two morphological units: a gently dipping upper slope, with a bathymetric bulge in front of the Crary Trough outlining the Crary Fan, and a steeply dipping (up to 15°) upper slope marking the Dronning Maud Land margin. The two units are also distinguished by their Cenozoic sedimentation rates. Intense fan growth occurred from the Early Oligocene to the Middle Miocene in front of the Crary Trough, while the Dronning Maud Land continental margin was sediment starved. Sedimentation rates strongly increased since the Middle Miocene on the Dronning Maud Land margin, but still remained lower than rates of the Crary Fan.

These distinct lateral differences may be attributed to two basic factors: the amount of sediment input and the flow velocity of the Antarctic Coastal Current.

The Crary Fan has a huge drainage area compared to its relatively narrow inlet, while the Dronning Maud Land margin has a long coastline with a smaller drainage area. The sediments being carved out from the Filchner Shelf, alone, have a vast volume, orders of magnitude greater than that removed from the smaller troughs of the Dronning Maud Land shelf. Thus, a much higher sediment input can be expected in front of the Crary Fan than on adjacent areas.

The Antarctic Coastal Current (ACC) reaches relatively high velocities on the Dronning Maud Land margin. At approximately 27° W, however, the ACC splits into two branches. The branch following the Filchner Shelf edge has a lower mean speed. The Coriolis force contributes to the erosion potential of the current by deflecting it leftward against the slope. The Coriolis force has more effect on the current along the Dronning Maud Land margin, due to its higher velocities and larger N-S component.

Limited sediment input and strong currents caused low deposition rates on the Dronning Maud Land margin until the Middle Miocene. Later, as a grounded ice sheet extended to the shelf break, sediment input increased, but still remain lower than that on the Crary Fan. The invigoration of current activity caused an effective winnowing of glaciomarine diamict covering the upper slope and led to very steep slopes of badly sorted, sand-prone lag deposits. These sediments are responsible for the 15° dip of the upper slope. The winnowed, fine-grained material may have been sedimented contemporaneously further downslope, or it could have been transported to the Crary Fan.

Higher sediment input and weaker currents are responsible for the vast fan in front of the Crary Trough. In the Middle Miocene, a grounded ice sheet reached the shelf edge and caused a significant change in the depositional process on the slope. The continued high sediment input and low current velocities prevented the formation of lag deposits on the Crary Fan. The sediments having a fine-grained component could not form as steep a slope as the unsorted lag deposits on the Dronning Maud Land margin.

At least two distinct phases of canyon cutting can be distinguished on the Dronning Maud Land margin. In places, sheet-drape of the current controlled, post-Middle Miocene sediments covers the canyon walls. This indicates that the canyon began to form before the deposition of the draping facies. Further upslope, the small tributaries of the Wegener Canyon appear to have been formed contemporaneously with the deposition of these current controlled sediments. This suggests a rejuvenation of the canyons, i.e. a second phase of canyon cutting.

A cyclic fill can be observed in the canyons on the western part of the Dronning Maud Land margin. Thicker, transparent seismic facies and units of high amplitude, discontinuous reflectors cover each-other in turn. Up to five such cycles can be detected. Some of the transparent units can be traced downslope and correlated with debris flow deposits interfingering with sediments of the easternmost channel/levee complex. The cyclicity may indicate that the formation of the debris flow facies is related to the glacial/interglacial fluctuations.

An estimate of the mass balance of glacial deposits shows that the channel/levee facies contain a considerable amount of glacially-eroded sediment removed from the Crary Trough. The diamictit apron of the upper slope can only account for about 1/3 of the sediments carved out from the Crary Trough; the rest must be included in the underlying channel/levee facies. The volume of the

upper slope diamictit apron is comparable to the volume of sediments eroded from the shelf north of Berkner Island. Consequently, most of the sediments eroded south of Berkner Island must have added to the channel/levee facies, and during the deposition of the channel/levee facies the grounding line must have advanced to a position near the northern tip of Berkner Island. It is speculated that during the ice advances, the position of the grounding line was limited by the sub-ice topography. Ice congested and remained grounded in the narrow passage between Berkner Island and East Antarctica, but it became afloat as it reached the broad shelf in front of the island. It may be possible that the presence of the West Antarctic Ice Sheet or a major see-level lowstand was required for the ice sheet to become grounded on the broad shelf north of Berkner Island. Modelling studies might answer this question.

Uniform sedimentation occurred on the flat top of Polarstern Bank, where highly continuous, subparallel reflectors built up a sheet-drape external geometry. Piston cores recovered hemipelagic sediments from these facies showing low sedimentation rates and no sign of current-controlled deposition. Thus, a condensed, but relatively continuous, sediment sequence can be expected that contains a record of the paleoceanographic, biostratigraphic and glacial history of the Weddell Sea.

The basic shortcoming of the proposed depositional model is the poor borehole control. While the interpretation of different sediment types and depositional processes is relatively well constrained, the proposed timing is subject to considerable uncertainties. Further drilling is needed to resolve this problem.

The compilation of the geophysical data has contributed nonetheless, to a better understanding of the tectonic structures in the Southeastern Weddell Sea. The presented data confirm the existence of a failed rift arm underlying the Filchner Shelf. The failed rift basin was probably formed as part of a broad back-arc extension during Middle-Late Jurassic times.

The Explora Escarpment could have developed in a later drift phase during strike-slip motion between Africa and Antarctica. Fracture zone trends indicate that the Mozambique Escarpment may not have been the conjugate part of the Explora Escarpment. New data do not support the structural continuity of the Andenes and Explora Escarpments. The Andenes Escarpment is interpreted as an oceanic plateau which formed on a fracture zone during the later drift phase. Thus, in this model, the two features do not represent a continuous continent-ocean transition. The two structures have

different morphology, their strikes are offset by about 70 km and no basement high can be found that connects them. The continent-ocean transition is probably located south of the Andenes Escarpment or it may cross the southern part of this Escarpment. The Polarstern Bank seamounts were formed on oceanic crust by a delayed volcanic event on a pre-existing fracture or fault zone in the Late Jurassic/Early Cretaceous.

The present continuity of the breakup-related tectonic structures indicates that no large-scale microplate movement occurred in the survey area since the early opening of the Weddell Sea.

The breakup related volcanism and the oldest seafloor spreading anomalies indicate that drifting started in the Mozambique Basin, in the Somali Basin, on the Falkland Plateau and on the Dronning Maud Land margin at about 170±10 Ma. The overlap of these ages may mean that seafloor spreading started simultaneously in these areas. It would follow that the rift arm on the Dronning Maud Land margin, the later failed rift beneath the Filchner Shelf and the rift arm south of the Falkland Plateau formed a triple junction. On the other hand, the scatter of these data does allow two distinct phases directly following each other. During the first phase the Weddell Rift could have been formed; a remnant of this event is the failed rift beneath the Filchner Shelf. During the second rift phase, seafloor spreading could have started in the Somali and Mozambique basins, and a new spreading axis formed between the Filchner-Ronne Shelf and the Falkland-Agulhas Plateau resulting in the opening of the Weddell Sea.

Acknowledgements

The chance to see Antarctica, as it really is, was what first drew me to Bremerhaven, and, I must say, I was not disappointed. But as I became immersed in Antarctica's glacial and tectonic history, the continent became even more fascinating and this mental adventure started to attract more and more of my imagination. During this work, I met many people, received lots of help and made more than a few friends. Some of them I would like to mention by name.

Wilfried Jokat introduced me to seismic data processing and interpretation. He started me on this thesis, helped and pushed me through its teething problems and its many ups and downs. Without him I would have never finished.

I would like to express my thanks to my colleagues and friends at the Alfred Wegener Institute for their support of science and every-day life at Bremerhaven, especially, to Karsten Gohl, Vera Schlindwine, Gabrielle Unzelmann-Neben, Michael Studinger and Jeremy Gallop. I'm indebted to Uwe Meyer for the stimulating discussions, for his patient help, for the gravity data and for being a friend.

I would like to thank John Firestone for his heroic proof-reading on somewhat short notice.

I would like to further acknowledge Yngve Kristoffersen and Karl Hinz for the seismic data, German Leitchenkov for the aeromagnetic map, Heinrich Hinze and Hans-Werner Schenke for the bathymetric map, Tilo Schöne for the satellite gravity map, L.A. Lawver for the boundaries of the microcontinents, Gerhard Kuhn, Phil Bart and Marc DeBatist for the helpful discussions, the AWI computer group for their invisible support and Bernd Hoppmann for his cooperation.

I owe many thanks to Heinz Miller, the head of the Geophysics Department at the AWI, who made this thesis possible. I thank him for the financial support, for the expeditions and conferences I could participate in, and for reading and correcting the manuscript.

During the last two years of this research I was supported by the Deutscher Akademischer Austauschdienst.

At last, but not least, I would like to thank my family, especially my sister Julianna, for standing behind me and for believing in me.

References

Allen, R. B., Tucholke, B. E., 1981. Petrology and implications of the continental rocks from the Agulhas Plateau, southwest Indian Ocean. *Geology*, 9 (10), 463-468.

Alley, R. B., Blankenship, D. D., Bently, C. R., Roony, S. T., 1987. Till beneath ice stream B3. Till deformation: evidence and interpretations. *J. Geopys. Res.*, 92, 8921-8929.

Anderson, J. B., Wright, R., Andrews, B., 1986. Weddell Fan and Associated Abyssal Plain, Antarctica: Morphology, Sediment Process, and Factors Influencing Sediment Supply. *Geo-Marine Letters*, 6, 121-129.

Barker, P. F., Burell, J., 1982. The influence upon Southern Ocean circulation, sedimentation and climate of the opening of the Drake Passage. In: Craddoc, C. (ed), Antarctic Geoscience, (Univ. of Wiscosin Press), 377-385.

Barker, P. F., Kennett, J. P., et al., 1988. *Proc. ODP Init. Repts.* 113, Ocean Drilling Program (College Station, TX), 785 pp.

Barker, P. F., Kennett J. P., et al., 1990. *Proc. ODP Sci. Results*, 113, Ocean Drilling Program (College Station, TX), 1033 pp.

Bart, P. J., De Batist, M., Miller, H., 1994. Neogene Collapse of Glacially Deposited, Shelf Edge Deltas in the Weddell Sea: Relationship between Deposition during Glacial Periods and Sub-Marine Fan Development. *Terra Antarctica*, 1(2), 317-318.

Bergh, H. W., 1987. Underlying Fracture Zone Nature of the Astrid Ridge off Antarctica's Queen Maud Land. *J. Geophys. Res.*, 92 (B1), 475-484.

Bouma, A. H., Stelting, C. E., Feeley, M. H., 1983. High-Resolution Seismic Reflection Profiles. In: Bally, A. W., (ed), Seismic Expression of Structural Styles, 1, American Association of Petroleum Geologists, Tulsa, Oklahoma, U.S.A.

Brancolini, G., Davey, F., 1994. The Cenozoic sedimentary geology of the Ross Sea - A Review. *Terra Antarctica*, 1, 325-328.

Canadian Hydrographic Service, 1982. General Bathymetric Chart of the Oceans (GEBCO), 5th Edition, Ottawa, Ontario, Canada

Ciesielski, P. F., Weaver, F. M., 1983. Neogene and Quaternary paleoenvironmental history of Deep Sea Drilling Project Leg 71 sediments, southwest Atlantic Ocean. In: Ludwig, W. J., Krasheninnikov, V. A. et al., *Init. Repts DSDP*, 71, U.S. Govt. Printing Office (Washington), 461-477.

Cooper, A. K., Barret P. J., Hinz, K., Traube, V., Leitchenkov, G., Stagg H. M. J., 1991. Cenozoic prograding sequences of the Antarctic continental margin: a record of glacio-eustatic and tectonic events. *Marine Geology*, 102, 175-213.

Cunningham, A. P., Larter, R. D., Barker, P. F., 1994. Glacially prograded sequences on the Bellinghausen Sea continental margin near 90°W. *Terra Antarctica*, 1, 267-268.

Dalziel, I. W. D., Elliott, D. H., 1982. West Antarctica: Problem Child of Gondwanaland. *Tectonics*, 1 (1), 3-19.

Dalziel, I. W. D., Grunow, A. M., 1992. Late Gondwanide Tectonic Rotations within Gondwanaland. *Tectonics*, 11 (3), 603-606.

Drewry, D. J. (ed), 1983. Antarctica: Glaciological and Geophysical Folio. Scott Polar Research Institute (Cambridge)

Drewry, D. J., Cooper, A. P. R. 1981. Processes and models of Antarctic glaciomarine sedimentation. *Ann. Glaciol.*, 2, 117-122.

Drewry, D. J., Jordan, S. R., Jankowsky, E, (1982): Measured properties of the Antarctic Ice Sheet: surface configuration, ice thickness, volume and bedrock carasteristics, *Ann. Glaciol.*, 3, 83-91.

Ehrmann, W. U., 1993. Die Känozoische Vereisungsgeschichte der Antarktis. *Berichte zur Polarforschung*, 142, 152 pp, Alfred Wegener Institute (Bremerhaven).

Elliott, D. H., 1991. Triassic-early Cretaceous evolution of Antarctica. In: Thomson M. R. A., Crame, J. A., Thomson, J. W. (eds): Geological evolution of Antarctica, Proceedings of the Fifth International Symposium on Antarctic Earth Sciences, Cambridge, 23-28 August 1987, Cambridge University Press, Cambridge, 541-548.

Elverhoi, A., 1984. Glaciogenic and associated marine sediments in the Weddell Sea, fjords of Spitzbergen and the Barrents Sea: a review. *Marine Geology*, 57, 53-88.

Erlank, A. J., Reid, D. L., 1974: Geochemistry, mineralogy and petrology of basalts. In: *Init. Repts. DSDP*, 25, U.S. Govt. Printing Office (Washington), 543-552.

Fahrbach E., 1993. Zirkulation und Wassermassenbildung im Weddellmeer. *Die Geowissenchafften,* 11 (7), 246-253.

Fahrbach, E., Rohardt, G., Krause, G., 1992. The Antarctic Coastal Current in the Southeastern Weddell Sea. *Polar Biol*, 12, 171-182.

Fahrbach, E., Rohardt, G., Schröder, M., Strass, V., 1994. Transport and structure of the Weddell Gyre. *Ann. Geophysical*, 12, 840-855.

Foldvik, A., Gammelsrod, T., Torresen, T., 1988. Notes on Southern Ocean hydrography, sea ice and bottom water formation. *Paleogeogr., Paleoclimatol., Paleoecol.*, 67, 3-17.

Foldvik, A., Gammelsrod, T., Torresen, T., 1985a. Circulation and water masses on the Weddell Sea Shelf. *Antarct. Res. Ser.*, 43, 21-34.

Foldvik, A., Kvinge, T., Torresen, T., 1985b. Bottom currents near the continental shelf break in the Weddell Sea. *Antarct. Res. Ser.*, 43, 5-20.

Fütterer, D. K., Kuhn, G., Schenke, H. V., 1990. Wegener Canyon bathymetry and results from rock dredging near ODP 691-693, Eastern Weddell Sea, Antarctica. In: Barker P. F., Kennett J. P., et al., *Proc. ODP Sci. Results*, 113, Ocean Drilling Program (College Station, TX), 39-47.

Fütterer, D. K., Melles, M., 1990. Sediment patterns in the southern Weddell Sea: Filchner Shelf and Filchner Depression. In: Bleil, U., Theide, J. (eds), Geological history of polar oceans: Arctic versus Antarctic. NATO ASI Series C, Kluwer, Dordrecht, 381-401.

Gordon, A. L., Goldberg, R. D., 1970. Circumpolar characteristics of Antarctic waters - Am. Geogr. Soc., Antarctic map folio ser., folio 13, 1-5.

Grobe, H. L., Mackensen, A., 1992. Late Quaternary climatic cycles as recorded in sediments from the Antarctic continental margin. In: Kennett, J. P., Warnke, D. A. (eds.), The Antarctic Paleoenvironment: A Perspective on Global Change. Part One. *Antarct. Res. Ser.*, 56, 349-376.

Grunow, A. M., 1993. New paleomagnetic data from the Antarctic Peninsula and their tectonic implications. *J. Geophys. Res.*, 98 (B8), 13815-13833.

Grunow, A. M., Kent, D. V., Dalziel, I. W. D., 1987. Ellsworth-Whitmore Mountains crustal block, Western Antarctica: New paleomagnetic results and their tectonic significance. In: McKenzie, G. D. (editor), Gondwana Six: Structure, Tectonics and Geophysics. Geophysical Monograph 40, Washington DC.; American Geophysical Union: 161-172.

Grunow, A. M., Dalziel, I. W. D., Kent, D. V., 1991. New paleomagnetic data from Thurston Island: Implications for Tectonics of West Antarctica and Weddell Sea opening. *J. Geophys. Res.*, 96 (B11), 17935-17954.

Hambrey, M. J., Barret, P. J., Ehrmann, W. U., Larsen, B., 1992. Cenozoic sedimentary processes on the Antarctic continental margin and the record from deep drilling. *Z. Geomorph.*, 86, 77-103.

Haq, B. H., Hardenbol, J., Vail, P. R., 1987. Chronology of fluctuating sea levels since the Triassic. *Science*, 235 (4793): 1156-1167.

Harris, W., Sliter, W. V., 1977. Evolution of the Southwestern Atlantic Ocean Basin, Results of Leg 36, Deep Sea Drilling Project. In: *Init. Repts. DSDP*, 36, U.S. Govt. Printing Office (Washington), 993-1011.

Haugland, K., Kristoffersen, Y., Velde, A., 1985. Seismic investigations in the Weddell Sea Embayment. *Tectonophysics,* 114, 293-313.

Henriet, J. P., Miller, H., 1990. Some speculations regarding the nature of the Explora-Andenes Escarpment. In: Bleil, U., Theide, J. (eds), Geological history of polar oceans: Arctic versus Antarctic. NATO ASI Series C, Kluwer, Dordrecht, 163-172.

Hinz, K., 1981. A Hypothesis on Terrestrial Catastrophes, Wedges of very thick Oceanward Dipping Layers beneath Passive Continental Margins, *Geol. Jb.*, 22, 3-28.

Hinz, K., Fritsch, J., Klein, A., Roeser, H. A., 1994. Geophysical investigations of the crustal structure off East Antarctica between longitudes 0° and 40° E, paper presented at Weddell Sea Tectonics and Gondwana Breakup Conference, British Antarctic Survey and Tectonic Studies Group of the Geological Society of London, Cambridge, UK, June 6-7, 1994.

Hinz, K., Krause, W., 1982. The continental margin of Queen Maud Land/Antarctica: Seismic sequences, structural elements and geological development. *Geol. Jb.*, 23, 17-41.

Hinz, K., Kristoffersen, Y., 1987. Antarctica, Recent Advances in the Understanding of the Continental Shelf. *Geol. Jb.*, 37, 54 pp.

Hunter, R. J., Jonhson, A. C., Aleshkova, N. D., 1994. Aeromagnetic data from the Weddell Sea: Synthesis and interpretation. Paper presented at Weddell Sea Tectonics and Gondwana Breakup Conference, British Antarctic Survey and Tectonic Studies Group of the Geological Society of London, Cambridge, UK, June 6-7, 1994.

Huybrechts, P., 1992. The Antarctic Ice Sheet and Environmental Change: a three dimensional study. *Berichte zur Polarforschung*, 99, 241 pp, Alfred Wegener Institute (Bremerhaven).

Huybrechts, P., 1993. Glacial Modelling of the Late Cenozoic East Antarctic Ice Sheet: Stability or Dynamism? Geografiska Annaler, 75(A), 221-237.

Hübscher, C., 1994. Crustal structures and location of the continental margin in the Weddell Sea/Antarctica, *Berichte zur Polarforschung*, 147, 233 pp.

Jokat, W., Fechner, N., Studinger, M., submitted. Geodynamic models of the Weddell Sea embayment in view of new geophysical data.

Jokat, W., Hüscher, C., Meyer, U., Oszko, L., Schöne, T., Versteeg, W., Miller, H., in press: The Continental Margin off East Antarctica between 10°W and 30°W. In: Storey, B., King, E. C., Livermore, R. A. (eds), Weddell Sea Tectonics and Gondwana Break-up, Geological Society Special Publications, London, 108, 129-141.

Johnson, A. C., Smith, A. M., 1992. New aeromagnetic map of West Antarctica (Weddell Sea Sector): Introduction to important features. In: Yoshida, Y., Kaminuma, K., Shiraishi, K. (eds): Recent progress in Antarctic Earth Science, Tokyo, 555-562.

Kaul, N., 1991. Detailed Seismic Investigations at the Eastern Continental Margin of the Weddell Sea off Kapp Norvegia, Antarctica, *Berichte zur Polarforschung*, 89, 120 pp.

Kennett, J. P., Barker, P. F., 1990. Latest Cretaceous to Cenozoic climate and oceanographic developments in the Weddell Sea, Antarctica: an ocean-drilling perspective. In: Barker, P. F., Kennett, J. P. et al., *Proc. ODP Sci. Results*, 113, Ocean Drilling Program (College Station, TX), 937-960.

Kristoffersen, Y., Hinz, K., 1991. Evolution of the Gondwana plate boundary in the Weddell Sea area. In: Thomson M. R. A., Crame, J. A., Thomson, J. W. (eds): Geological evolution of Antarctica, Proceedings of the Fifth International Symposium on Antarctic Earth Sciences, Cambridge, 23-28 August 1987, Cambridge University Press, Cambridge: 225-230.

Kristoffersen, Y., Haugland, K., 1986. Geophysical evidence for the East Antarctic plate boundary in the Weddell Sea. *Nature*, 322, 538-541.

Kudryavtzev, G., Leitchenkov, G., Miloradovskaya, E., 1994. Deep Seismic Sounding across the Filchner-Ronne ice shelf, poster presented at Weddell Sea Tectonics and Gondwana Breakup Conference, British Antarctic Survey and Tectonic Studies Group of the Geological Society of London, Cambridge, UK, June 6-7, 1994.

Kuhn, G., Ehrmann, W. U., Melles, M., Schmiedl, G., Hambrey, M. J., 1992: Glaciomarine sedimentary processes in the Weddell Sea and Lazarev Sea. In: The Expeditions Antarktis IX/1-4 of the RV Polarstern in 1990/91. *Berichte zur Polarforschung*, 100, 223-244, Alfred Wegener Institute (Bremerhaven).

Kuhn, G., Weber, M. 1993. Acoustic characterisation of sediments by Parasound and 3.5 kHz systems: Related sedimentary processes on the southeastern Weddell Sea continental slope, Antarctica. *Mar. Geol., 113*, 201-217.

Kuvaas, B., Leitchenkov, G., 1992. Glaciomarine turbidite and current controlled deposits in Prydz Bay, Antarctica. *Marine Geology*, 108, 365-381.

Kuvaas, B., Kristoffersen, Y., 1991. The Crary Fan: a Trough-mouth Fan on the Weddell Sea Continental Margin, Antarctica. *Marine Geology*, 97, 345-362.

Kvasov, D. D., Verbitsky, M. Y., 1981. Causes of Antarctic Glaciation in the Cenozoic. *Quaternary Research,* 15, 1-17.

LaBrecque, J. L., Ghidella, M., 1994. Magnetic Anomaly Map of the Weddell Basin and Antarctic Peninsula, poster presented at Weddell Sea Tectonics and Gondwana Breakup Conference, British Antarctic Survey and Tectonic Studies Group of the Geological Society of London, Cambridge, UK, June 6-7, 1994.

LaBrecque, J. L., Barker, P., 1981. The age of the Weddell Sea Basin, *Nature,* 290, 489-492.

LaBrecque, J. L., Candle, S., Bell, R., Raymond, C. 1986. Aerogeophysical survey yields new data in the Weddell Sea. *Antarctic Journal of US*, 21 (5), 69-71.

LaBrecque, J. L., Hayes, D. E., 1979. Seafloor spreading history of the Agulhas Basin. *Earth and Planetary Science Letters*, 45 (2), 411-428.

Larter, R. D., Cunningham, A. P., 1993. The depositional pattern and distribution of glacial-interglacial sequences on the Antarctic Peninsula Pacific margin. *Marine Geology*, 109, 203-219.

Lawver, L. A., Gahagan, L. M., Coffin, M. F., 1992. The development of paleoseaways around Antarctica. *Antarct. Res. Ser.*, 56, 7-30.

Lawver, L. A., Royer, J. Y., Sandwell, D. T., Scotese, C. R., 1991. Evolution of the Antarctic continental margins. In: Thomson M. R. A., Crame, J. A., Thomson, J. W. (eds): Geological evolution of Antarctica, Proceedings of the Fifth International Symposium on Antarctic Earth Sciences, Cambridge, 23-28 August 1987, Cambridge University Press, Cambridge, 533-539.

Lawver, L. A., Scotese, C. R., 1987. A Revised Reconstruction of Gondwanaland. In: McKenzie, G. D. (ed), Gondwana Six: Structure, Tectonics and Geophysics. Geophysical Monograph 40, Washington DC, American Geophysical Union, 17-23.

Lorenzo, J. M., Mutter, J. C., 1987. Extension in the central Falkland Basin. *EOS*, 68 (44), 1479.

Ludwig, W. J., 1983. Geological Framework of the Falkland Plateau. In: Ludwig, W. J., Krasheninnikov, V. A. et al., *Init. Repts. DSDP*, 71, U.S. Govt. Printing Office (Washington), 281-293.

Marshall, J. E. A., 1994. The Falkland Islands: A key element in Gondwana paleogeography. *Tectonics*, 13, 499-514.

Martin, A. K., Hartnady, C. J. H., 1986. Plate tectonic development of the Southwest Indian Ocean, a revised reconstruction of East Antarctica and Africa. *J. Geophys. Res.*, 91 (B5), 4767-4786.

McGinnis, J. P., Hayes, D. E., 1994. Sediment Drift Formation along the Antarctic Peninsula. *Terra Antarctica*, 1, 275-276.

Melles, M., Kuhn, G., 1993. Sub-bottom profiling and sedimentological studies in the southern Weddell Sea, Antarctica: evidence for large-scale erosional/depositional process. *Deep-Sea Res.*, 40 (4), 739-760.

Mercer, J. H., Stott, L. D., 1984. Cenozoic marine sedimentation and ice volume variation on the East Antarctic craton. *Geology*, 12: 287-291.

Meyer, U., in press. Untersuchung des südöstlichen Weddell Meeres auf der Basis mariner Potentialfeld Daten. PhD thesis, University of Bremen.

Miller, H., De Batist, M., Jokat, W., Kaul, N., Steinmetz, S., Unzelmann-Neben, G., Versteeg, W., 1991. Revised Interpretation of Tectonic Features in the Southern Weddell Sea, Antarctica, from New Seismic Data. *Berichte zur Polarforshung*, 60, 33-38.

Miller, H., Henriet, J. P., Kaul, N., Moons, A., 1988. A Fine Scale Seismic Stratigraphy of the Eastern Margin of the Weddell Sea. In: Bleil, U., Thiede, J. (eds): Geological History of the Polar Oceans: Arctic versus Antarctic, NATO ASI Series.

Moons, A., DeBatist, M., Henriet, J. P., Miller, H., 1992. Sequence stratigraphy of the Crary Fan, Southeastern Weeddell Sea. In: Yoshida, Y., Kaminuma, K., Shiraishi, K. (eds): Recent progress in Antarctic Earth Science, Tokyo, 613-618.

Norton, I. O., Sclater, J. G., 1979. A model for the evolution of the Indian Ocean and the breakup of Gondwanaland. *J. Geophys. Res.*, 84 (B12), 6803-6830.

Orsi, A. H., Nowlin, W. D., Withworth, T., 1993. On the circulation and stratification of the Weddell Gyre. *Deep-Sea Research*, 40, 169-203.

Parson, B., Sclater, J. G., 1977. An analysis of the variation of ocean floor bathymetry and heat flow with age. *J. Geophys. Res.*, 82 (5), 803-827.

Powell, R. D., 1984. Glaciomarine processes and indicative lithofacies, modelling of ice shelf and tidewater glacier sediments based on quaternary examples. *Marine Geology*, 57, 1-52.

Rebesco, M., Larter, R. D., Barker, P. F., Camerlenghi, A., Vanneste, L. E., 1994. The history of sedimentation on the continental rise west of the Antarctic Peninsula. *Terra Antarctica*, 1, 277-279.

Salvin, S. M., Douglas, R. G., Stehli, F. G., 1975. Tertiary marine paleotemperatures. *Geological Society of America Bulletin, 86*, 1499-1510.

Sandwell, D. T., McAdoo, D. C., 1988. Marine Gravity of the Southern Ocean and Antarctic margin from Geosat. *J. Geophys. Res.*, 93 (B9), 10389-10396.

Sangree, J. B., Widmier, J. M., 1977. Seismic Interpretation of Clastic Depositional Facies. In: C. Payton (ed), Seismic Stratigraphy - Applications to Hydrocarbon Exploration, Am. Assoc. Pet. Geol. Mem., 26, 165-185.

Savage, M. L., Ciesielski, P. F., 1983. Revised history of glacial sedimentation in the Ross Sea. In: Oliver, R. L., James, P. R., Jago, J. B. (eds), Antarctic Earth Sciences, Canberra, 555-559.

Schenke, H. W., Hinze, H., Niederjasper, F., Schöne, T., Hoppmann, B., in prep. Bathymetric Chart of the Weddell Sea.

Sea Ice Climatic Atlas, Antarctica, 1985, Volume 1. Naval Oceanography Command Detachment, Asherille.

Sheriff, R. E., Geldart, L. P., 1983. Exploration Seismology, Volume 1-2, Cambridge University Press, Cambridge.

Simpson, E. S. W. et al., 1974. Site 249. In: *Init. Repts. DSDP*, 25, U.S. Govt. Printing Office (Washington), 278-304.

Solheim, A., 1990. Shallow geological and geophysical data from the southeastern Weddell Sea. Paper presented at the International Workshop on Antarctic Offshore Acoustic Stratigraphy (ANTOSTRAT), Asilomar Conference Facility, Pacific Grove, California, June 7-10, 1990. Overview and Extended Abstracts. U.S. Geological Survey, Open-File Report, 90-309, 246-250.

Stefansson, V., 1947. Great Adventures and Explorations. Dial Press, New York. pp. 788.

Storey, B. C., 1991. The crustal blocks of West Antarctica within Gondwana: reconstruction and breakup model. In: Thomson M. R. A., Crame, J. A., Thomson, J. W. (eds): Geological evolution of Antarctica, Proceedings of the Fifth International Symposium on Antarctic Earth Sciences, Cambridge, 23-28 August 1987, Cambridge University Press, Cambridge, 587-592.

Storey, B. C., Alabaster, T., Hole, M. J., Pankhurst, R. J., Wever, H .E., 1992. Role of subduction plate boundary forces during the initial stages of Gondwana breakup: evidence from the proto-Pacific margin of Antarctica. In: Storey, B. C., Alabaster, T., Pankhurst, R. J. (eds): Magmatism and Causes of Continental Break-up, Geological Society Special Publications, 68, London, 149-165.

Sundborg, A., 1965. The river Klarälven, a study in Fluvial process. *Geofisika Annaler*, 38, 125-316.

Syvitski, J., 1994. Glacial sedimentation processes. *Terra Antarctica*, 1, 251-253.

Tanahashi, M., Eittreim, S., Wannesson, J., 1994. Seismic stratigraphic sequences of the Wilkies Land Margin. *Terra Antarctica*, 1, 391-393.

Vail, P. R., Mitchum, J. R., Todd, R. G., Widmier, J. M., Tomphson, S., Sangree, J. B., Bubb, J. N., Hatleid, W. G., 1977a. Seismic stratigraphy and global changes of sea level. In: C. Payton (ed), Seismic Stratigraphy - Applications to Hydrocarbon Exploration, Am. Assoc. Pet. Geol. Mem., 26, 49-212.

Vail, P. R., Mitchum, J. R., Todd, R. G., Tomphson, S., 1977b. Global cycles of relative changes of sea level. In: C. Payton (ed), Seismic Stratigraphy - Applications to Hydrocarbon Exploration, Am. Assoc. Pet Geol. Mem., 26, 83-96.

Vaughan, D. G. et al., 1994. Map of subglacial and seabed topography 1:2000000 Filchner-Ronne Shelf Ice/Weddell Sea, Antarktis. Institut für Angewandte Geodäsie, Frankfurt am Main.

White, R., McKenzie, D., 1989. Magmatism at Rift Zones: The Generation of Volcanic Continental Margins and Flood Basalts. *J. Geophys. Res.*, 94 (B6), 7685-7729.

Yilmaz, Ö., 1987. Seismic Data Processing, Investigations in Geophysics, Volume 2, SEG, Tulsa.